# Simple Analytical and Numerical Techniques for Modelling Flame Spread on Solids

*Gregory North, Björn Karlsson, Daniel Gojkovic, Patrick van Hees*

**Department of Fire Safety Engineering**
**Lund University, Sweden**

**Brandteknik**
**Lunds tekniska högskola**
**Lunds universitet**

**Report 7014, Lund 2001**

# Simple Analytical and Numerical Techniques for Modelling Flame Spread on Solids

*Gregory North, Björn Karlsson, Daniel Gojkovic, Patrick van Hees*

**Lund 2001**

Simple Analytical and Numerical Techniques for Modelling Flame Spread on Solids

By Gregory North, Björn Karlsson, Daniel Gojkovic, Patrick van Hees

**Report: 7014**
**ISSN: 1402-3504**
**ISRN: LUTVDG/TVBB--7014--SE**

Number of pages: 123
Illustrations: Gregory North

Keywords
Flame spread, fire growth, surface materials, linings, flamspridning, effektutveckling, ytskiktsmaterial



Brandteknik
Lunds tekniska högskola
Lunds universitet
Box 118
221 00 Lund

brand@brand.lth.se
http://www.brand.lth.se

Telefon: 046 - 222 73 60
Telefax: 046 - 222 46 12

Department of Fire Safety Engineering
Lund University
P.O. Box 118
SE-221 00 Lund
Sweden

brand@brand.lth.se
http://www.brand.lth.se/english

Telephone: +46 46 222 73 60
Fax: +46 46 222 46 12

# Abstract

This report describes the work performed by Lund University, Sweden within a joint project between Lund University and the Swedish National Testing and Research Institute (SP), Borås. The project, called "Development of Engineering Tools for the Prediction of Flame Spread", had the aim of increasing the knowledge of flame spread modelling both with respect to thermal flame spread models and pyrolysis models. This report concentrates on the thermal theory models for flame spread.

The report shows how information on time to ignition and rate of heat release from bench-scale tests can be used to estimate time to ignition and fire growth in certain full-scale scenarios. The Cone Calorimeter is used to get bench-scale data on time to ignition and the energy release rate of a given material. The theoretical thermal models are described and a statistical package called @Risk is used to determine the values of a number of constants inherent in the models. These constants are then used in the models, allowing flame spread and energy release rate to be calculated for a number of simple full-scale scenarios, using data from the Cone Calorimeter test as input.

# Acknowledgments

This work has been financed by Brandforsk (Swedish Board for Fire Research) with the project number 307-971 and was a joint collaboration between Lund University and SP (Swedish National Testing and Research Institute). A reference group monitored the work, the group was Jan Blomqvist, Staffan Bengtson, Bengt Hägglund, Göran Holmstedt, Bror Persson, Birgit Östman, Björn Karlsson, Patrick van Hees, Heimo Tuominen, Örjan Thorné, Tomas Kemeny and Susanne Hessler. Their assistance is acknowledged.

# Table of Contents

# List of Figures



## Appendix Figures

# List of Tables



## Appendix Tables

# Nomenclature

| Symbol | Description | Units |
|---|---|---|
| a | Dimensionless Constant | (-) |
| A | Dimensionless Constant | (-) |
| $A_0$ | Initial Pyrolysis Area | $m^2$ |
| c | Specific Heat Capacity | $kJkg^{-1}K^{-1}$ |
| $C_1$ | Constant | $m^2s^{-1}$ |
| $C_2$ | Constant | s |
| $C_3$ | Constant | $s^{-1}$ |
| f | Fraction of Initial Pyrolysis Length | (-) |
| H | The Height of the Combustible Material | m |
| $\Delta H_C$ | Heat of Combustion | $kJkg^{-1}$ |
| k | Thermal Conductivity of a Solid Fuel | $kWm^{-1}K^{-1}$ |
| $k\rho c$ | Apparent Thermal Inertia | $kW^2sm^{-4}K^{-2}$ |
| K | Flame Height and Area coefficient which is dependent on the Burner Location | $mkW^{-1}$ or $m^2kW^{-1}$ |
| $\dot{m}$ | Mass Loss Rate of the Fuel | $kgs^{-1}$ |
| n | Exponential Constant in Flame Height Correlations | (-) |
| $\dot{q}''$ | Heat Flux per unit Area | $kWm^{-2}$ |
| $\dot{q}''_{fs}$ | Heat Flux for Flame Spread | $kWm^{-2}$ |
| $\dot{q}''_{start}$ | Pre-flame Spread Heat Flux | $kWm^{-2}$ |
| $\dot{q}''_e$ | External Radiation Heat Flux per Area | $kWm^{-2}$ |
| $\dot{Q}$ | Energy Release Rate | kW |
| $\dot{Q}_c$ | The Total Heat release rate of the Combustible Lining Material | kW |
| $\dot{Q}_{c^*}$ | Transient Total Heat release rate of the Combustible Material | kW |
| $\dot{Q}_{exp}$ | Full-scale Experimental Heat release rate | kW |
| $\dot{Q}_{tot}$ | Total Energy Release Rate, including the Burner | kW |
| $\dot{Q}''$ | Energy Release Rate per unit fuel Area, measured in the Cone Calorimeter | $kWm^{-2}$ |
| $s_1$ | Constant | $s^{-1}$ |
| $s_2$ | Constant | $s^{-1}$ |
| $t$ | Time | s |
| $t_{ig}$ | Time to Ignition | s |
| $t_p$ | Dummy Variable of Integration | s |
| $t_{pi}$ | Post-ignition Time | s |
| $t_{start}$ | Time to Ignition, due to the Burner Flame | s |
| T | Temperature | °C or K |

| | | |
|---|---|---|
| $T_{ig}$ | Ignition Temperature of a Material | °C or K |
| V | Flame Spread Velocity | $ms^{-1}$ or $m^2s^{-1}$ |
| W | Width of the Pyrolysis Front | m |
| x | Distance | m |
| $x_f$ | Flame Height | m |
| $x_{fb}$ | Flame Height from the Burner | m |
| $x_p$ | Height of the Pyrolysis Front | m |
| $x_{po}$ | Initial Height of the Pyrolysis Front | m |
| y | Distance into the Combustible Material | m |
| $y_{max}$ | Height of the Wall (Numerical Model) | m |
| | | |
| $\alpha$ | Constant | $s^{-1}$ |
| $b$ | Constant | $s^{-1}$ |
| $\Delta$ | Constant | $s^{-2}$ |
| $\Phi$ | Flame Heating Parameter | $kW^2m^{-3}$ |
| $c$ | Combustion Efficiency | (-) |
| $\lambda$ | The Decay Coefficient when simulating results from the Cone Calorimeter | $s^{-1}$ |
| $\sigma$ | Stefan Bolzmann constant | $Wm^{-2}K^{-4}$ |
| $r$ | Density | $kgm^{-3}$ |
| $t$ | Flame Spread Time to Ignition, used in the flame spread calculations | s |

## Subscripts

| Symbol | Description |
|---|---|
| 0 | Initial |
| F | Flame |
| g | Gas |
| ig | Ignition |
| n | Time Period of current interest |
| p | Pyrolysis |
| *t* | Time |
| o,ig | Minimum for Ignition |
| e | External |
| b | Burner |
| ave | Average |
| max | Maximum |
| s | Surface |

# 1. INTRODUCTION

This report describes the work performed by Lund University within a joined project between Lund University and SP (Swedish National Testing and Research Institute), Borås, Sweden. The project, called "Development of Engineering Tools for the Prediction of Flame Spread", has the aim of increasing the knowledge of flame spread modelling both with respect to thermal flame spread models and pyrolysis models.

This report concentrates on the theory of thermal models for flame spread. Such models need information on the time to ignition of a material at a given heat flux and information on the energy release rate history from a Cone Calorimeter or another such apparatus. Many different ways of arriving at a time to ignition value are possible and this report shows a very simple but effective way in which this can be done.

The flame spread equations are derived, showing that these can be solved either numerically (using numerical input data directly from the Cone Calorimeter) or analytically (using a mathematical representation of the data from the Cone calorimeter).

The analytical solutions have the advantage that they can be inserted into a statistical program, such as @Risk, and important information on various constants and parameters in the equations can be arrived at by comparing thousands of test simulations to full-scale experimental data. In this way, a number of ambiguous constants, such as the flame height constant K, can be determined.

Having determined these constants using the analytical model, they can be inserted into the equivalent numerical model. This allows information from the Cone Calorimeter on a numerical form to be used to predict full-scale flame spread and fire growth behaviour for a number of simple full-scale scenarios.

This report describes the aforementioned steps. Chapter 2 is used to describe the theory behind the models, Chapter 3 discusses experiments carried out in full-scale, which allows decisions to be made on which scenarios will be modelled. Chapter 4 shows how time to ignition data in bench-scale experiments can be used to estimate time to ignition in a number of full-scale scenarios. Chapter 5 discusses the analytical model and the sensitivity analysis carried out using @Risk. Chapter 6 discusses the numerical model and the results are presented in Chapter 7. Chapter 8 gives some conclusions and the concluding chapters and appendices give more detailed background to the undertaken work.

# 2. BACKGROUND THEORY ON UPWARD FLAME SPREAD

Many people have studied flame spread on solid combustible materials previously to varying extents. A selection of this past research has been reviewed in [1]. One specific area of this research involves the incorporation of the governing expressions into mathematical models. It is these expressions that will be discussed within this section.

## 2.1 Introduction

Mainly two types of methods for predicting flame spread have been proposed in the literature in recent years. Firstly, thermal theories have been used, where input data from the Cone Calorimeter are used to predict the flame spread and the resulting Heat Release Rate (HRR). The large-scale scenario that has been used for the verification of this method has generally been the Room/Corner Test (see Section 3.3 for more information). Work has also been undertaken using Computational Fluid Dynamic (CFD) and pyrolysis models to predict fire growth for the same full-scale experimental tests. Both methods require the properties of the examined material, which are usually determined from a bench-scale test apparatus such as the Cone Calorimeter. These parameters needed would generally be the thermal properties (such as k, $\rho$, c, $T_{ig}$) and properties to do with combustion, such as the heat of combustion and the latent heat of evaporation.

The analysis undertaken in this part of the research and described in Chapters 2 through 5 involved the development of an analytical flame spread model and implementation of this into a zone model in a full-scale scenario, including a flame spread algorithm, to investigate the flame spread phenomenon. An analytical model was used so that sensitivity analysis of the variables could be undertaken using the program @RISK. This sensitivity analysis was required, as it has been shown in previous research that relatively small variations in data can produce widely differing results in some models. This risk analysis program was designed for use with spreadsheets and therefore is ideally suited to analytical models. Verification of the model was achieved by comparing the individually calculated material values to equivalent experimental data that had been previously studied.

The following Chapter details the flame spread theory that was used in the analytical model to describe the flame spread travel, vertically up various interior wall linings and horizontally across ceilings.

## 2.2 Wind-aided Flame Spread Theory over Thick Solids

This type of flame spread results from an external wind or the buoyancy-induced flow of a

flame as it spreads up a wall or under a ceiling. The spread can be acceleratory and generally dominates over opposed flow flame spread.

The following analysis considers wind aided flame spread on thermally thick materials, or thin materials attached to a backing board. The developed theory [17] was built on a quasi-steady thermal model and no account of the complex chemical kinetics was taken. It was also assumed that the fuel is sufficiently thick so as to not be completely consumed during the flame spread process, implying that the material will not burn out. The set-up for this analysis is shown in Figure (2.1),

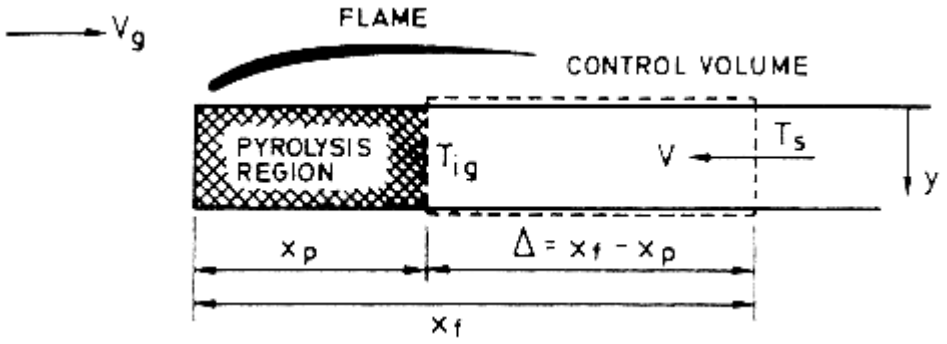


**Figure 2.1:** Energy Conservation Analysis in Wind-aided Flame Spread [17]

Starting from the general heat conduction equation in one dimension,

$$\mathrm{K}\frac{d^2\mathrm{T}}{d\mathrm{y}^2} = \rho \mathrm{c}\frac{d\mathrm{T}}{dt} \qquad \ldots(2.1)$$

and applying the initial condition, $T(y,0)=T_0$, and the boundary condition at y=0 (thus ignoring the convective and radiative cooling and other heat losses),

$$\dot{q}''(0,t) = \dot{q}''_e = -\mathrm{k}\frac{d\mathrm{T}}{d\mathrm{y}}$$

it is possible to arrive at the following expression for the ignition temperature, $T_{ig}$,

$$\mathrm{T}_{ig} - \mathrm{T}_0 = \frac{2\dot{q}''_e}{\sqrt{\pi}}\sqrt{\frac{t}{\mathrm{k}\rho \mathrm{c}}} \qquad \ldots(2.2)$$

and rearranging for the flame spread time to ignition, $t$, we get,

$$t = \frac{\pi \mathrm{k}\rho \mathrm{c}\left(\mathrm{T}_{ig} - \mathrm{T}_0\right)^2}{4\dot{q}''^{\,2}_e} \qquad \ldots(2.3)$$

If the flame spread time to ignition is replaced with the heating distance (assumed to be equal to $x_f - x_p$) divided by the velocity of the pyrolysis front, namely,

$$V = \frac{x_f - x_p}{\tau} \qquad \ldots(2.4)$$

an expression for the flame spread velocity can be obtained. This expression is given as,

$$V = \frac{4\dot{q}''^2_e \left(x_f - x_p\right)}{\pi k \rho c \left(T_{ig} - T_0\right)^2} \qquad \ldots(2.5)$$

The flame spread time to ignition, $\tau$, in equation (2.3) depends only on the fuel properties, ambient temperature and the level of heat flux from the flame to the fuel. Inherent in the equations is the assumption that $\tau$ is approximately constant while ($x_f$ - $x_p$) varies.

To simplify the underlining theory so a complete expression for V can be written, expressions for $x_f$ and $x_p$ must be found. Saito et al [32] suggested such expressions and developed an equation for V. Certain approximations were required for this solution to be obtained. The main assumptions were,

1. The material is thermally thick, homogeneous and it's thermal properties are constant with temperature.
2. Chemical kinetics are excluded, so that very fast as well as very slow rates of flame spread are not fully dealt with and extinction conditions are therefore only discussed approximately.
3. The flame length, $x_f$, depends on a power of $\dot{Q}$, the rate of heat release.
4. Heat flux, $\dot{q}''$, from the flame only occurs at constant flux within the region $x_p < x < x_f$ (see Figure (2.2)).

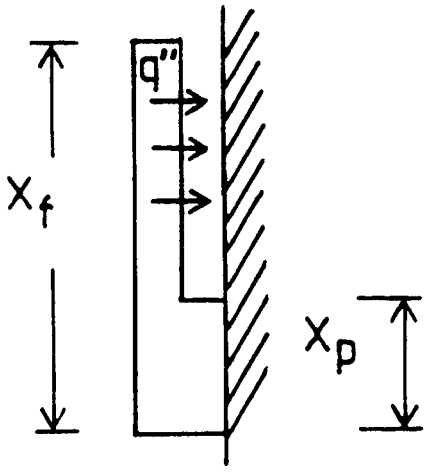


**Figure 2.2:** Constant Heat Flux Region, $x_p < x < x_f$ [17]

As mentioned above, in setting up an equation for the flame spread velocity, V, expressions are needed for $x_f$ and $x_p$. The height of the pyrolysis zone, $x_p$, as a

by,

$$x_p(t) = x_{po} + \int_0^t V_p(t_p)dt_p \qquad \ldots(2.6)$$

where $x_{po}$ is the value of $x_p$ at an initial time $t$ = 0 and $t_p$ is the dummy variable of integration.

The height of the flame is most commonly correlated with the total heat release rate, $\dot{Q}_{tot}$, and takes the form,

$$x_f(t) = K\dot{Q}_{tot}(t) \qquad \ldots(2.7)$$

The value of K depends on the location of the fire scenario, be that under a ceiling, in a corner or on an open wall. This particular variable was used in the tuning of the model, as detailed in Chapters 5 and 7.

In order to set-up the equation for the time dependent velocity of the pyrolysis front, V($t$), steady state assumptions are needed for the initial conditions. The burner output, $\dot{Q}_b$, is assumed to produce a constant, steady flame height in front of the virgin fuel. The flame produces a heat flux that is assumed to be constant over the flame height and zero above it. After a certain time, governed by the a material dependent flame spread time to ignition value, the material behind the flame ignites and the pyrolysis height, $x_{po}$, of this region, at $t$ = 0, is thus given by,

$$x_{po} = K\dot{Q}_b \qquad \ldots(2.8)$$

The flame height occurring at time, $t$ = 0, is termed $x_{fo}$ and is due to the energy released by the burner and the energy released from the initially burning material and is given by,

$$x_{fo}(t_0) = K\left(\dot{Q}_b + x_{po}W\dot{Q}''(0)\right) \qquad \ldots(2.9)$$

In the above equation, $\dot{Q}''(0)$ is the heat released per unit area by the material at ignition and W is the width of the flame front. It is assumed that the width, W, takes the same value as the width of the burner.

So that the time dependent flame height for $t$ > 0 can calculated, equation (2.7) shows that an expression for the total heat release rate, $\dot{Q}_{tot}$, is needed. This expression is influenced by three different sources, namely,

1. The constant output from the gas burner, and
2. The initial burning material at time $t$ = 0, and
3. The contribution resulting from the upward movement of the pyrolysis front.

By taking these effects into account, the total heat release rate, $\dot{Q}_{tot}$, is given by,

$$\dot{Q}_{tot}(t) = \dot{Q}_b + x_{po} W \dot{Q}''(t) + \int_0^t \dot{Q}''(t - t_p) W V(t_p) dt_p \qquad \ldots(2.10)$$

The heat release rate of the burning material, $\dot{Q}''$, is assumed to change with time, therefore denoted, $\dot{Q}''(t)$, and $t_p$ is the dummy variable of integration.

Now that all the variables in equation (2.5) have been described by obtainable variables, an equation for the flame spread velocity can be derived. This is achieved by substituting equation (2.10) into (2.7) and combining this with (2.6). This substitution arrives at the following Volterra integral equation for the flame spread velocity, V($t$),

$$V(t) = \frac{1}{t}\left[ K\left( \dot{Q}_b + x_{po} W \dot{Q}''(t) + \int_0^t W \dot{Q}''(t - t_p) V(t_p) dt_p \right) - \left( x_{po} + \int_0^t V(t_p) dt_p \right) \right] \qquad \ldots(2.11)$$

The analysis has so far assumed that K has the units of $mkW^{-1}$. This choice of unit implies that the width of the burning material remains constant. For materials placed under a ceiling, the characteristic width of the flame spread is not constant, therefore a flame spread velocity expression in terms of area can be useful. To allow the analysis to continue in a unit area ($m^2kW^{-1}$) basis as opposed to unit length ($mkW^{-1}$), thus incorporating flame spread under ceilings as well as vertically up walls, equation (2.11) can be rewritten as,

$$V(t) = \frac{1}{t_{ig}}\left[ K\left( \frac{\dot{Q}_b}{W} + x_{po} \dot{Q}''(t) + \int_0^t \dot{Q}''(t - t_p) V(t_p) dt_p \right) - \left( x_{po} + \int_0^t V(t_p) dt_p \right) \right] \qquad \ldots(2.12)$$

The two terms in the brackets on the right hand side represent $x_f$ and $x_p$ respectively and $t_p$ is again the dummy variable of integration.

Two further assumptions that are included in this analysis are,

1. The initial pyrolysing length, $x_{po}$, is dependent on the burner output, $\dot{Q}_b$. This output is assumed to be constant at all times.
2. Preheating of the combustible material beyond the flame tip is not accounted for (such as preheating by a hot gas layer). The flame is assumed to be the only source of heat and therefore $T_s$, as indicated in Figure (2.2), is assigned the same value as $T_0$.

To solve equation (2.12), a mathematical representation is needed for the time dependent heat release rate of the given material. This can be achieved by using Cone Calorimeter data and developing simple heat release rate expressions. The Cone Calorimeter data can

be used directly in the equation (2.12) but it must then be solved numerically by a computer (as done in Chapter 6). Alternatively, the Cone Calorimeter results can be approximated to a mathematical function and inserted into the flame spread equation (2.12), which can then be solved analytically. This has been undertaken to allow extensive sensitivity analysis and is described in the following Chapters.

### 2.2.1 Heat Release Rate Representations

To analytically solve equation (2.12), it is necessary to mathematically represent the time dependent Heat Release Rate (HRR) and the flame length of the material under investigation. There are many types of mathematical representations that can be made [17] but in this research only two were investigated - a peak heat flux followed by an exponential decay (Peak/Decay) or an averaged, straight heat flux (Averaged). These two HRR representations can be seen graphically in Figures (2.3) and (2.4) in the following sections.

The Peak/Decay model assumes that the heat flux from the combustible material peaks as the item ignites and then decays exponentially over time. The value of this peak, $\dot{Q}''_{max}$, and the rate of decay, $\lambda$, are material dependent and were therefore required input variables in the developed flame spread model. The expression of such a heat release rate representation is,

$$\dot{Q}''(t) = \dot{Q}''_{max} e^{-\lambda t}$$

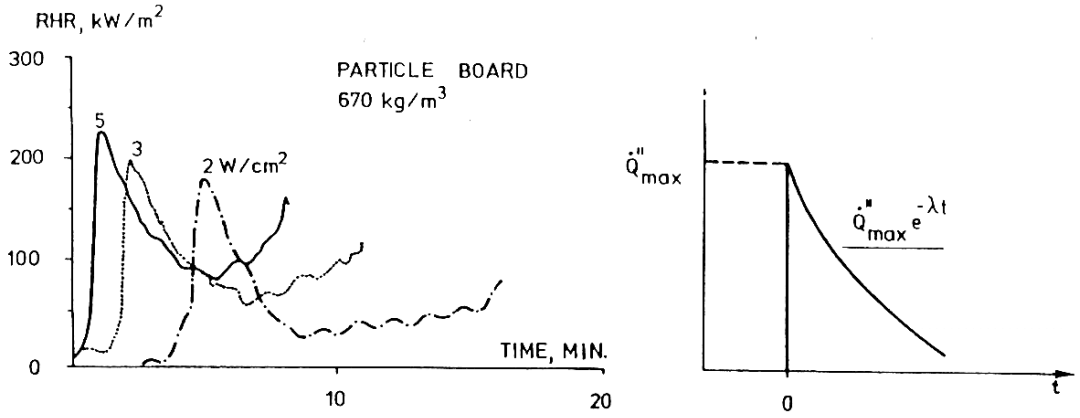


**Figure 2.3:** Cone Calorimeter Results and the Peak/Decay HRR Representation [17]

The Averaged model assumes that the exponential decay of the previously described model is so small so that it can be ignored and the material can then be represented by a constant heat release rate per unit area, $\dot{Q}''_{ave}$. This model holds reasonably well for materials that burn slowly over a relatively long time period. The figure below shows an actual heat release rate curve for a particular material, on the left, and a constant representation of the same curve, on the right. The form of the expression for the Average heat release rate representation is,

$$\dot{Q}''(t) = \dot{Q}''_{ave}$$

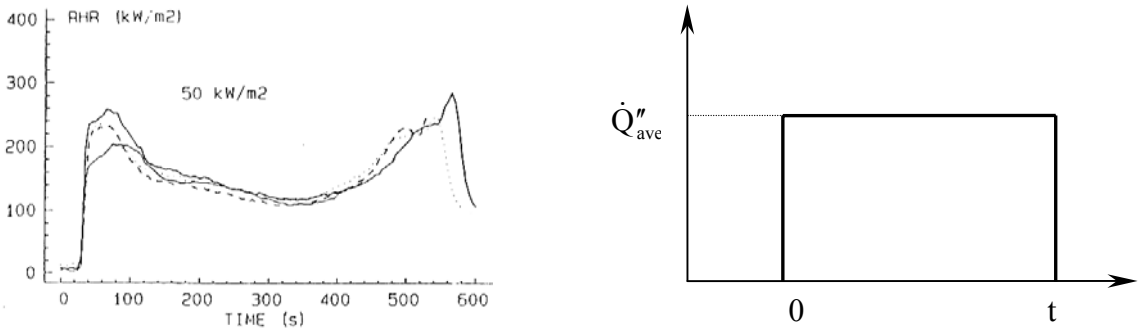


**Figure 2.4:** Cone Calorimeter Test Results [21] and the Average HRR Representation

## 2.2.2 Upward Flame Spread Expressions

We noted that the Average HRR representation was in fact simply a special case of the Peak/Decay HRR case where $\dot{Q}''_{ave}$ equalled $\dot{Q}''_{max}$ and the decay coefficient, $\lambda$, equalled zero. Both representations could therefore be easily included in the model. The HRR representation is now carried out by replacing the variables described above with $\dot{Q}''$ and $\lambda$. The development of the upward flame spread expressions for each HRR representation are described in [27, 17].

A full written description of the variables in the expressions can be found in Chapter 5.

### 2.2.2.1 Flame Spread Velocity, $V(t)$

By applying the assumptions as described previously and taking Laplace transformations followed by inverse Laplace transforms of equation (2.12), the following equation is obtained for the flame spread velocity, V($t$), with units of ms$^{-1}$,

$$V(t) = \frac{C_1}{s_2 - s_1}\left[s_2 e^{s_2 t} - s_1 e^{s_1 t}\right] \qquad \ldots(2.13)$$

where,

$$s_{1,2} = -\frac{1}{2\tau}(1 - a + \lambda\tau) \pm \frac{1}{2}\sqrt{\Delta} \qquad \ldots(2.14)$$

$$\Delta = \frac{1}{\tau^2}(1 - a + \lambda\tau)^2 - \frac{4\lambda}{\tau} \qquad \ldots(2.15)$$

$$a = K\dot{Q}'' \qquad \ldots(2.16)$$

$$\dot{Q}_b = \frac{A_o}{K} \qquad \ldots(2.17)$$

$$x_{po} = \frac{K\dot{Q}_b}{W} \qquad \ldots(2.18a)$$

which changed to the following equation when the tuning variable, f (see Section 5.2.1.5), was included to,

$$x_{po} = \frac{fK\dot{Q}_b}{W} \qquad \ldots(2.18b)$$

and

$$C_1 = \frac{K\dot{Q}'' x_{po}}{\boldsymbol{t}} \qquad \ldots(2.19)$$

The conditions for the velocity to accelerate are that $s_1$ or $s_2$ or both are positive, ie. for the region $\boldsymbol{l t} < \left(1-\sqrt{a}\right)^2$ and $\boldsymbol{l t} > \left(1+\sqrt{a}\right)^2$. A decelerating velocity is therefore described by the following limits,

$$V(t) \text{ decelerates if} \qquad \left(1-\sqrt{a}\right)^2 < \boldsymbol{l t} < \left(1+\sqrt{a}\right)^2$$

If the $V(t)$ decelerates, then (2.18) no longer applies and $V(t)$ becomes,

$$V(t) = \frac{C_1 e^{\boldsymbol{a}t}}{\boldsymbol{b}}\left[\boldsymbol{a}\sin(\boldsymbol{b}t) + \boldsymbol{b}\cos(\boldsymbol{b}t)\right] \qquad \ldots(2.20)$$

where,

$$\boldsymbol{a} = -\frac{1}{2\boldsymbol{t}}(1 - a + \boldsymbol{l t}) \qquad \ldots(2.21)$$

$$\boldsymbol{b} = \frac{1}{2}\sqrt{\Delta} \quad \text{(when } \Delta \text{ is positive)} \qquad \ldots(2.22a)$$

$$\text{or } \boldsymbol{b} = \frac{1}{2}\sqrt{-\Delta} \quad \text{(when } \Delta \text{ is negative)} \qquad \ldots(2.22b)$$

For the complex solution, ie. when $\Delta$ is negative, $s_{1,2}$ becomes complex and is written in the form, $\boldsymbol{a} \pm i\boldsymbol{b}$.

The limits of the accelertory or deceleratory behaviour for the flame spread velocity can be represented graphically in Figure (2.5).

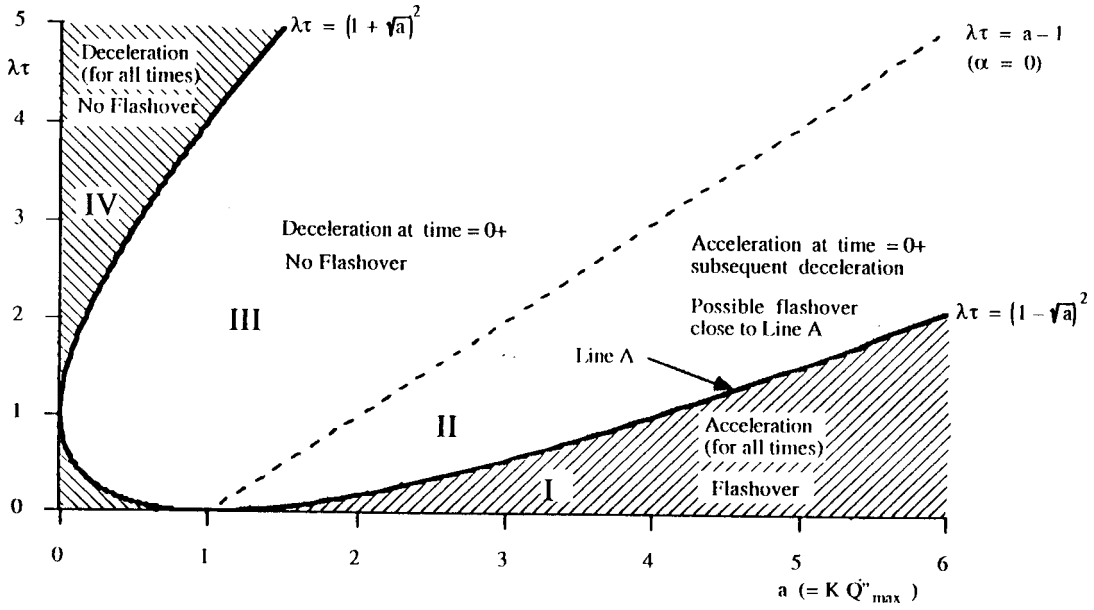


**Figure 2.5:** Regions of Flame Front Acceleration and Deceleration [17]

Four regions are indicated in Figure (2.5) which depend on the value that the product $\lambda\tau$ takes. The description of the flame spread can be summarised in Table (2.1).

**Table 2.1:** Summary of Flame Spread Characteristics

| Region [a] | Expression | Flame Front Description | Graphical Representation |
|---|---|---|---|
| I | $\lambda\tau < \left(1-\sqrt{a}\right)^2$ | Acceleration over all times | 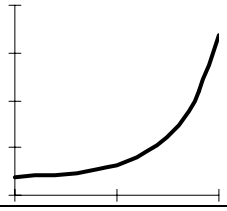 |
| II | $\left(1-\sqrt{a}\right)^2 < \lambda\tau < (a-1)$ | Oscillatory decay with initial acceleration | 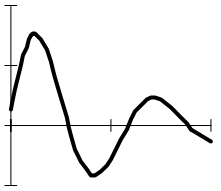 |
| III | $(a-1) < \lambda\tau < \left(1+\sqrt{a}\right)^2$ | Oscillatory decay with initial deceleration | 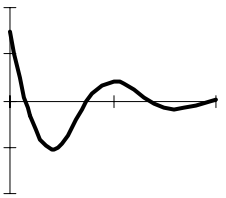 |
| IV | $\lambda\tau > \left(1+\sqrt{a}\right)^2$ | Deceleration over all times | 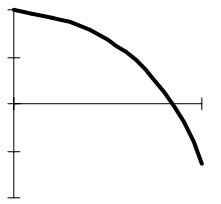 |

[a] The region described in this column refers to the region within Figure (2.5)

Note that the solutions for the flame spread velocity are only valid for positive values of $V(t)$ since the flame height is always considered to be positive. This limitation is of particular importance for oscillatory flame spread described in regions II and III as the validity of $V(t)$ ceases once the velocity becomes negative for the first time.

In order to calculate how far the flame front has travelled and the resulting heat release rate, the expressions, in terms of velocity, for the pyrolysing area, $A_p(t)$, and the heat release rate, $\dot{Q}_c(t)$, must be derived. Again the flame spread behaviour, be that accelertory or deceleratory, must be considered.

#### 2.2.2.2 Pyrolysing Length, $x_p(t)$

The expression for the Pyrolysis Length, in metres (m), can be obtained by integrating equations (2.13) and (2.20), thus giving,

for $\lambda t < \left(1-\sqrt{a}\right)^2$ and $\lambda t > \left(1+\sqrt{a}\right)^2$

$$x_p(t) = x_{po} + \frac{C_1}{s_2 - s_1}\left[e^{s_2 t} - e^{s_1 t}\right] \qquad \ldots(2.23)$$

and for $\left(1-\sqrt{a}\right)^2 < \lambda t < \left(1+\sqrt{a}\right)^2$

$$x_p(t) = x_{po} + \frac{C_1 e^{at}}{\beta}\sin\left[\beta t\right] \qquad \ldots(2.24)$$

#### 2.2.2.3 Flame Front Length, $x_f(t)$

An expression for the Flame Front Length, in metres, is given by,

$$x_f(t) = K\left[\dot{Q}_c(t) + \dot{Q}_b\right] = K\dot{Q}_{tot}(t) \qquad \ldots(2.25)$$

where $\dot{Q}_c(t)$ is given by equation (2.26).

#### 2.2.2.4 Heat Release Rate, $\dot{Q}_c(t)$

The heat released, in kW, from the combustible material is obtained from the equation,

$$\dot{Q}_c(t) = x_{po}\dot{Q}''e^{-\lambda t} + \int_0^t \dot{Q}''e^{-\lambda\left(t-t_p\right)}V(t)dt_p \qquad \ldots(2.26)$$

Inserting equations (2.13) and (2.20) and performing the integration then gives,

for $\lambda t < \left(1-\sqrt{a}\right)^2$ and $\lambda t > \left(1+\sqrt{a}\right)^2$

$$\dot{Q}_c(t) = W\left[x_{po}\dot{Q}''e^{-\lambda t} + \frac{C_1}{s_2 - s_1}\left(\frac{s_2\dot{Q}''\left(e^{s_2 t} - e^{-\lambda t}\right)}{s_2 + \lambda} - \frac{s_1\dot{Q}''\left(e^{s_1 t} - e^{-\lambda t}\right)}{s_1 + \lambda}\right)\right] \quad \ldots(2.27)$$

and for $\left(1-\sqrt{a}\right)^2 < \lambda t < \left(1+\sqrt{a}\right)^2$

$$\dot{Q}_c(t) = W\left[x_{po}\dot{Q}''e^{-\lambda t} + C_1 C_2\dot{Q}''\left[e^{\alpha t}\left(\cos(\beta t) + \frac{C_3}{\beta}\sin(\beta t)\right) - e^{-\lambda t}\right]\right] \quad \ldots(2.28)$$

where,

$$C_2 = \left[\frac{1}{\lambda}\left(\alpha^2 + \beta^2\right) + 2\alpha + \lambda\right]^{-1} \quad \ldots(2.29)$$

$$C_3 = \frac{1}{\lambda}\left(\alpha^2 + \beta^2\right) + \alpha \quad \ldots(2.30)$$

And $C_1$, $\alpha$ and $\beta$ are given by equations (2.19), (2.21) and (2.22a,b) respectively.

# 3. FLAME SPREAD EXPERIMENTS

The flame spread phenomenon can be experienced by various test methods, including the Room/Corner and the Single Burning Item tests. These two methods, currently standard tests throughout Europe, were used to verify the results obtained from the two mathematical models. This Chapter describes the experiments that were used for this comparison in this research as well as the materials investigated and the data collection and standardisation procedures.

## 3.1 Introduction

The experiments that have been used as a comparison for the mathematical models in this report included research undertaken using the Room/Corner and the Single Burning Item (SBI) tests. Three different research studies using the Room/Corner test apparatus have been used for the verification which included the results from the SBI Research Program [34], the Swedish Institute for Wood Technology Research (Trätek) [17] and a Nordic fire research program named "EUREFIC [17, 35].

## 3.2 Background to Experiments

The experimental results used in this report give details of specific fire behaviour for numerous materials. This behaviour is primarily in terms of,

1. The quantity of energy that is released by a material, and
2. The way in which flames spread over the material.

A bench-scale apparatus such as the Cone Calorimeter or the ISO Ignitibility Test generally describes the first of these behaviours. The second behaviour has been described for the given materials by the aforementioned Room/Corner or SBI test.

These two behaviours were fundamental in the development of the model described in this report. The energy release rate prediction found from the initial test method is a required input into the model and without the second test, experimental comparison with the model could not be easily made.

Each result from the experiments were found by slightly different methods. These differences are described in the following three sections of this Chapter and further information can be found in the given references.

To characterise the initial behaviour of the materials, Cone Calorimeter results were used. The Cone Calorimeter apparatus utilises the principle of oxygen consumption to calculate the heat released by the material. The relevant results from this test are, for each exposure level, the time to ignition, mass loss rate and the rate of heat release.

This device was used in all the experimental studies on each material. The typical set-up of this device, in the horizontal orientation, is seen in Figure (3.1).

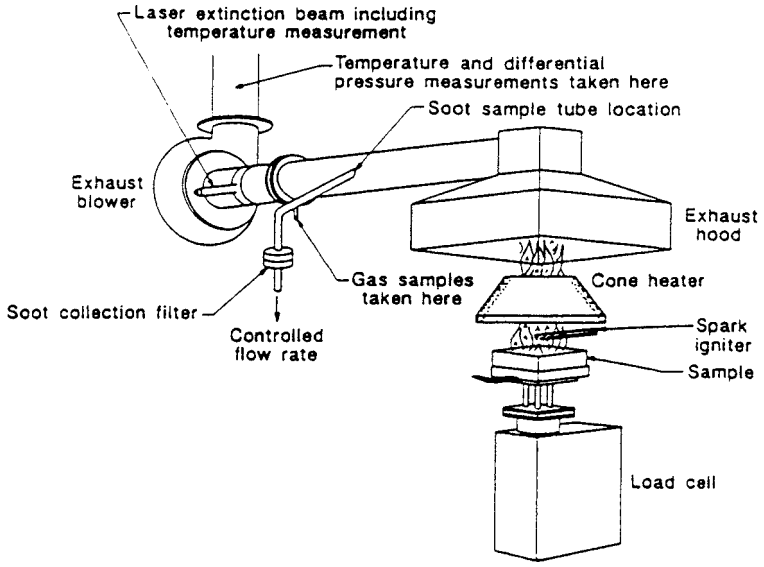


**Figure 3.1:** Typical Cone Calorimeter Experimental Set-up [17]

Once the energy release behaviour was determined, the flame spread characteristics were investigated in the Room/Corner and SBI tests.

## 3.3 Room/Corner Scenario

This is a large-scale test method for the measurement of the burning behaviour of surface lining materials used in buildings. The test apparatus consists of a small compartment (3.6m long, 2.4m wide and 2.4m high) with one open door and a gas burner. A gas collection system is also supplied with the necessary instrumentation to measure the fire gas properties. The Swedish and Eurefic data (described overleaf) used in this report are just a small collection of the many different materials that have been investigated in this apparatus. The experimental set-up for the Room/Corner test is shown in Figure (3.2).

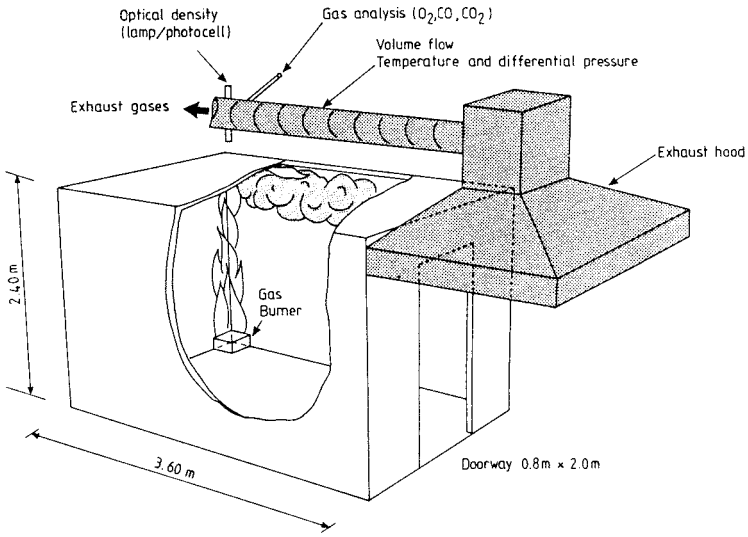


**Figure 3.2:** Room/Corner Experimental Set-up [33]

The ignition source in these tests was a propane gas burner placed on the floor in one corner of the room. During the first ten minutes of the test, the burner was run at 100kW and after ten minutes, if flashover had not occurred in the compartment, it was increased to 300kW for ten more minutes.

The combustion products, leaving the room through the door, from this test were collected in a hood connected to an exhaust system. The rate of heat released from the fire was calculated within this system by the same principle as in the Cone Calorimeter test, namely, oxygen consumption.

### 3.3.1 Swedish "S" Series Experiments

The Swedish, as well as the Eurefic experiments, used the European Standard Room/Corner test. Thirteen different materials from this study have been incorporated into this research. As mentioned previously, the materials were also tested in the Cone Calorimeter at irradiance levels of between 25–75kWm$^{-2}$. These materials, given in table 3.1, were fixed to the ceiling and to the walls of the test compartment, excluding the wall where the door was located as the test procedure required.

The materials and the code used in this Swedish study are given in Table (3.1).

**Table 3.1:** Materials used in Swedish "S" Series Experiments

| S Series Materials | |
|---|---|
| Material No. | Material Name |
| S1 | Insulating Fibre Board |
| S2 | Medium Density Fibre Board |
| S3 | Particle Board |

| | |
|---|---|
| S4 | Gypsum Plasterboard |
| S5 | PVC covering on S4 |
| S6 | Paper covering on S4 |
| S7 | Textile covering on S4 |
| S8 | Textile covering on Mineral Wool |
| S9 | Melamine-faced Particle Board |
| S10 | Expanded Polystyrene |
| S11 | Rigid Polyurethane Foam |
| S12 | Wood Panel (Spruce) |
| S13 | Paper covering on S3 |

Note that these particular materials have been termed the "S" series materials as denoted by the "S" prior to the material number. Further properties for these materials can be found in Appendix A.

### 3.3.2 Eurefic "E" Series Experiments

The Eurefic data is from the Nordic research program "EUREFIC - EUropean REaction to FIre Classification". This program is managed by the co-operation of the fire institutes in Denmark, Finland, Norway and Sweden. The purpose of the tests, incorporated into this research, was to gain sufficient data for the use in the development and validation of a calculation model for scaling test results from the Cone Calorimeter to large scale test results of the room fire test, NT FIRE 025.

The eleven different materials included from this study have only been those tested in the horizontal orientation in the Cone Calorimeter, since this was the case for all the other materials. The experimental flame spread data for these materials was obtained from the Room/Corner Test apparatus. These materials are described in Table (3.2).

**Table 3.2:** Materials used in Eurefic "E" Series Experiments

| **E Series Materials** | |
|---|---|
| Material No. | Material Description |
| E1 | Painted Gypsum Paper Plaster Board |
| E2 | Ordinary Plywood |
| E3 | Textile Wall-covering on Gypsum Paper Plaster Board |
| E4 | Melamine Faced High Density Non-combustible Board |
| E5 | Plastic Faced Steel Sheet on Mineral Wool |
| E6 | FR Particle Board - type B1 |
| E7 | Faced Rockwool |
| E8 | FR Particle Board |
| E9 | Polyurethane Foam Covered with Steel Sheet |
| E10 | PVC-wall Carpet on Gypsum Paper Plaster Board |
| E11 | FR Polystyrene |

Note that these particular materials have been termed the “E” series materials as denoted by the “E” prior to the material number. Further properties for these materials can be seen in Appendix A.

## 3.4 Single Burning Item (SBI) Scenario

The test was developed by the Official Laboratories Group (OLG) based on the guidelines set out by the EU Regulatory Group (RG) and is one of the test methods to be used to determine the classification of building products in the future European classification system.

This test attempts to simulate a small single burning item placed in a corner of a room so therefore end-use conditions of the specimens, such as the typical mounting procedure, must be closely followed. The corner of a room is used as the fire origin as it is assumed to be the most favourable location for fire development.

Two test specimens, with dimensions $1.0 \times 1.5$m and $0.5 \times 1.5$m, are positioned on the test apparatus to form an overlapping “room corner” and a triangular test burner is placed on the floor beside the specimens. This burner, with a side length of 250mm, is a diffusion burner fuelled by propane. The output of the burner is 30kW, which continues for the tests’ duration of 21 minutes. There is a floor in the test configuration but no ceiling. The combustion products from the fire are collected in a hood and transported through a duct containing thermocouples, a pressure sensor, a smoke measurement system and a sample probe. The test rig is placed in an enclosure in order to avoid any draft around the test specimen and to protect the operator from the combustion products.

The test outputs are the heat release rate (calculated using oxygen depletion), time to ignition (determined as a 6kW rise in the heat release rate), lateral flame spread on the large wing of the test specimen, smoke production and burning droplets/particles information. The experimental set-up for the SBI test is shown in Figure (3.3).

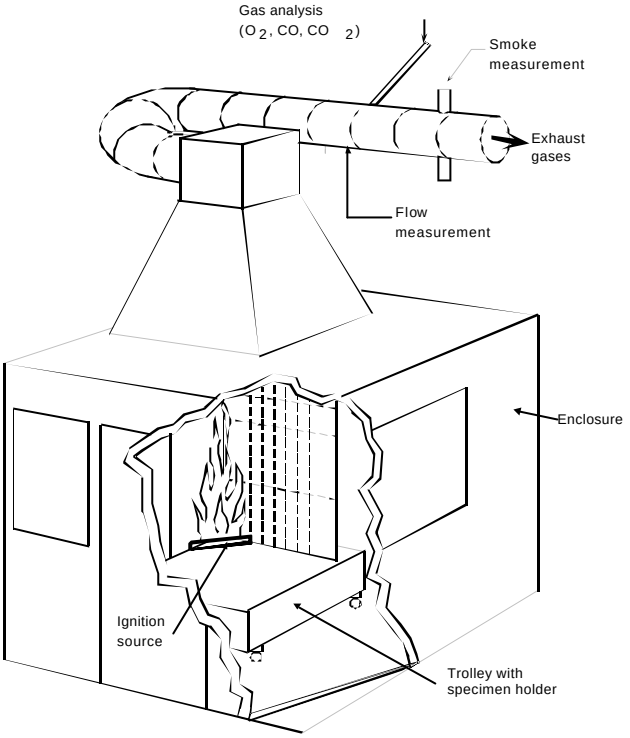


**Figure 3.3:** SBI Experimental Set-up [34]

## 3.4.1 "M" Series Experiments

Thirty different building products, selected by the European Commissions' group of regulators, were included in a study and data was available for most. These materials are listed in Table (3.3).

**Table 3.3:** Materials used in "M" Series Experiments

| **M Series Materials** | |
|---|---|
| Material No. | Material Name |
| M1 | Plasterboard |
| M2 | FR PVC |
| M3 | FR extruded Polystyrene board |
| M4 | PUR foam panel with Al. Foil faces |
| M5 | Varnished mass timber, Pine |
| M6 | FR Chipboard |
| M7 | FR Polycarbonate panel (3 layered) |
| M8 | Painted Plasterboard |
| M9 | Paper wall covering on Plasterboard |
| M10 | PVC wall carpet on Plasterboard |
| M11 | Plastic-faced Steel sheet on Mineral Wool |
| M12 | Unvarnished mass timber, Spruce |
| M13 | Plasterboard on Polystyrene |

| | |
|---|---|
| M14 | Phenolic foam |
| M15 | Intumescent coat on Particle board |
| M16 | Melamine faced MDF board |
| M17 | PVC water pipes |
| M18 | PVC covered electric cables |
| M19 | Unfaced Rockwool |
| M20 | Melamine faced Particle board |
| M21 | Steel clad expanded Polystyrene sandwich panel |
| M22 | Ordinary Particle board |
| M23 | Ordinary Plywood, Birch |
| M24 | Paper wall covering on Particle board |
| M25 | Medium density fibre tiles |
| M26 | Low density fibre board |
| M27 | Plasterboard/FR PUR foam core |
| M28 | Acoustic mineral fibre tiles |
| M29 | Textile wall paper on Calcium silicate board |
| M30 | Paper-faced glass wool |

Note that these particular materials have been termed the "M" series materials as denoted by the "M" prior to the material number. Further properties for these materials can be seen in Appendix A.

Room/Corner scenario HRR data was also available for most of the "M" materials so they were also tested in the Room/Corner scenario flame spread model.

Experimental data for the SBI scenario was unavailable for materials M17 and 18 and for the Room/Corner scenario, experimental data was also missing for materials M17, 18, 21 and 27-30.

## 3.5 Heat Release Rate Data Collection and Standardisation

Two different types of experimental data were used as input in this research. One of these collections came from bench-scale tests and the other collection came from full-scale tests.

The bench-scale, ie. Cone Calorimeter, test data was used for the determination of the heat release rate representation data for the individual materials, namely the heat flux level, $\dot{Q}''$, and the decay coefficient, $\lambda$.

The full-scale, ie. Room/Corner or SBI, test data was required for the comparison between the calculated and experimental HRR data. This HRR data came directly from the Room/Corner or the SBI experiments, which required modification to remove various discrepancies to ensure that the model and the associated analysis could be undertaken

optimally.

The following section describes the way in which this data was obtained.

### 3.5.1 Cone Calorimeter Data Manipulation

Raw data from the Cone Calorimeter experiments for the individual materials was tabulated within a spreadsheet and manipulated so that the desired values for the flame spread model, namely the heat flux level, $\dot{Q}''$, and the decay coefficient, $\lambda$, could be determined. These values were needed to describe the HRR representation of each material as mentioned in the previous chapter.

Figure (3.4) shows the typical output from a Cone Calorimeter test that was found for each material modelled.

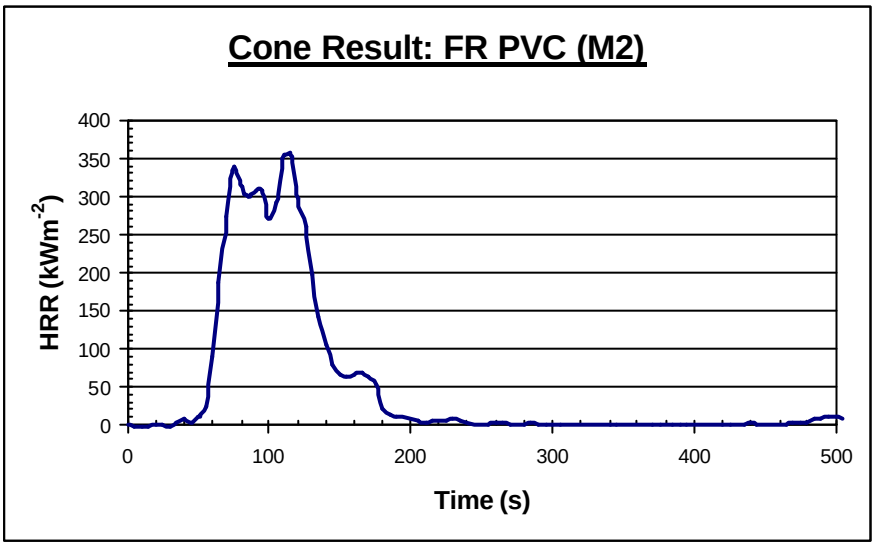


**Figure 3.4:** Typical Raw Data from a Cone Calorimeter Experiment

From this figure, the data was time shifted so that the maximum heat release rate now occurred at time, t = 0. This resulted in the formation of Figure (3.5), which is in the form of a Peak/Decay HRR representation described in Figure (2.3).

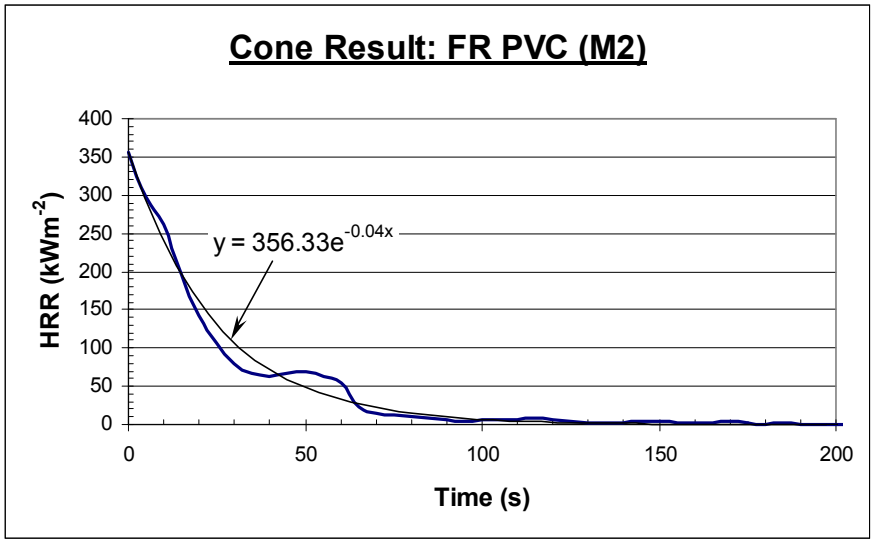


**Figure 3.5:** Typical Manipulated Cone Calorimeter Data

An exponential trendline was placed over the data points and the heat flux level, $\dot{Q}''$, and the decay coefficient, $\lambda$, could be found, as shown by the thin line in Figure (3.5). This technique was undertaken for all the materials studied in this research and a full list of the values can be found in the Appendix A.

## 3.5.2 Experimental Upward Flame Spread Data Standardisation

The HRR results collected from the Room/Corner or SBI experiment showed some significant variation between the different specimens so that the results needed to be standardised. This standardisation involved the removal of the initial irrelevant stages of the HRR data until a certain value was achieved. In the Room/Corner and the SBI test, this initial value was 20 and 50kW respectively. Once these HRR values were obtained, the experimental time was reset to zero. In doing this process the effects of the start times of the measuring equipment (Data Logger) and any initial experimental differences in the burner ignition would effectively be removed.

# 4. IGNITION TIME / HEAT FLUX ASSOCIATION

## 4.1 Introduction

Many different variables are needed to fully describe a complex phenomenon such as flame spread. Such variables include the properties, location and orientation of the specimen, the properties of the testing equipment as well as various environmental factors to name but a few. In an attempt to develop a model that focused on the dominant factors and therefore reduced the number of necessary inputs, which can also be difficult to obtain, simplifications were needed. This approach is supported by Williams [40] who stated in a 1976 report that,

> *"…there is merit (in neglecting) all but the essential phenomena and in studying thoroughly limiting cases in which different phenomena are controlling."*

One area of simplification used in the model was the development of a time to ignition expression for each material and it is this that is the topic of the following Chapter.

## 4.2 Background Theory

The heat flux level, $\dot{q}''_e$, exposed to a material from an experimental apparatus, such as the Cone Calorimeter, can be varied over a considerable range typically varying from around 0 to 110 $kWm^2$ for the standard bench-scale device. It is this change in radiated heat flux level that obviously plays a significant role in the time that a given material would take to ignite. An equation has been established in Chapter 2, which can be used to describe this time duration, namely equation (2.3). This equation is,

$$t_{ig} = \frac{\pi k \rho c \left(T_{ig} - T_0\right)^2}{4 \dot{q}''^2_e}$$

and is a solution of the one-dimensional heat conduction equation, using relatively simple initial and boundary conditions. The material properties are included in the terms "$k\rho c$" and $T_{ig}$, and the apparatus term is given by $\dot{q}''_e$. The ambient temperature, $T_0$, also introduces an environmental term.

The standard procedures for obtaining the $k\rho c$ and the $T_{ig}$ value for a material are available [34] but it has been shown [27] that there is a relatively large spread in the results, indicating that that reliability of the material properties determined is questionable. A further reason for not following the ASTM procedure was that bench-scale ignition data is sparse for many of

the materials studied within this research. Often only one heat flux level (typically 50 kWm$^{-2}$) is used in the experimental tests which is insufficient for the ASTM approach. It was therefore decided to use the experimental ignition data directly, instead of following the procedures outlined in [34]. All available ignition data pertaining to the materials studied here were therefore gathered and a simpler statistical analysis was used to derive an equation for determining the time to ignition at different heat flux levels.

From previous testing, results had shown that for cellulosic materials the value of $(T_{ig} - T_0)^2$ varies to a lesser extent than for the other variables, since $T_{ig}$ is typically in the range 350-450°C and the ambient temperature around 20°C. Note that the vast majority of materials tested for this report are cellulosic. In general, it can also be assumed that the conductivity, k, increases with density, ρ. From this, it was anticipated that the time to ignition may be satisfactory represented by some form of the equation,

$$t_{ig} = C\frac{\rho^{X1}}{\dot{q}''^{X2}_e} \qquad \ldots(4.)$$

where the constant C incorporated the less dominant variables of equation (2.3) and X1 and X2 were some powers associated with the two remaining dominant variables.

This simplified equation was investigated so that the "best" expression, when comparing the experimental to the calculated time to ignition values, could be incorporated into the developed flame spread model. Note that all the available materials from the experimental studies were used in this investigation.

# 4.3 Analysis

This type of analysis had been previously undertaken using only the "S" series materials [27]. The results from this report indicated that the equation,

$$t_{ig} = 113\left(\frac{\rho}{\dot{q}''^{2}_e}\right) \qquad \ldots(4.2)$$

produced very satisfactory results when compared to several other forms of the simplified time to ignition equation. This particular equation again showed similar satisfactory results in this research when applied to all the materials, namely the "S", "E" and "M" series. These results are shown below.

# 4.4 Results

The first step taken in the verification of equation (4.2) was to plot the materials so that the slope, C, of the trendlines, linking the points of each material, could be determined. The

time to ignition of the materials was plotted on the y-axis and the known density divided by the exposed heat flux value squared was plotted on the x-axis. Figure (4.1) shows this technique.

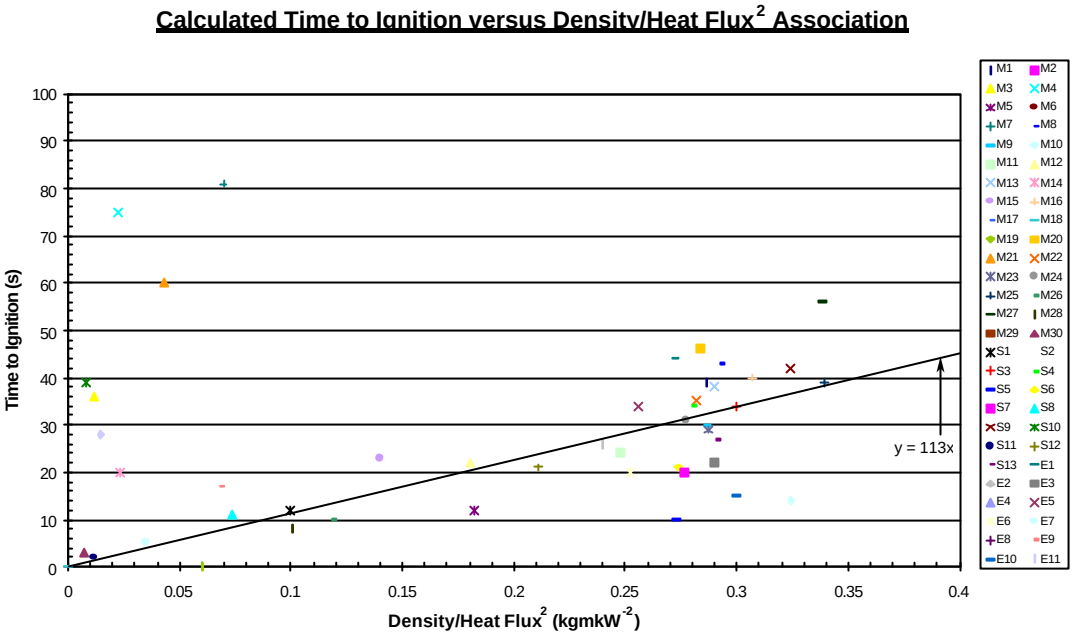


**Figure 4.1:** Time to Ignition, $t_{ig}$, versus $\frac{r}{\dot{q}_e''^2}$ Investigation

It can be seen from this Figure that the value of 113 for "C" in equation (4.2) fits the majority of the materials well. It is noted that "C" equal to 113 poorly approximates some of the synthetic materials, such as Polycarbonate and Polystyrene. These materials have relatively low density/heat flux$^2$ values and are located on the extreme left of Figure (4.1). Materials M2, M6, M29, E4 and E8 are also not shown on this figure as they have significantly larger time to ignitions or density/heat flux$^2$ values. Material M19 is the only material that does not ignite at the heat flux level examined by this Figure (50kWm$^{-2}$) so therefore lies on the x-axis.

Since the value of "C" had been verified, equation (4.2) could then be used to calculate the time to ignition, it was possible to determine the reliability of the estimation that this equation gave. The results, when this equation was compared to experimental values, are given in Figure (4.2).

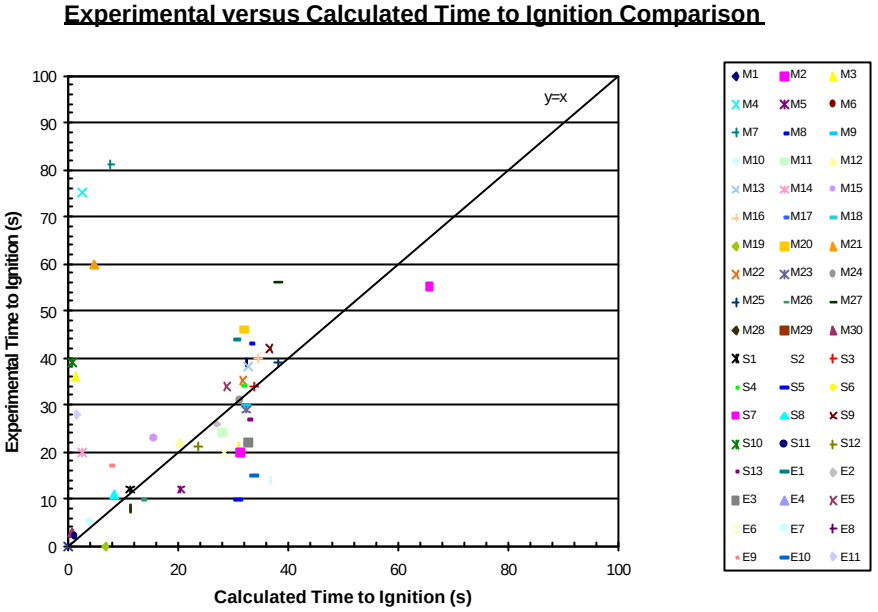


**Figure 4.2:** Time to Ignition @50kWm$^{-2}$ Comparison

Since equation (4.2) was to be used at heat flux levels other than just 50kWm$^{-2}$, further analysis was needed to ensure that the performance of the equation did not significantly deteriorate. This analysis required time to ignition data for the materials at different heat flux level. Such data from the experimental studies was limited for the materials investigated in this research but some analysis was possible. Ignition data was available for most of the "S" series materials at the 75kWm$^{-2}$ level and for the "E" series materials at the 35kWm$^{-2}$ level. Figures (4.3) and (4.4) show the results from the 35 and 75kWm$^{-2}$ investigation.

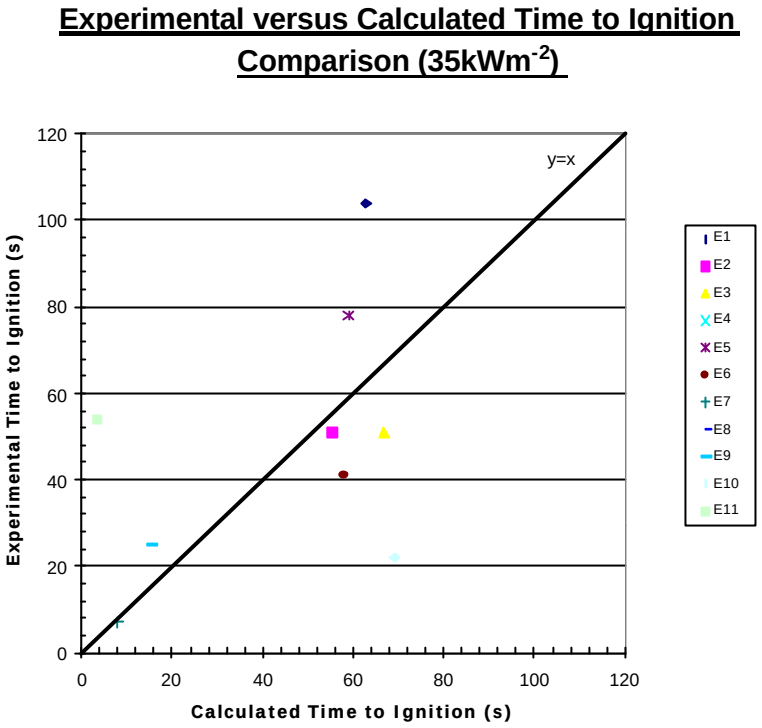


**Figure 4.3:** Time to Ignition @35kWm$^{-2}$ Comparison

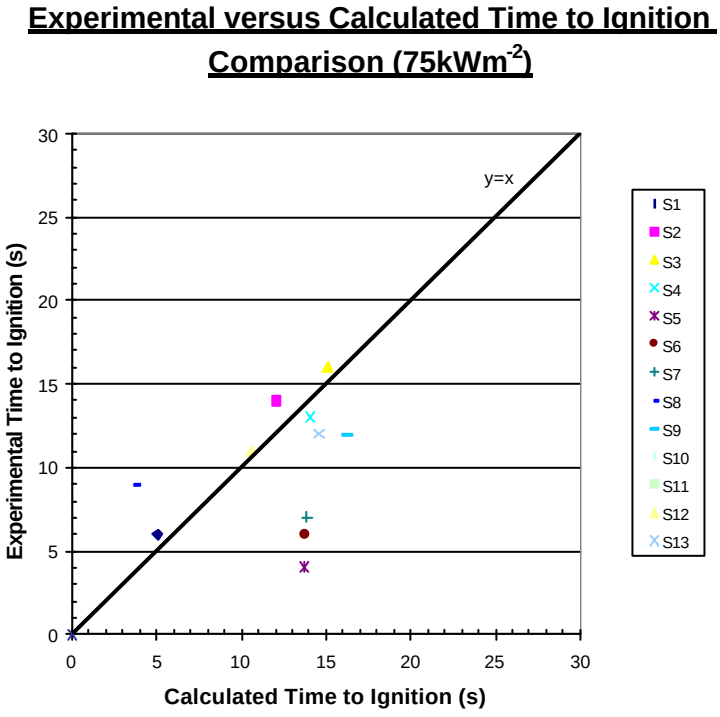


**Figure 4.4:** Time to Ignition @75kWm$^{-2}$ Comparison

The results of the experimental to calculation time to ignition comparison show that the

equation $t_{ig} = C\frac{\rho}{\dot{q}_e''^2}$ represents the materials relatively well for the investigated heat flux ranges. It is recommended that the "C" value of 113 should be used for the time to ignition calculation within the flame spread model used in this work.

# 4.5 Conclusions

This Chapter investigated the relationship between the time to ignition and the density/heat flux squared ratio in a attempt to develop a simplified equation for the time to ignition for various materials at different heat flux values. This analysis followed similar analysis carried out in [27]. The heat flux level of 50kWm$^{-2}$ was used for the main analysis on the "S", "E" and "M" series materials since almost all the materials ignited at this level and the data was available. In investigating the effect of different heat flux levels, 35 and 75kWm$^{-2}$ were used. Only the "S" series materials were used at the 75kWm$^{-2}$ level and the "E" series materials at the 35kWm$^{-2}$ level due to the limited quantity of data available.

It was found that the following equation gives satisfactory calculated times when compared to actual experimental values, especially for the cellulosic materials. This equation is,

$$t_{ig} = 113\left(\frac{\rho}{\dot{q}_e''^2}\right)$$

The next step in the research involved incorporating this equation into a model to determine the upward flame spread for different materials. The level of significance of the errors in the flame spread model resulting from the time to ignition expression simplification, as presented in this Chapter, could then be determined. The following chapters of this report are dedicated to this flame spread model development and analysis.

# 5. Analytical Model and Sensitivity Analysis

The upward flame spread expressions, described in Chapter 2, were inserted into a spreadsheet so that the phenomenon could be modelled. This Chapter describes the variables within this model and the sensitivity analysis theory.

## 5.1 Sample Spreadsheet Model

Figure (5.1) shows the arrangement of the analytical flame spread model in the MICROSOFT EXCEL spreadsheet. It should also be noted that the figure actually only shows the top part of the model, as the flame spread calculations are undertaken for approximately six hundred seconds (Post-ignition time).

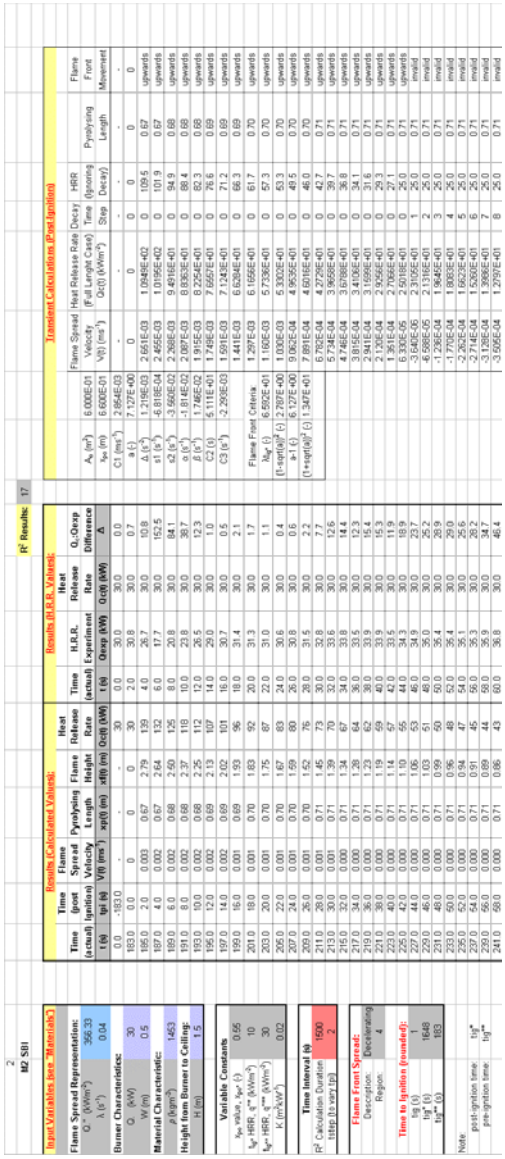

**Figure 5.1:** Analytical Flame Spread Model for a Typical Material

## 5.2 Spreadsheet Model Description

This flame spread analysis was undertaken in MICROSOFT EXCEL and utilised many different functions. One particular function that was used frequently was the IF statement. This statement specifies a logical test to perform and takes the following form,

$$\text{"IF" statement} = \text{IF}[\text{logical test}, \text{value if true}, \text{value if false}] \quad \ldots(5.1)$$

The following section describes the logic behind the inputs, outputs and transient calculations that were incorporated into the model. This spreadsheet calculated upward flame spread and then compared the results to the experimental data found from the "S", "E" and "M" studies. For a full description of the origin of the equations used in this model, the reader is directed to Chapter 2 - being the section on "Background Theory on Upward Flame Spread". The actual physical form of the spreadsheet model for a typical material can be seen in Figure (5.1).

### 5.2.1 Input Variables

Only six input variables and four tuning variables were needed in the model, which were used to describe such things as the material being investigated, the location of the material, the burner characteristics as well as some constants for the heat flux and time to ignition considerations. These variables are described below.

#### 5.2.1.1 Flame Spread Representation

***Heat Flux,*** $\dot{Q}''$***:***

This variable described the maximum or average heat flux level produced by the material in the Cone Calorimeter test, as described by the chosen heat release rate representation. Details of this representation technique can be found in Chapter 3. The units if this variable are $kWm^{-2}$. The value of this variable for each material investigated was obtained by a curve fitting technique from the Cone Calorimeter data and the results for all the materials can be found in Appendix A.

***Decay Coefficient,*** $\lambda$***:***

This value describes the materials' post-ignition exponential rate of decay of the heat released during burning. For a material represented by the constant heat release rate, this value should be set to zero but since this creates infinity errors in the model, a value of $1\times10^{-10}$ was used. Again, details of this representation technique are described in Chapter 3. The units if this variable are $s^{-1}$. The value of this variable for each material investigated

was obtained by a curve fitting technique from the Cone Calorimeter data and the results can be found in Appendix A.

#### 5.2.1.2 Burner Characteristics

***Burner Output,*** $\dot{Q}_b$ ***:***

The experimental set-ups of the individual full-scale testing methods govern the heat output of the burner. In the Room/Corner experiment the burner should be set to 100kW. This value remains at this level for the first ten minutes of the test, which was the time period of interest in the model. In the SBI test, the burner output reduces to 30kW, which is maintained throughout the entire test duration of 21 minutes.

***Burner Width,*** W***:***

The width of the burner is taken as the total distance that the burner is attached to the wall. Again, this value is dependent on the full-scale testing equipment. In the Room/Corner experiment a square burner is used and the burner width is taken as 0.34m (twice the burner side length of 0.17m). The SBI test incorporates a triangular burner that results in a total burner width of 0.5m (individual side length of 0.25m).

#### 5.2.1.3 Material Characteristics

***Density,*** $\rho$***:***

The density of a material is generally published as part of the results from Cone Calorimeter tests but the value of this variable has sometimes been difficult to establish. Some materials and test methods also require the use of a backing board, therefore significantly modifying the expected density value. In such instancies, the density value used in the model was either the published "effective" values or a value calculated by a taking a mass weighting of the individual densities of the components of the test sample. The units for density are $kgm^{-3}$.

#### 5.2.1.4 Height from the Burner to Ceiling

***Material Height,*** H***:***

This variable was needed to establish a limit to the distance that the pyrolysis front can spread on the material. In the SBI test, the upward flame spread is modelled only on the vertical wall of the specimen whereas the Room/Corner apparatus allows for the spread of the flame also across the ceiling. In this case, the height of the material is calculated by dividing the total assumed surface area of the material by the width of the burner. The total surface area was assumed to be the sum of the ceiling area and the wall area. The wall area equals the distance from the top of the burner/base of the flame to the ceiling multiplied by

the width of the pyrolysis front (assumed to be equal to the burner width). This calculation can be described by,

$$\text{Material Length} = \frac{\text{Total Pyrolyised Area}}{\text{Pyrolysis Width}} \qquad \ldots(5.2)$$

where the total pyrolyised area is given by

$$\text{Total Pyrolyised Area} = (\text{Ceiling Length} \times \text{Ceiling Width}) + (\text{Wall Height} \times \text{Burner Width}) \qquad \ldots(5.3)$$

The dimensions of the Room/Corner test compartment are 3.6m long, 2.4m wide and 2.4m high. Such dimensions and a burner width of 0.34m give a total height of approximately 27m. In the SBI apparatus the material height was 1.5m. The length assumes that the flame pyrolysis width remains constant.

#### 5.2.1.5 Tuning Variables

To allow for "model tuning", due to the unknowns, the following four constants were been developed. This tuning process, to account for the removed complexity, allows the development of simple models that focuses on the dominant phenomena as recommended by Williams [23].

The actual values that these four tuning variables took for the Room/Corner and the SBI scenarios were calculated by performing sensitivity analysis on the model. Details of this analysis can be found in section 5.3 and in Chapter 7.

The variable constants used in the model are described below.

***Fraction of Initial Pyrolysis Length,*** f***:***

In the applied theory, it is assumed that the initial heat flux, prior to the burning of the material, is constant across the gas burner flame height and zero below it (see Figure (2.2)). Since this assumption over-estimates the heat transferred from the burner flame to the material, this factor has been incorporated to more closely represent reality. The range of values of "f", due to this overestimation, was between 0 and 1.

***Heat Flux during Flame Spread,*** $\dot{q}''_{fs}$ ***:***

This factor is used to describe the heat flux level for the flame spread time to ignition value, $\tau$, used in the model equations once the material is burning. This was based on the result from the initial analysis in this research, which found a dependence on the assumed exposed heat flux for the time to ignition (see Chapter 4). The unit of this flux is $kWm^{-2}$.

***Pre-flame Spread Heat Flux,*** $\dot{q}''_{start}$***:***

Once the burner is started, the material being tested takes a period of time to ignite. The simplified time to ignition equation derived in the previous section is used to describe this time, $t_{start}$, and $\dot{q}''_{start}$ is the heat flux level used in this equation. The unit of this flux is again $kWm^{-2}$.

***Flame Area Coefficient,*** K***:***

This factor is burner location dependent and assumes values depending on the original flame spread experimental test method. The location of the burner in this research is either in a corner or on a wall. Values for K are typically in the range of 0.008 and 0.02. The units of K were $m^2kW^{-1}$ in the analytical model.

#### 5.2.1.6 Time Step Interval

***Time Step,*** $t_{step}$***:***

To allow for simple modification of the time step size between the calculation times ($t_{pi}$), this factor has been introduced. The value, in seconds, that this variable takes was generally dependent on the speed of the flame spread. Values between two and five seconds gave satisfactory detail to the model. This value must be the same as for the experimental data used in the model if a direct comparison is to be made.

## 5.2.2 Output Variables

The constructed spreadsheet model gives various outputs. The following section describes each of these outputs.

#### 5.2.2.1 Flame Front Spread

In the hope of adding clarity for the user of the model, in terms of the movement of the flame front, these two outputs have been included to determine the characteristics of the overall flame spread, as indicated by the regions I, II, III and IV in Figure (2.5).

***Region:***

In the Figure (2.5) four specific regions are identified. The IF statement, below, is used to determine which region the flame spread velocity is situated.

$$\text{Region} = \text{IF}\left[ l t \le \left(1-\sqrt{a}\right)^2, 1, \text{Region}_{a} \right] \qquad ...(5.4a)$$

$$\text{Region}_b = \text{IF}\left[ \tau t \le (1-a), 2, \text{Region}_c \right] \quad \text{...(5.4b)}$$

$$\text{Region}_c = \text{IF}\left[ \tau t \le \left(1+\sqrt{a}\right)^2, 3, 4 \right] \quad \text{...(5.4c)}$$

where "a" is described by equation (2.16) and $\tau$ by equation (5.7).

***Description:***

This calculation looks at the numerical result from the following "Region" calculation and gives a written statement on the flame spread velocity characteristic. The equation used for this calculation is,

IF("Region"=1,"Accelerating",IF("Region"=4,"Decelerating","Oscillating")) ...(5.5)

### 5.2.2.2 Time Variables

The follow section details the different time variables incorporated into the model. These times were rounded to the nearest second to simplify the calculation of the average $R^2$ value.

In the model calculations, two different ignition times have been used. The first ignition time, $t_{start}$, is used to describe the time it takes for the material to ignite. Before this time, the only heat that is being released is that from the gas burner. The second ignition time, $\tau$, is used in the transient calculations of the model and describes the post-ignition time behaviour of the material. For further information on the use of this variable, the reader is directed Section (2.2.2).

Figure (5.2) indicates the effects that these two ignition times can have on the heat release rate for a typical material.

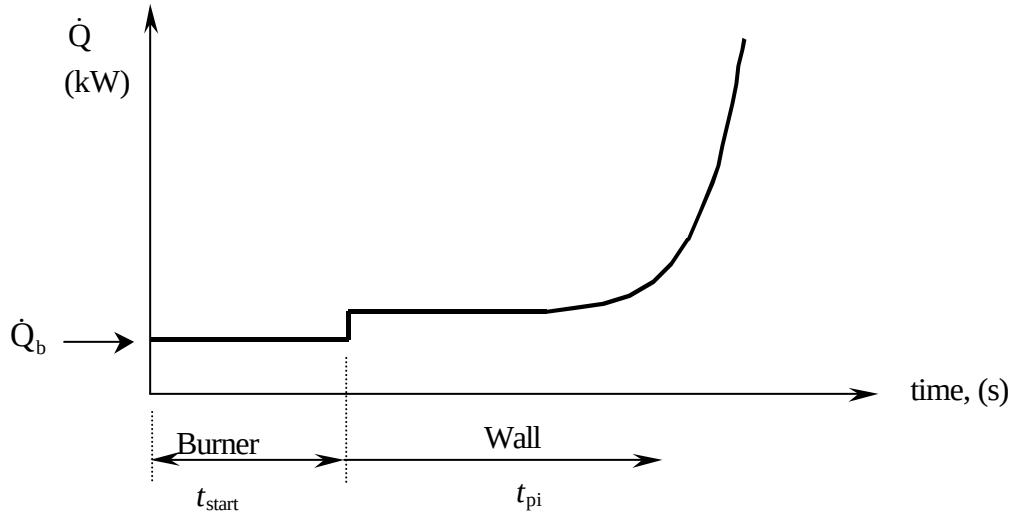


**Figure 5.2:** Characteristic Representation of the Different Ignition Times

As well as these time to ignition variables, other variables were included to describe the times during the calculations. All of these variables are described below.

***Burner Start Time to Ignition,*** $t_{start}$***:***

The burner start time to ignition value attempted to calculate the time between the actual burner at the experimental time "zero" (see section 3.5.2) and the time when the material ignited. For simplicity, it is assumed that the burner flame gives a constant irradiant heat flux to the material behind the burner over an area, $A_w$.

Previous research [17] has shown that using the total incident heat flux from the burner, ie. 100 or 30kW, to describe the time to ignition of the material underpredicts the time and improved values were obtained when the heat flux level was reduced. Because of these inaccuracies, the same general time to ignition approximation equation is used to describe is value. In the model, this equation is given as,

$$t_{start} = 113\left(\frac{\rho}{\dot{q}''^{2}_{start}}\right) \qquad \ldots(5.6)$$

***Flame Spread Time to Ignition, t:***

Once the burner has ignited the material, this value is used in the models transient calculations as described in the previous sections. The equation used in the model was,

$$t = 113\left(\frac{\rho}{\dot{q}''^{2}_{fs}}\right) \qquad \ldots(5.7)$$

***Time (Actual),*** $t$**:**

This time scale is the basis for the comparison of the data sets as it links the experimental and modelled times. The time used in the model equations is added to the time to ignition for the material. As a result, the following equation is used for the actual time, $t$, namely,

$$t = t_{pi} + t_{start} \qquad \ldots(5.8)$$

The first value for $t$ equals zero and subsequent values are the sum of the current time step and the time to ignition.

The total time for the Room/Corner model must not exceed ten minutes (600 seconds). This limitation is due to the experimental testing procedure of increasing the burner output from 100 to 300kW if the material has not reached flashover by this stage. This change in burner output does not occur in the SBI scenario, therefore there is no ten minute limitation in this model. It should also be noted that this is a pre-flashover model so if flashover occurs within this ten minutes, all the values after this event are also invalid.

***Time (Post Ignition),*** $t_{pi}$***:***

Once flame spread starts, the flame spread equations require a time, so the value of the variable $t_{pi}$ is used. This time is governed by two simple equations in the spreadsheet, one being for the initial time and the second for the times following this. The initial time value of $t_{pi}$ is negative as the burner starts before the material ignites ($t_{pi} = 0$). The heat release rate is set to the burner output value between the first and second $t_{pi}$ values. The $t_{pi}$ equations are,

Initial Time Value;

$$t_{pi} = -t_{start} \qquad \ldots(5.9)$$

Following Time Values;

$$t_{pi} = (0, 1, 2, 3...) \times t_{step} \qquad \ldots(5.10)$$

This equation is incorporated into the model so that the post-ignition (ie. when the flame spread phenomenon is being modelled) time step interval can be changed.

### 5.2.2.3 Calculated Values

The four variables below, as described in Section (2.2.2), are the main outputs of interest in this model. The HRR values were directly used to compare the validity of the model with the experimental results.

***Flame Spread Velocity,*** $V(t)$***:***

The general logic statements used for the calculation of this velocity, at given time $t_n$, are,

$$V(t) = \text{IF}(\text{"Flame Front Movement "="invalid "},0, V_1(t)) \qquad \ldots(5.11a)$$

$$V_1(t) = \text{IF}(\text{"Pyrolysing Length" ="H"},0, V(t_n)) \qquad \ldots(5.11b)$$

These equations calculate when the flame spread equations are still valid and that the calculation does not continue past the height of the wall, thus resulting in a zero velocity at this point. Any combustion of surfaces above the wall material of interest is not included in the model.

The statements above, are applied to the two equations (2.13) and (2.20) that calculates the flame spread velocity, $V(t)$, of the flame front. This velocity has units of $ms^{-1}$.

***Pyrolysing Length,*** $x_p(t)$***:***

The following statements are used to describe the length of the pyrolysis front at a given time, $t_n$.

$$x_p(t) = \text{IF}\left[\text{MIN}\left(V_c(t_0) : V_c(t_n)\right) < 0, x_p(t_{n-1}), x_{p1}(t_n)\right] \quad \ldots(5.12a)$$

$$x_{p1}(t_n) = \text{IF}\left[x_{pc}(t_{n-1}) \geq H, H, x_{p2}(t_n)\right] \quad \ldots(5.12b)$$

$$x_{p2}(t_n) = \text{IF}\left[\text{MIN}\left(x_{pc}(t_0) : x_{pc}(t_n)\right) < 0, \text{MAX}\left(x_p(t_0) : x_p(t_{n-1})\right), x_{p3}(t_n)\right] \quad \ldots(5.12c)$$

$$x_{p3}(t_n) = \text{IF}\left[\text{MAX}\left(x_{pc}(t_0) : x_{pc}(t_{n-1})\right) > x_{pc}(t_n), \text{MAX}\left(x_p(t_0) : x_p(t_{n-1})\right), x_{p4}(t_n)\right] \quad \ldots(5.12d)$$

$$x_{p4}(t_n) = \text{IF}\left[\left(x_{pc}(t_n) > H\right), H, x_{pc}(t_n)\right] \quad \ldots(5.12e)$$

The logic equations above ensure that the calculated pyrolysing length, $x_p(t)$, value is correct. The checks here are undertaken to see that no flame spread velocity (equation (5.12a)) or pyrolysing length (equation (5.12c)) values are negative. Checks are also carried out to ensure that the pyrolysis length doesn't decrease (equation (5.12d)), as this would imply that the material was becoming unburnt. Equations (5.12b) and (5.12e) ensure that the pyrolysis length does not become larger than the actual height of the wall, H.

The subscript "$t_0$" indicates the initial value and "$t_{n-1}$" indicates the previous value of the pyrolysing length. The subscript "c" added to the pyrolysing length symbol, $x_p$, and the velocity, V, indicates that the value is taken from the transient calculations. This particular subscript is also used in other variables calculated in the spreadsheet.

The logic equations above are applied to equation (2.23) or (2.24), which calculates the pyrolysing length, $x_p(t)$, of the flame. This length has units of metres, m.

***Heat release rate,*** $\dot{Q}_c(t)$***:***

The following logic statements are used to describe the heat release rate of a material at a given time, $t_n$.

$$\dot{Q}_c(t) = \text{IF}\left["\text{Flame Front Movement}" = "\text{invalid}", \dot{Q}_{c*}(t_n)e^{-lt} + \dot{Q}_b, \dot{Q}_{c1}(t_n)\right] \quad \ldots(5.13a)$$

$$\dot{Q}_{c1}(t_n) = \text{IF}\left[x_p(t_n) = H, \dot{Q}_{c*}(t_n)e^{-lt} + \dot{Q}_b, \dot{Q}_{c2}(t_n)\right] \quad \ldots(5.13b)$$

$$\dot{Q}_{c2}(t_n) = \text{IF}\left["\text{Decay Time Step}" = 0, \dot{Q}_c(t_n) + \dot{Q}_b, \dot{Q}_{c*}(t_n)e^{-lt} + \dot{Q}_b\right] \quad \ldots(5.13c)$$

The subscript "*" on $\dot{Q}_c(t)$ indicates that it is a transient calculation value of the heat release rate value where the pyrolysing length, $x_p(t)$, has stopped. This value is needed so

that the λ decay of the heat release rate can start once the upward flame spread has stopped.

These statements are applied to equations (2.26) or (2.27) which calculates the heat release rate, $\dot{Q}_c(t)$, of the flame. The unit for this variable is kW.

***Flame Height,*** $x_f(t)$***:***

This variable was calculated after the heat release rate as this variable is used in the calculation. The flame height is governed by the following simple equation;

$$x_f(t) = K\dot{Q}_c(t) \qquad \ldots(5.14)$$

#### 5.2.2.4 Experimental Results

The experimental results collected for this research from the Room/Corner and SBI tests are given in these columns of the spreadsheet and are described below.

***Time (actual),*** $t_{exp}$***:***

This column contains the time data from the experimental studies following the data standardisation outlined in section (3.5.2).

***Experimental Heat release rate,*** Exp. HRR***:***

Again the data given here was directly taken from the experiments after some modifications were undertaken. These changes are detailed in section (3.5.2). The unit of this variable is kW.

#### 5.2.2.5 Comparison Result

A value was needed that could describe the degree of fit of the calculated to the experimental heat release rate results. This value was used as the input variable to the sensitivity analysis of the model which was undertaken in @RISK. The following variables and equations were used in the determination of this value,

***Difference,*** δ***:***

An $R^2$ approach was used in this analysis. This method was broken down into two steps. Firstly, the squares of the differences were calculated and then these values were averaged and square rooted in the second step. The equations for the first step, as described by this variable, δ, are shown below, at the given time period, $t_n$,

$$\boldsymbol{d} = \mathrm{IF}\left[\boldsymbol{d}_1, 0, \left(\dot{\mathrm{Q}}_{\mathrm{exp}}(t_{\mathrm{n}}) - \dot{\mathrm{Q}}_{\mathrm{c}}(t_{\mathrm{n}})\right)^2\right] \quad \ldots(5.15a)$$

$$\boldsymbol{d}_1 = \mathrm{OR}\left[\dot{\mathrm{Q}}_{\mathrm{exp}}(t_{\mathrm{n}}) = 0, t_{\mathrm{n}} > 600, \mathrm{AND}\left(\dot{\mathrm{Q}}_{\mathrm{c}}(t_0 : t_{\mathrm{n}}) > 1000, \dot{\mathrm{Q}}_{\mathrm{exp}}(t_0 : t_{\mathrm{n}}) > 1000\right)\right] \quad \ldots(5.15b_1)$$

$$\boldsymbol{d}_1 = \mathrm{OR}\left[\dot{\mathrm{Q}}_{\mathrm{exp}}(t_{\mathrm{n}}) = 0, t_{\mathrm{n}} > 2000, \mathrm{AND}\left(\dot{\mathrm{Q}}_{\mathrm{c}}(t_0 : t_{\mathrm{n}}) > 1000, \dot{\mathrm{Q}}_{\mathrm{exp}}(t_0 : t_{\mathrm{n}}) > 1000\right)\right] \quad \ldots(5.15b_2)$$

The logic applied to these equations were,

- Limiting the experimental heat release rate data when the values became zero - once the end of the experimental data was reached, no comparison is needed.
- Limiting the time period of interest – only the first 600 seconds of the Room/Corner scenario model can be used to describe the flame spread behaviour of the material in question due to the burner output change. For this scenario, equation ($5.15b_1$) was used. For the SBI scenario, this burner output change does not occur so the 600 second limit was extended to 2000 seconds, so equation ($5.15b_2$) replaced ($5.15b_1$). This arbitrarily set limit was chosen as the flame spread movement had occurred by this time.
- Limiting the maximum heat release rate to 1000kW – once the flashover occurs, assumed to be at a HRR of 1000kW, the model was no longer valid.

If "true", all of these logic steps resulted in a zero value for $\delta$, which removed the influence on the comparison for the particular time period in question.

***$R^2$ Results:***

The second part of the comparison equation gave the actual result that was used in the sensitivity analysis. It was this value that was minimised to calculate when the experiment and calculated values had the closest fit. The equation used is shown below and includes the sum of the difference values, $\delta$, from the first time period, $t_0$, to the final time, $t_{\mathrm{n}}$. The units of this term is kW.

$$\mathrm{R}^2 \text{ Result} = \mathrm{SQRT}\left[\frac{\mathrm{SUM}(\boldsymbol{d}_0 : \boldsymbol{d}_{\mathrm{n}})}{\mathrm{COUNTIF}((\boldsymbol{d}_0 : \boldsymbol{d}_{\mathrm{n}}), "> 0")}\right] \quad \ldots(5.16)$$

## 5.2.3 Transient Variables

Transient calculations were used in the model, as seen in Figure (5.1), primarily to keep the equations in each cell to a manageable size. The secondary reason was that some

equations, such as that describing the heat release rate, were rather complex which gave no option other than using these extra transient columns.

While the inclusion of such columns removes the "cleanliness" of the model, they provide extra insight into the specific behaviour/values of parts of the theory at the given calculated times. Some of these variables are detailed below.

#### 5.2.3.1 Decay Time Step, $t_{ds}(t_n)$

This variable is used in the heat release rate calculation. It's purpose is to count the number of the time periods once the pyrolysis front has reached the top of the material. The logic used is given by the equations below, at time, $t_n$,

$$t_{ds}(t) = \text{IF}\left[x_p(t_n) = H, \text{COUNTIF}\left(x_p(t_n) = H\right), t_{ds1}(t_n)\right] \quad \ldots(5.17a)$$

$$t_{ds1}(t_n) = \text{IF}\left[\text{FFM} = \text{"Upwards"}, 0, t_{ds}(t_{n-1}) + 1\right] \quad \ldots(5.17b)$$

#### 5.2.3.2 HRR(No Decay), $\dot{Q}_{ND}(t)$

This variable is used in conjunction with the Decay Time Step, $t_{ds}(t_n)$, in the heat release rate calculation. The value of this variable never decreases and it remains constant once the pyrolysis front starts to mathematically decrease. The governing equations are, at time, $t_n$,

$$\dot{Q}_{ND}(t) = \text{IF}\left[x_p(t_n) - x_p(t_{n-1}) \le 0, \dot{Q}_{ND}(t_{n-1}), \dot{Q}_{ND1}(t_n)\right] \quad \ldots(5.18a)$$

$$\dot{Q}_{ND1}(t_n) = \text{IF}\left[\dot{Q}_{c*}(t_{n-1}) \ge 1\times E + 300, 1\times E + 300, \dot{Q}_{ND2}(t_n)\right] \quad \ldots(5.18b)$$

$$\dot{Q}_{ND1}(t_n) = \text{IF}\left[\dot{Q}_{c*}(t_{n-1}) \le -1\times E + 300, -1\times E + 300, \dot{Q}_c(t_n)\right] \quad \ldots(5.18c)$$

The final two equations above ensure that the upper and lower number limits[1] in MICROSOFT EXCEL are not reached, therefore removing such possible calculation limit errors.

#### 5.2.3.3 Flame Front Movement, FFM.

The description of the movement of the flame front, given by the equations below, are used by most of the other variables in the model to ensure that the movement is still valid. These equations firstly check to see that, at time $t_n$, the velocity is positive, then that the pyrolysis front isn't at the top of the material and finally that the pyrolysis front direction is still

[1] MICROSOFT EXCEL upper and lower number limit is $1\times10^{307}$ and $-1\times10^{307}$ respectively

upwards (positive).

$$FFM(t) = IF\left[MIN\left(V\left(t_0^*\right): V\left(t_n^*\right)\right) < 0, \text{"invalid"}, FFM_1\left(t_n\right)\right] \quad \ldots(5.19a)$$

$$FFM_1\left(t_n\right) = IF\left[x_p\left(t_n\right) = H, \text{"stopped"}, FFM_2\left(t_n\right)\right] \quad \ldots(5.19b)$$

$$FFM_2\left(t_n\right) = IF\left[MAX\left(x_p\left(t_0^*\right): x_p\left(t_n^*\right)\right) > x_p\left(t_n^*\right), \text{"backwards"}, \text{"upwards"}\right] \quad \ldots(5.19c)$$

# 5.3 Model Assessment

Once the model had been set-up and the comparison materials determined, a tuning and performance assessment of the model was undertaken. This assessment involved the determination of the best values for the four tuning variables. This task is described below and the results of the comparison are given in Chapter 7.

## 5.3.1 Background Information

To determine the variation that would occur in the results of the analytical flame spread model when the values of the different variables were modified, sensitivity analysis was undertaken. This analysis was performed in a risk analysis package called @RISK. It was the desire to pursue such analysis that was instrumental in the initial creation of the analytical, as opposed to a numerical, model that was developed in this research. The following section describes the sensitivity analysis undertaken and the results of the analysis are given in Chapter 7.

### 5.3.1.1 Background to Sensitivity Analysis and @RISK

***Sensitivity Analysis***

In any modelling approach, many different variables are used to describe the outputs and for most situations and these variables are often not known with complete certainty. These outputs will therefore include a degree of uncertainty.

Often, this uncertainty is small, which generally occurs when all the variables can be simply described or are well known, but it can often become very significant when a complex phenomenon is being described. Uncertainty in the values of the input variables can also arise due to their values being based on either objective or subjective decisions.

For the uncertainty of a model to be quantified, all the possible values of the variables which influence the outputs need to be investigated. This process is termed “Sensitivity Analysis”.

One technique that can be used to perform sensitivity analysis is to describe the input

variables by probability distributions. There are many different types of probability distributions available which can describe the range of possible values and their likelihood of occurrence for each input variable.

One program that can be used for this type of sensitivity analysis is @RISK. This program was utilised in this analysis so that the uncertainty variables within the upward flame spread model could be assessed.

***@RISK***

@RISK is used in conjunction with either Lotus 1-2-3 or Microsoft Excel (used in this research) and applies a quantitative procedure that determines the likely range of outcomes for a given scenario. In general, the technique encompasses:

1. **Developing a Model**, by defining the activity in a spreadsheet.
2. **Identifying the Uncertainties**, by providing probability distributions for the models uncertain input variables.
3. **Analysing the Model by Simulation**, which determines the values and distribution(s) of the selected output(s). This is accomplished by calculating the summary statistics of many iterations of the model. Each iteration selects a different input value governed by the distribution associated to the particular input variable.

The results from the simulation of the model can then be used to determine the most appropriate course of action that should next be taken. This method clarifies the behaviour of the model to any changes in the values of the input variables.

#### 5.3.1.2 Simulation Inputs

The purpose of the simulation was to determine the values of the four particular tuning variables that are incorporated in the flame spread model. A range of possible values for these input variables was known from previous research and by examining their specific definitions. These variables are described earlier in Section (5.2.1.5) and the values and distributions that they initially took in the analysis is described below.

***Fraction of Initial Pyrolysis Length,*** f***:***

This variable is used to reduce the heat transfer overestimation that occurs in the initial phases of the model. The range of values that this variable is assumed to take is between 0.05 and 0.95.

As previously mentioned, @RISK requires that the variables be given a distribution that describes their uncertainty. The choice of these distributions was made difficult due to the complexity of the model. This complexity is not only in terms of the phenomenon that is being analysed but also in terms of the interaction that occurs between the equations. Since

the influence that each variable has is uncertain, a uniform distribution has been chosen for all four input variables. The shape of this simple distribution function for an arbitrary variable is given in Figure (5.3).

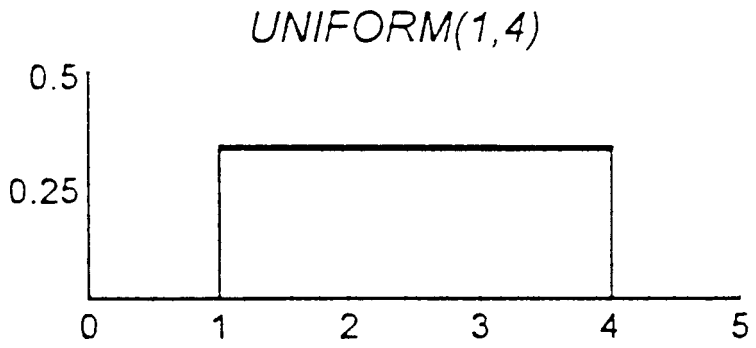


**Figure 5.3:** A Typical Uniform Probability Distribution [28]

It is assumed in using this function that the probability of obtaining any value throughout its range is equal.

***Heat Flux for Flame Spread,*** $\dot{q}''_{fs}$ ***, and Pre-flame Spread Heat Flux,*** $\dot{q}''_{start}$ ***:***

These time to ignition factors are assumed to be covered by a range of between 5 and 70 $kWm^{-2}$. Again, a uniform distribution was applied to these variables.

***Flame Area Coefficient, K:***

This factor is burner location dependent and is assumed to have values ranging from between 0.003 to 0.03 $m^2kW^{-1}$. This area coefficient is also given a uniform distribution.

**Summary**

The values that were used in the initial analysis of the flame spread model are summarised in Table (5.1),

**Table 5.1:** Flame Spread Model Input Variables

| Input Variable | Units | Values | | |
|---|---|---|---|---|
| | | Minimum | Maximum | Distribution |
| f | (-) | 0.05 | 0.95 | Uniform |
| $\dot{q}''_{fs}$ | $kWm^{-2}$ | 5 | 70 | Uniform |
| $\dot{q}''_{start}$ | $kWm^{-2}$ | 5 | 70 | Uniform |
| K | $m^2kW^{-1}$ | 0.003 | 0.03 | Uniform |

#### 5.3.1.3 Simulation Outputs

The main reason for performing the sensitivity analysis was to optimise the tuning variables so that the heat release rate calculated in the model would fit the experimental data to its best ability. Because of this, the output of particular interest was the comparison equation, "$R^2$ Results". This value was calculated for the each individual materials as well as being averaged over all of the materials. The philosophy used in this optimisation was to;

> "Obtain the four input variable values, applied to all the materials, when the averaged $R^2$ value was minimised."

These values would therefore indicate the best fit of all the materials to their individual experimental data for the given experimental scenario.

The technique used in @RISK from the post-simulation summary data to implement this philosophy was to;

1. Sort the raw simulation results of the averaged $R^2$ value in ascending order so that the minimum value could be obtained, as well as at which iteration it occurred.
2. View the data from the iteration, found in Step 1, and determine the values of the four input variables.

#### 5.3.1.4 Simulation Settings

@RISK allows various settings to be chosen for a simulation. These options include varying,

- the number of iterations performed,
- the sampling type,
- convergence monitoring parameters, and
- the (random) seed number generation setting.

During the model simulation the following settings and values were chosen,

**Table 5.2:** Simulation Settings Summary

| Setting | Values: RC[1] Scenario | Values: SBI[2] Scenario |
|---|---|---|
| Iteration Number | 5000 | 5000 |
| Seed | 1 | 1 |
| Sampling Technique | Latin Hypercube | Latin Hypercube |
| Standard Recalc. | Expected Value | Expected Value |
| Convergence Limit | Every 100 iterations | Every 100 iterations |

[1] The Room/Corner scenario tests involving the "S", "E" and "M" series materials.

[2] The SBI scenario test involving the "M" series materials.

The value of the iteration number was chosen so that sufficient accuracy of the results could be achieved. If too few iterations were chosen, the level of uncertainty of the results would have increased significantly.

The value chosen for the seed determines the repeatability of the results obtained from @RISK. The program uses a complex algorithm to generate the random numbers for choosing values from the distribution function used in the simulation. The seed value determines the sequence that this algorithm follows. By setting a non-zero seed value, the same "random" sequence will occur during each iteration whereas a zero seed value produces a new, random, seed every iteration therefore removing any future repeatability of the analysis.

# 6. NUMERICAL MODEL

The analytical model was not just evaluated against experimental data. An evaluation against a numerical model not only provided the opportunity to see how the well the analytical model corresponded to the numerical model but it also gave the opportunity to further evaluate the numerical model.

The numerical model used for the evaluation was the zone model "WPI/Fire Code", modified to incorporate flame spread [12]. This flame spread model differed only slightly from that used in the analytical model, as the flame spread expressions were developed using the Euler method instead of Laplace Transformations. Both models are based on the same fundamental equations.

## 6.1 The Flame Spread Algorithm

Instead of solving equation (2.5) using the Volterra type integral in equation (2.11), Baroudi et al [3] integrated equation (2.5) directly using the first order forward Euler method [10]. Thus equation (2.5) became,

$$x_p(t_{i+1}) = \left(1 - \frac{\Delta t_{i+1}}{t_{ig}}\right) x_p(t_i) + \left(\frac{\Delta t_{i+1}}{t_{ig}}\right) x_f(t_i) \qquad \ldots(6.1)$$

where

$$\Delta t_{i+1} = t_{i+1} - t_i \qquad \ldots(6.2)$$

The velocity of the pyrolysis front at $t = t_{i+1}$ can be expressed as the mean velocity between $x_p(t_{i+1})$ and $x_p(t_i)$, shown in equation (6.3).

$$\frac{dx_p(t_{i+1})}{dt} \approx \frac{x_p(t_{i+1}) - x_p(t_i)}{\Delta t_{i+1}} \qquad \ldots(6.3)$$

The integral in equation (2.10) was approximated using the trapezoidal integration rule [10] and thus the total HRR can be written as:

$$\dot{Q}_{tot}(t) = \dot{Q}_b + x_{p0} W \dot{q}''(t) + W \sum_{p=1}^{p=i} \dot{q}''(t - t_p) \frac{x_f(t_p) - x_p(t_p)}{t_{ig}} w_p \qquad \ldots(6.4)$$

where

$$t_{p=1} = t(0) \text{ and } t_{p=i} = t$$

The weight $\omega_p$, which comes from the trapezoidal integration, equals $\frac{\Delta t_{i+1}}{2}$ except when $p = 1$ and $p = i$, where $\omega_p$ equals $\Delta t_{i+1}$. This was the equation used in the numerical model *Thimes* [3] along with the equations for the flame height and the pyrolysis front addressed in the section above. There was also the condition that when the flame height was shorter than the pyrolysis height, the flame height was set equal to the height of the pyrolysis front, ie. when,

$$x_f(t_{i+1}) < x_p(t_{i+1})$$

then set: $$x_f(t_{i+1}) = x_p(t_{i+1})$$

This accounted for the coincidence of the flame and pyrolysis heights during the periods when the flame was receding [3]. This algorithm was part of the computer program *Thimes* developed by Baroudi et al [3].

## 6.2 The Zone Model - WPI/Fire Code

As mentioned earlier, the flame spread algorithm was incorporated into the WPI/Fire Code zone model. The WPI/Fire Code is a single room zone-type compartment fire model prepared at the Worcester Polytechnic Institute. It is based on the HARVARD fire model [24] and the FIRST fire model [25] but had additional physics options developed by Beller [4] and Caffrey [8]. Beller [4] provides physics options for:

1. Calculating ceiling heat transfer based on the presence of a ceiling jet
2. Momentum driven mass flow through a ceiling vent

Caffrey [8] provides physics options for evaluating the formation of a hot spot on the wall or in a ceiling [1]. The following section is a very brief summary of the physical model provided by the WPI/Fire Code.

The WPI/Fire Code models a single room as having two gas layers, a cool lower layer at ambient conditions, and a hot upper layer that forms from the fire plume.

The basic model was a deterministic and time dependent solution of simplified energy and mass conservation equations. The model also provided for formation of a fire plume over the burning object. It calculated the heat transfer between the fire, the walls, the ceiling and other objects. It provided the mass flow through multiple vents in the wall. It also determined the environmental conditions in the room including layer temperatures and toxic gas species concentration.

The three types of burning objects could be simulated were,

1. A fire growing on a horizontal surface of polyurethane

2. A pool fire
3. A liquid /gas fuel burner fire

Each object was limited by the oxygen available. An object also may not be initially burning, but ignition occurs once the calculated surface temperature reaches a user-defined ignition temperature.

The fire plume above an object entrains air from the lower layer and carries it into the upper layer due to buoyancy resulting in a hotter, less dense gas. The model provides for selection of one of six empirical fire plume models [5], namely,

1. Morton, Taylor, Turner (line source)
2. Morton, Taylor, Turner (point source)
3. McCaffrey
4. Zukoski
5. Delichatsios/FM
6. Tokunga, Sakai, Kawagoe, Tanaka and Hasemi

The plume entrainment in the model was also able to be changed by specifying whether the object is located away from all walls, against a wall or in a corner.

The upper layer was formed when the ceiling stops the gases of the fire plume. The basic program assumed, contrary to real fire dynamics, that the plume stops at the layer interface. The convective heat transfer to the upper walls and ceiling from this layer was assumed to be from a mass at a uniform temperature. This may under-predict the convective heat transfer in the early stage of the hot layer formation. The selection of Beller's [4] alternative physics routine for extended ceiling convective heat transfer accounted for the presence of a ceiling jet and increased the calculated convective heat transfer from the upper layer to the walls and the ceiling.

Wall vents are treated differently from the ceiling vents. Wall vents allowed for the natural outflow of hot gases and inflow of supply air, or both, depending on its position relative to the layer interface. Natural flow is driven by the pressure differential and mass conservation. By selecting Beller's ceiling vent physics option, a momentum driven mass flow through a ceiling vent could be approximated [1].

## 6.3 Flame Spread Algorithms Incorporated into the WPI/Fire Code

Since the WPI/Fire Code used the mass loss rate instead of the heat release rate as input data, several changes had to be made, partly to the flame spread algorithm and partly to the zone model. One correction that was made in [12] was that the flame spread algorithm created a table of the mass loss rate instead of the rate of heat release. This mass loss rate table is further used as input to the WPI/Fire Code. This is described in Figure (6.1).

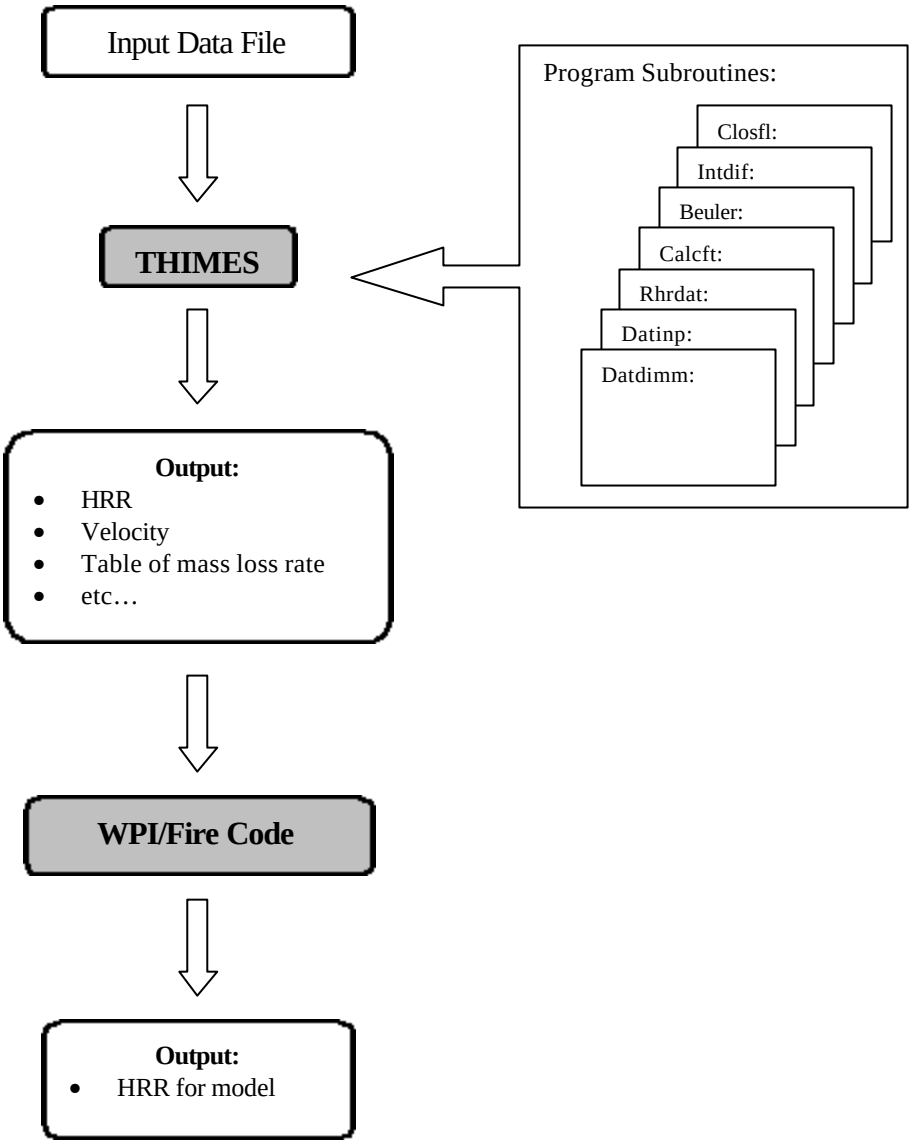


**Figure 6.1:** Flowchart describing the incorporation of the flame spread model, Thimes, into the zone model, WPI/Fire Code

# 6.4 Input Variables

All the input variables that the flame spread model uses are stored in an input data file. An example of such a file is shown in Appendix C. Some of the input data variables will be further discussed here. The values of the input data variables for the numerical model are the same as the ones used for the analytical model and can be found in Chapter 5.

**Flame Height Correlation Factor, K:**

Since Baroudi et al [2] expressed K in the units of $mkW^{-1}$, but the expressions used in the analytical model expressed this in $m^2kW^{-1}$, the value of K used in the numerical model had to be divided by the burner width for both the Room/Corner and the SBI simulations.

The value of this variable varied depending on the scenario, ie. the value depends on whether the fire is against a wall or in a corner. A sensitivity analysis made in [12] showed that this value should be chosen carefully since a small change in the value would have great impact on the flame spread velocity. A more sophisticated sensitivity analysis can be found in Chapter 7.

**Flame Spread Time to Ignition, t :**

The time to ignition varied with the external heat flux for each specific material used in the experiment. The value of the time to ignition is also scenario dependent just as the K value. The heat flux behind the flame in a corner scenario is greater than in a wall scenario. The values for $\tau$ were the same as those used in the analytical simulations and are given in Appendix A.

**Burner Characteristics:**

There are several variables describing the burner characteristics in the numerical model. $W_{burner}$ was the burner width. In a corner scenario the value of this variable was the sum of the width of the two sides that are against the walls. $\dot{Q}_b$ was the burner heat release rate per unit width. $\Delta H_c$ was the heat of combustion for the gas used in the burner.

**Cone Data:**

This material behaviour data from the Cone Calorimeter experiments are presented in two columns as seen in Appendix C (RHR curve values). One column is for the time step and the other for the heat release rate per unit area. The same heat release rate data from the Cone Calorimeter was used as in the analytical simulations.

# 6.5 Output Data

The output data from the WPI/Fire Code is of the same form as from most zone models e.g. layer height, rate of heat release, gas temperatures etc. The main variable used for the comparison is the rate of heat release in the enclosure. A typical part of an output data file time step is shown in Appendix C.

The full heat release rate results from the simulations are given in Appendices D, E, F and G, where they are also compared to the full-scale experimental data.

# 7. RESULTS

In this Chapter, the results from the flame spread model sensitivity analysis will be summarised. These results were obtained from the calculated analytical and numerical models from the following scenarios and material collections:

- Room/Corner scenario,
  - 13 "S" series materials
  - 11 "E" series materials
  - 23 "M" series materials
- SBI scenario,
  - 28 "M" series materials

Further information on each material collection can be found in Chapter 3 and Appendix A. Once the four tuning variables were found, the measured heat release rates from these experiments were compared to the equivalent experimental scenario for validation of the model.

## 7.1 Room/Corner Model Analysis

The program @RISK provided the basis for the determination of the four tuning variables that were used in both the analytical and numerical flame spread models. The final values for these variables were determined by a two step process. Firstly, the program ran the simulations for each scenario, namely the Room/Corner and the SBI, for the complete set of materials for which the tuning variables were to be used to describe. From this analysis, final tuning variable values were determined. This second step involved the fine tuning of the values so that they had a realistic quantity of significant figures while still ensuring that this small change did not effect the accuracy of the model.

### 7.1.1 Sensitivity Analysis of the Tuning Variables

Once the Room/Corner model was developed, @RISK was used to find the values of the four tuning variables that produced the closest agreement between the calculated and the experimental data. @RISK initially gave the Fraction of Initial Pyrolysis Length variable, f, a value of 0.18, the Heat Flux for Flame Spread variable, $\dot{q}''_{fs}$, a value of 30.4, the Pre-flame Spread Heat Flux variable, $\dot{q}''_{start}$ a value of 47.2 and the Flame Area Coefficient, K, a value of 0.018.

### 7.1.2 Final Optimised Results and Comparisons

Final tuning of these four variable values was then undertaken. This step only produced slightly different values for $\dot{q}''_{fs}$ and $\dot{q}''_{start}$. The final results for the Room/Corner scenario are

presented in Table (7.1),

**Table 7.1:** Minimum Input Values for the Room/Corner Model

| Input Variable | Value | Unit |
|---|---|---|
| F | 0.18 | (-) |
| $\dot{q}''_{fs}$ | 30 | $kWm^{-2}$ |
| $\dot{q}''_{start}$ | 50 | $kWm^{-2}$ |
| K | 0.018 | $m^2kW^{-1}$ |

The corresponding correlation analysis of the model investigated the effect that modifying the four tuning variable values by ±10% had on the $R^2$ value for all the materials. It was found that any change in the variable values increased the $R^2$ value which justified the choice of the variable values (to produce a minimum $R^2$ value). This trend can be seen in Figure (7.1).

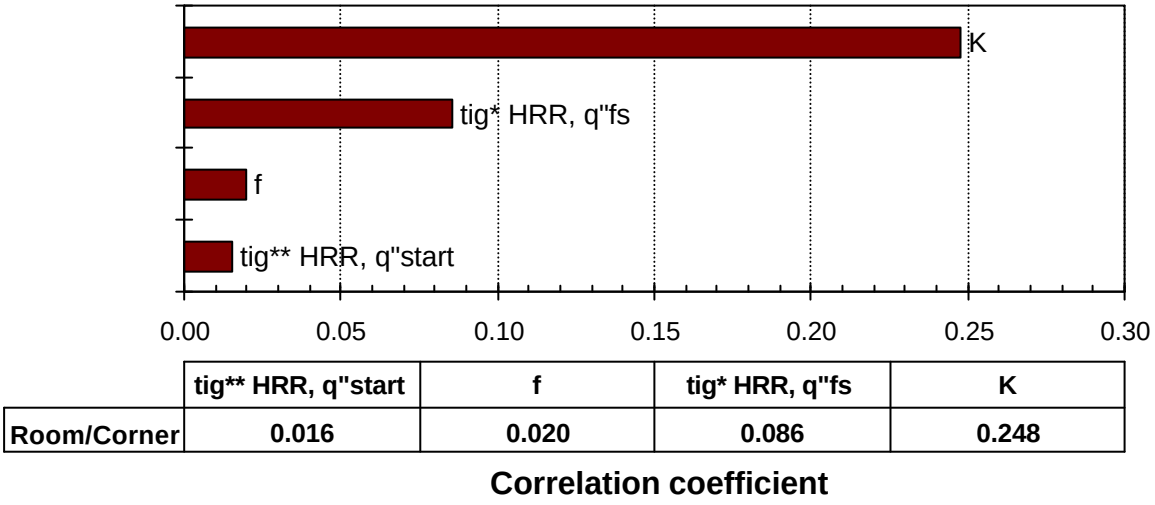


**Figure 7.1:** $R^2$ Correlation Values for the Room/Corner Scenario

This analysis also showed that the most sensitive value to any variation was the Flame Area Coefficient, K. It's correlation value was almost three times the next closest variable, namely $\dot{q}''_{fs}$. The correlation values for the Pre-flame Spread Heat Flux variable, $\dot{q}''_{start}$, and the Fraction of Initial Pyrolysis Length variable, f, were found to have a smaller influence on the value of the average $R^2$ value for the Room/Corner model.

Since the time that a material will take to go to flashover in a compartment is very important, a comparison between the experimental and calculated (analytical and numerical) time to flashover was made. Flashover is assumed to occur when the heat release rate exceeds 1000kW. This comparison is made in Figure (7.2) overleaf.

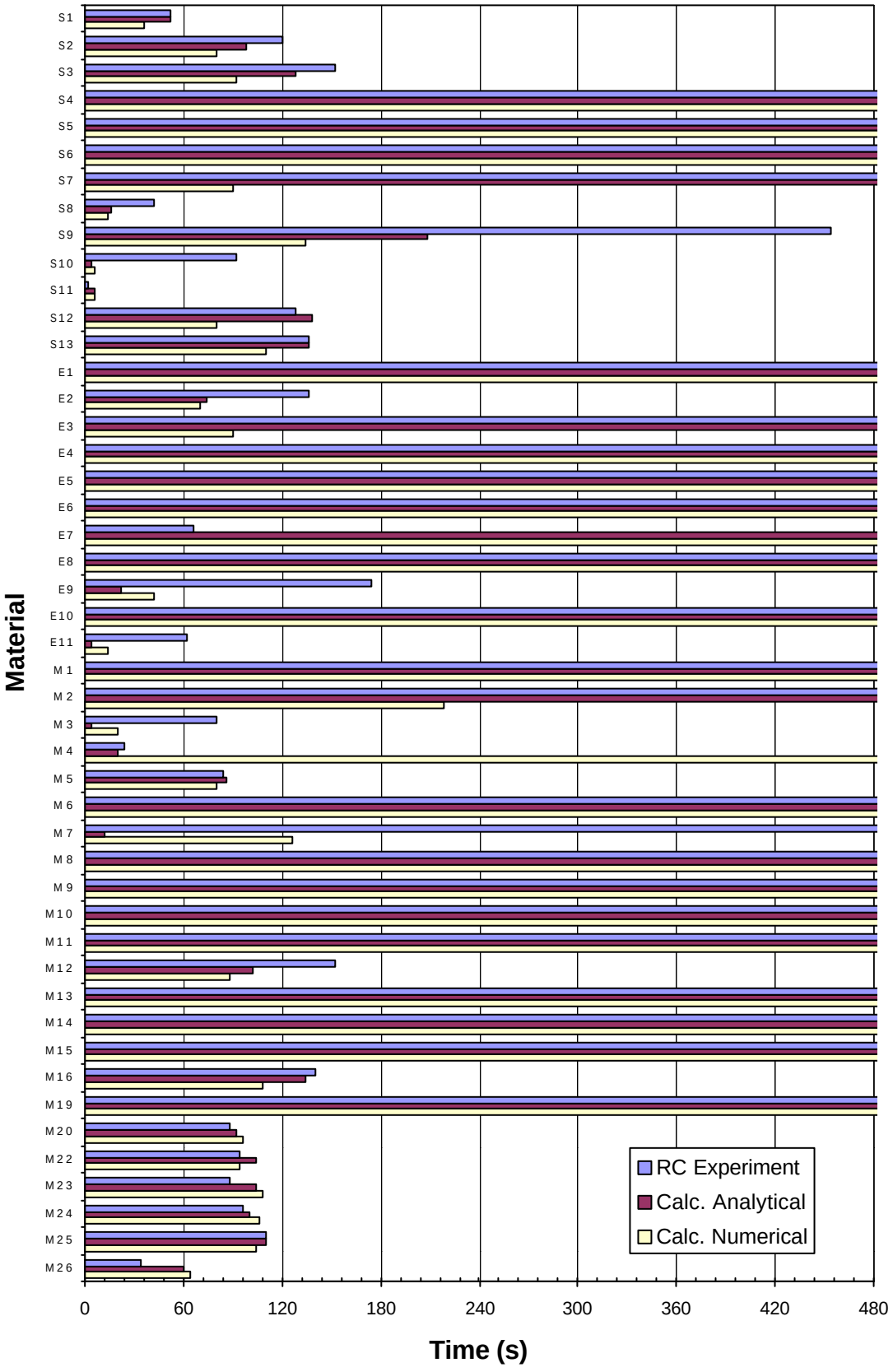


**Figure 7.2:** Room/Corner Scenario Time to Flashover Comparison

In Figure (7.2), some materials can be seen that did not go to flashover within the initial 100kW (burner output) phase of the experimental procedure. It can be seen that the model was generally very good at predicting the time to flashover.

In model RC, using the Room/Corner experiment results, very good overall comparison was found between the calculated heat release rate and the corresponding experimental results for the "S", "E" and "M" series materials. An example of the success of the model is shown in Figure (7.3), which shows material M24.

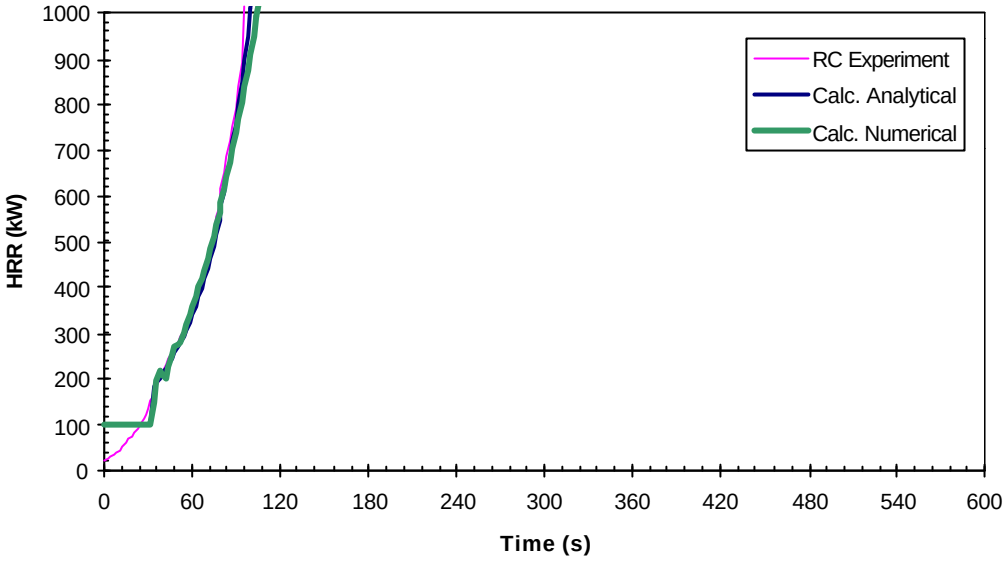


**Figure 7.3:** Material M24 (Paper wall covering on Particle board) HRR Comparison – RC Test Scenario

This particular figure shows a flashover material and Figure (7.4) shows the modelling results for a non-flashover material.

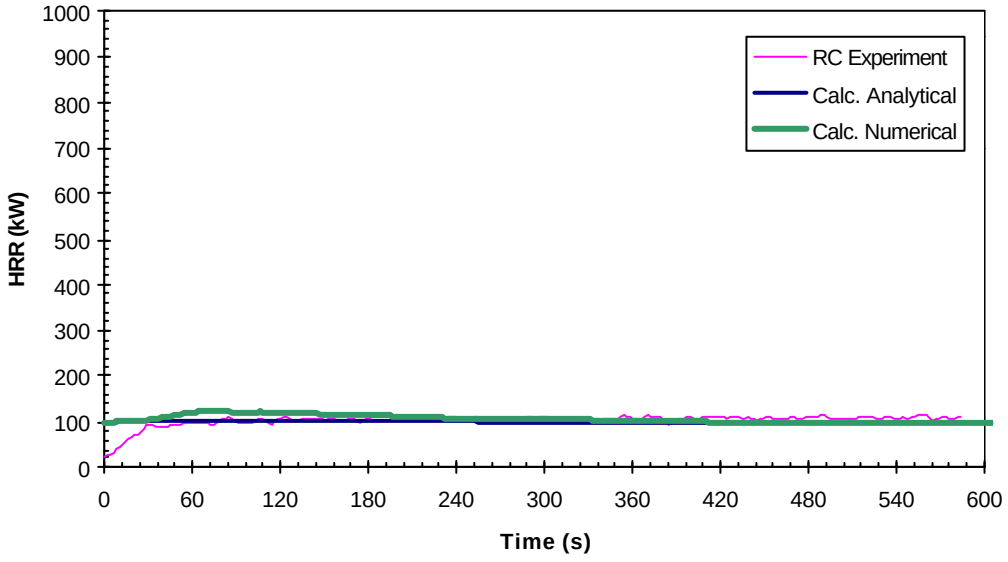


**Figure 7.4:** Material M19 (unfaced Rockwool) HRR Comparison – RC Test Scenario

A complete set of figures for the "S", "E" and "M" series materials can be seen in Appendices D, E and F.

# 7.2 SBI Model Analysis

In this model, only the "M" series materials were analysed since no experimental comparison data was available on the SBI scenario for the "S" and "E" materials. The method used was identical to that described for the Room/Corner model and is detailed below.

## 7.2.1 Sensitivity Analysis of the Tuning Variables

This model, as could be expected, produced a different averaged $R^2$ value than in the previous @RISK analysis. @RISK initially gave the Fraction of Initial Pyrolysis Length variable, f, a value of 0.523, the Heat Flux for Flame Spread variable, $\dot{q}''_{fs}$, a value of 7.05, the Pre-flame Spread Heat Flux variable, $\dot{q}''_{start}$ a value of 27.71 and the Flame Area Coefficient, K, a value of 0.0202.

## 7.2.2 Final Optimised Results and Comparisons

The optimisation of the variable values produced slightly different values for all four variables this time. These values, corresponding to the optimum fit between the experimental to calculated heat release rate, were applied to the model and a description of the actual effect that this had is described in the next section. The results from the analysis in this section is given in Table (7.2),

**Table 7.2:** Minimum Input Values for the SBI Model

| Input Variable | Value | Unit |
|---|---|---|
| f | 0.55 | (-) |
| $\dot{q}''_{fs}$ | 10 | $kWm^{-2}$ |
| $\dot{q}''_{start}$ | 30 | $kWm^{-2}$ |
| K | 0.020 | $m^2kW^{-1}$ |

Once the optimal input values were found, analysis of varying the four tuning variables by ±10% was again investigated. Similar correlation results were found to those in the Room/Corner model. Again the Flame Areas Coefficient, K, was found to have the largest influence on the $R^2$ value but this time it was more closely followed by the Heat Flux for Flame Spread variable, $\dot{q}''_{fs}$. This variable was then followed by a similar step back to the Fraction of the Initial Pyrolysis Length variable, f. The Pre-Flame Spread Heat Flux

variable, $\dot{q}''_{start}$, exhibited the least significance on the $R^2$ value. These results are shown in Figure (7.5),

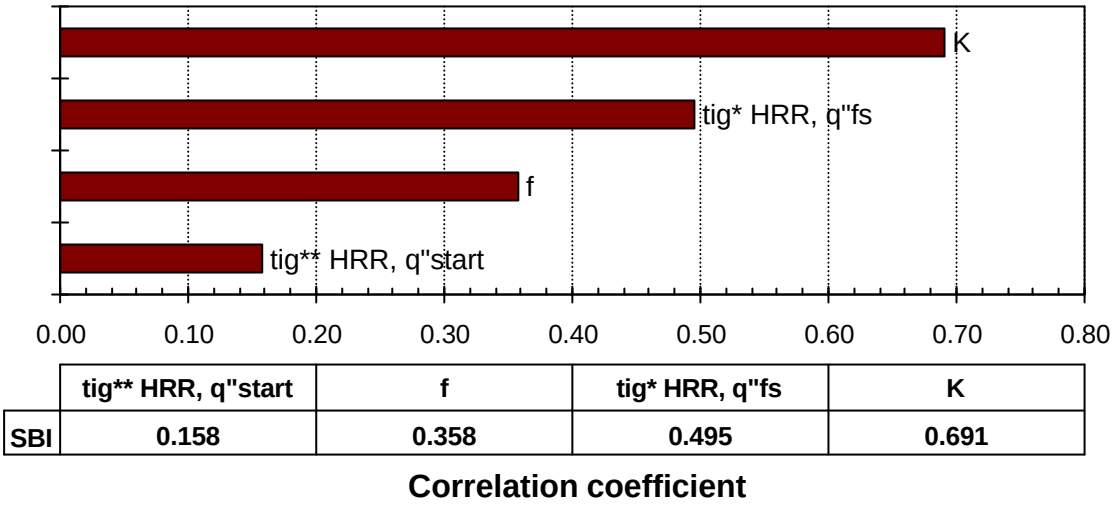


**Figure 7.5:** $R^2$ Correlation Values for the SBI Scenario

In this analysis, since it was found that none of the "M" series materials went to flashover in the SBI scenario, a new method of comparison was needed. This technique was to compare the reported with the calculated FIGRA (SBI) values for all the materials. The FIGRA (SBI) is an index used to describe the growth rate of a fire and has the units of $Ws^{-1}$. It is calculated by dividing the peak heat release rate of the fire (excluding the influence from the ignition source) by the time at which this occurs. A further detailed explanation of this calculation is given in [30]. From this value, the designated "
material can be determined as shown in Table (7.3).

**Table 7.3:** FIGRA (SBI) Classification Limits for the Euroclasses

| Euroclass | FIGRA (SBI) Limit Values ($Ws^{-1}$) |
|---|---|
| A1 | ≤120 |
| A2 | ≤120 |
| B | ≤120 |
| C | ≤250 |
| D | ≤750 |
| E | ≤750 |
| F | >750 |

The higher the FIGRA (SBI) value, and therefore the Euroclass, the greater the fire risk that the material possesses. A material of class "A1" is non-combustible whereas a class "F" material would progress to flashover extremely quickly.

Table (7.4) and Figure (7.6) show the results of the reported versus the calculated (analytical) FIGRA (SBI) investigation for the "M" series materials.

**Table 7.4:** FIGRA (SBI) Values for "M" series Materials

| Material | FIGRA (SBI) Values | | | |
|---|---|---|---|---|
| | Reported [1] | Euroclass | Calculated [2] | Euroclass |
| M1 | 45 | A1 | 103 | A1 |
| M2 | 87 | A1 | 365 | D |
| M3 | 1390 | F | 14252 | F |
| M4 | 1838 | F | 1613 | F |
| M5 | 688 | D | 844 | F |
| M6 | 27 | A1 | 244 | C |
| M7 | 0 | A1 | 7027 | F |
| M8 | 47 | A1 | 38 | A1 |
| M9 | 205 | C | 251 | D |
| M10 | 374 | D | 358 | D |
| M11 | 98 | A1 | 127 | C |
| M12 | 0 | A1 | 775 | F |
| M13 | 0 | A1 | 190 | C |
| M14 | 119 | A1 | 206 | C |
| M15 | 47 | A1 | 0 | A1 |
| M16 | 382 | D | 663 | D |
| M19 | 0 | A1 | 0 | A1 |
| M20 | 601 | D | 760 | F |
| M21 | 0 | A1 | 0 | A1 |
| M22 | 399 | D | 367 | D |
| M23 | 398 | D | 394 | D |
| M24 | 477 | D | 519 | D |
| M25 | 432 | D | 310 | D |
| M26 | 1074 | F | 466 | D |
| M27 | 0 | A1 | 162 | C |
| M28 | 58 | A1 | 63 | A1 |
| M29 | 168 | C | 139 | C |
| M30 | 4080 | F | 10119 | F |

[1] Values taken from [34]

[2] Values calculated from the analytical flame spread model.

These results are also shown graphically below,

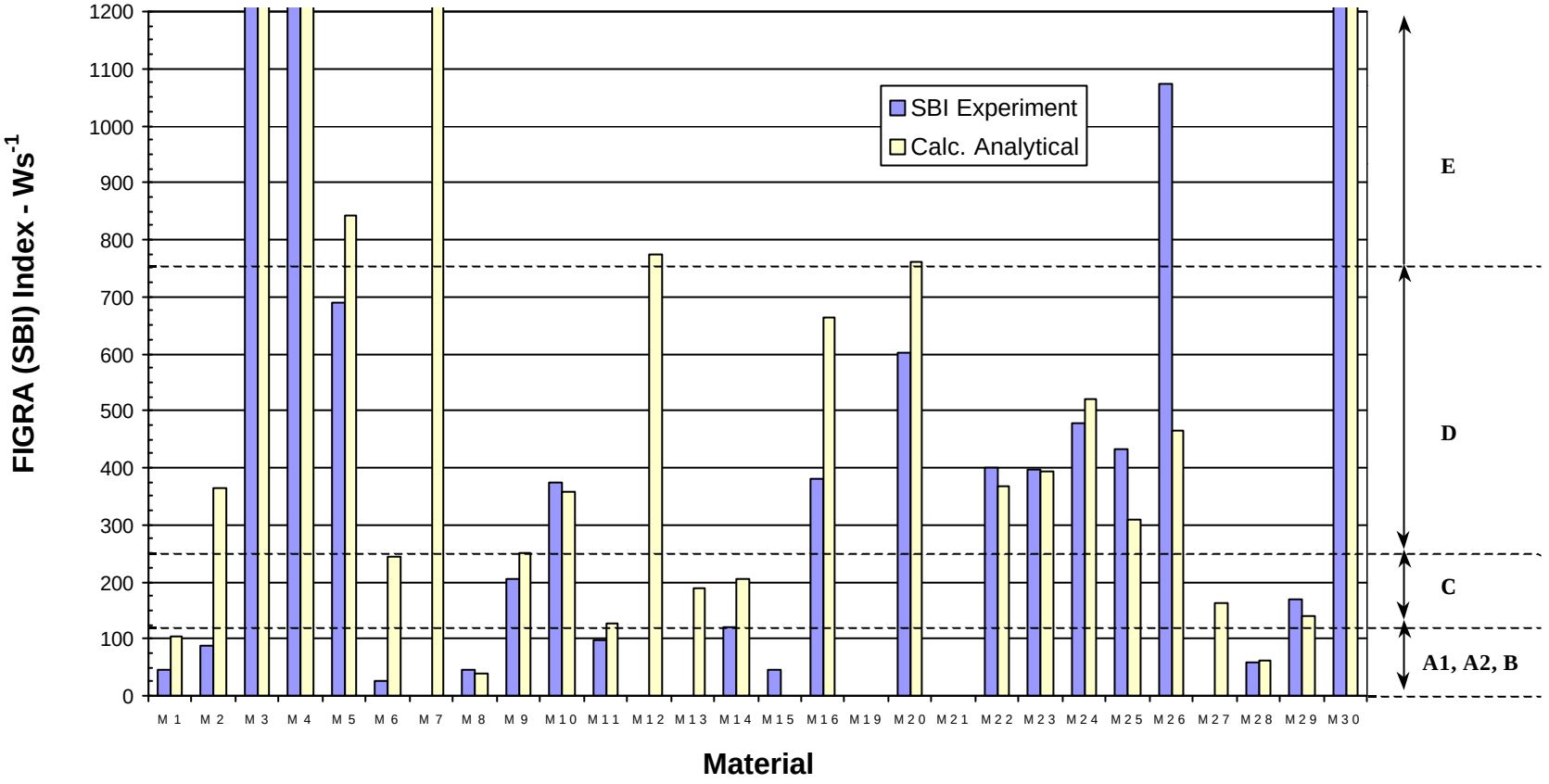


**Figure 7.6:** FIGRA (SBI) Comparison – SBI Scenario

(Note: The Euroclass zones are shown on the right of the Figure)

Figure (7.6) shows that the SBI scenario model also predicted the FIGRA (SBI) value satisfactorily in most cases.

The application of the input variable values into the SBI scenario flame spread model also gave very good results. The material M24, indicated in Figure (7.7), again shows the success that the analytical model had in calculating the heat release rate values. This material, as with all the "M" series materials, did not go to flashover in the experimental test.

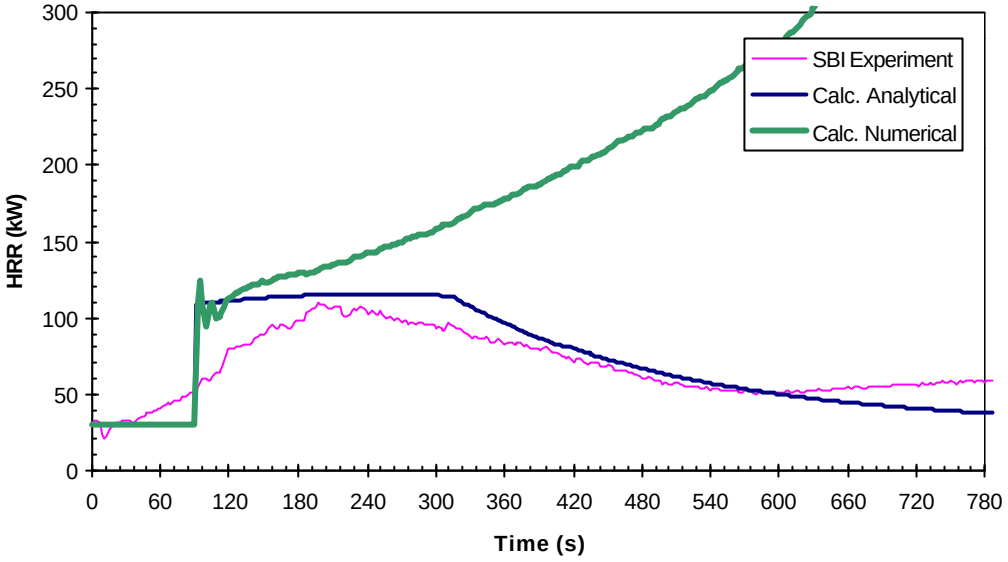


**Figure 7.7:** Material M24 (Paper wall covering on Particle board) HRR Comparison – SBI Test Scenario

A complete set of figures for the "M" series materials can be seen in Appendix G.

# 7.3 Summary

In the assessment of the two models, Room/Corner and SBI, to their experimental studies, sensitivity analysis was applied so that the optimal values of the four input tuning variables could be determined. It was found from the analysis that the values of these variables differed between that of the model RC, which incorporated the "S", "E" and "M" series materials, and model SBI, which investigated only the "M" series materials. The values of these optimised tuning variables are summarised in Table (7.5),

**Table 7.5:** Optimal Tuning Values for Model RC and SBI

| Input Variable | Model RC Values | Model SBI Values | Unit |
|---|---|---|---|
| f | 0.18 | 0.55 | (-) |
| $\dot{q}''_{fs}$ | 30 | 10 | $kWm^{-2}$ |
| $\dot{q}''_{start}$ | 50 | 30 | $kWm^{-2}$ |
| K | 0.018 | 0.020 | $m^2kW^{-1}$ |

It was found by using the Regression Correlation function in @RISK that each input value influenced the average $R^2$ result to differing extents. For both models, the flame area coefficient, K, was found to have the most influence on the minimum average $R^2$ result. The Heat Flux for Flame Spread variable, $\dot{q}''_{fs}$, Fraction of the Initial Pyrolysis Length variable, f, and the Pre-Flame Spread Heat Flux variable, $\dot{q}''_{start}$, followed K in a descending order of influence. One interesting outcome from this analysis was that the influences on the $R^2$ value by all the tuning variables was considerably more significant for the SBI scenario than for the Room/Corner scenario.

The two optimised models were found to give very good comparisons between the calculated (analytical and numerical) and experimental heat release rates. The models can therefore be used to satisfactorily calculate the flame spread characteristics for the materials investigated.

# 8. CONCLUSIONS AND FUTURE WORK

***Time to Ignition Equation Investigation***

In the first part of the research, a simplified expression for the time to ignition of a material, was developed. This development involved the investigation of several possible expressions but all but one of these were excluded since their performance was found to be poor. The simplified equation that was finally chosen was incorporated into the analytical and numerical flame spread model. The analysis undertaken for this equation used data from the "S", "E" and the "M" series materials and the results in the comparison between the calculated and experimentally determined time to ignition values were found to be satisfactory.

The strength of the ignition model is it's simplicity; one only needs as input the material density and ignition data from a single experiment. Some accuracy is always lost when models are simplified and better results are quite possible by making the ignition model more elaborate. The cost, however, is that more input data becomes necessary and more elaborate bench-scale experiments are required.

The ignition model was one of the most important components of the overall flame spread model, and any improvements in the ignition calculations will result in better prediction of the final results on fire growth in the full scale scenarios. Improvements to the ignition model described in this report could be made by, for example, dividing the material into different groups (eg. wood, plastics, etc) and determining statistically derived expressions for each group of materials.

***Analytical Flame Spread Model Development and Assessment***

As with most models of complex phenomenon, many simplifications were incorporated into the model developed in this research. These simplifications neglected all but the essential aspects of vertical flame spread on combustible materials in an attempt to make the model easy to use and so that the sensitivity analysis performed would be relatively computationally inexpensive.

One of these simplifications involved representing the heat release rate, from Cone Calorimeter results, of each material by a mathematical expression. This expression was either described by a Peak/Decay or an Average representation.

Tuning of the model was undertaken by four input variables that were optimised by sensitivity analysis. This optimisation compared the fit of the calculated values to the experimental data collected from three different studies. Two of the studies, namely the "S" and "E" series tests, used only the European Standard Room/Corner test method. The other study on the "M" series materials used the Room/Corner test and the Single Burning Item test method.

The results from using the analytical model described in the report to represent the complex phenomena of upward flame spread on solid materials were found to be very satisfactory based on the generally close comparison between the calculated and experimental values.

A complete listing of the heat release rate graphs for all the materials and scenarios can be found Appendices D, E, F and G.

***Numerical Flame Spread Model Development and Assessment***

A considerable number of numerically based flame spread models have been developed. Some are very elaborate and can take account of pyrolysis and mass transport of pyrolysis products from the surface of the combustible material. Other models are so called thermal models, where it is assumed that ignition and full pyrolysis starts when any part of the combustible surface reaches a certain ignition temperature, and also assume that the heat release from the material can be estimated using bench-scale experimental data. It is the latter type of models that have been used and discussed in this report.

In some instances, such models are not connected to a room fire model, so it is assumed that the burning item is not affected by any environmental changes in the room as the fire grows. An example of such models is Thimes [2]. In this work we have briefly described a model where Thimes has been incorporated into a full room fire model. This opens up possibilities of linking the environmental variables, such as gas temperature, to variables that control the flame spread, such as surface temperature and time to ignition. Such a link has not been pursued to any extent in the work presented here, but any future development would allow such a link to be made. In general, it can be stated that the current numerical model performs in a satisfactory manner, but further development would enhance the performance.

***Future Work***

In the future, further effort could be placed into applying different mathematical representations of the heat release rate for the materials. In doing so, the model should be more capable of describing a wider variety of materials, especially those polymeric materials, that produce a pool fire on combustion.

The simplified time to ignition expression developed in this research has been shown to be satisfactory for the materials investigated. But, as described above, it's simplicity may limit the applicability somewhat. By dividing the materials into different categories and statistically developing an expression for each category, the applicability may improve considerably. Any future use of such expressions should be accompanied with similar associated analysis undertaken in this research so to ensure its acceptability.

Designers often wish to place many different materials on the same vertical wall, such as timber placed below paper covered plasterboard. The effect, due to the different material properties and combustion behaviour, that such an arrangement would have on the flame spread development on the materials would be a very interesting and important progression of the current model. Such a model could be used to determine the flame front behaviour and its variation due to changing the individual material types and/or arrangement. This model could be used by engineers to prove that their particular complex wall design would still provide the necessary level of fire safety as imposed by the relevant sections of a countries building code.

# 9. REFERENCES


1) Barnett, J.B., Satterfield, D.B., *User's guide to WPI/HARVARD Version 2,* Centre for Fire Safety Studies, Worcester Polytechnic Institute, August 1990.
2) Baroudi, D., Kokkala, M., Parker, W., *THIMES a computer program for upward flame calculations*, Internal Report, Technical Research Centre of Finland (VTT), 1997.
3) Baroudi, D., Kokkala, M., Parker, W., *Upward Flame Spread on Wooden Surface Products: Experiments and Numerical Modelling,* Technical Research Centre of Finland (VTT), 1997.
4) Beller, D.K., *Alternate Computer Models of Fire Convection Phenomena for the Harvard Computer Fire Code*, Worcester Polytechnic Institute, 1987.
5) Beyler, C.L., *Fire Plumes and Ceiling Jets*, Fire Safety Journal, Vol. 11, 1986.
6) Brenton, J.R., Drysdale, D.D., *Upward Flame Spread over Vertical Fuel Surfaces*, Unpublished manuscript supplied by the author, 1999.
7) Buchanan, A.H. (Editor), *Fire Engineering Design Guide*, Centre for Advanced Engineering, University of Canterbury, New Zealand, July 1994.
8) Caffrey, P.J., *Computer Modelling of Hot Spot Formation on Walls Using Non-Ventilated Heat Transfer Phenomenon*, Worcester Polytechnic Institute, 1989.
9) Cooper, L.Y., Compartment Fire-Generated Environment and Smoke Filling, *The SFPE Handbook of Fire Protection Engineering*, National Fire Protection Association, Quincy, Second Edition, Section 3, Chapter 10, 1995.
10) Edward, C.H., Penney, D. E., *Calculus & Analytic Geometry*, 2nd Edition. 1956.
11) Frantzich, H., *Uncertainty and Risk Analysis in Fire Safety Engineering*, Report TVBB-1016, Department of Fire Safety Engineering, Lund University, Sweden, 1998.
12) Gojkovic, D., Hultquist, H., *Incorporating Flame Spread and Fire Growth Algorithms into a Computation Zone model*, Report 5029, Department of Fire Safety Engineering, Lund University, Sweden, 1999.
13) Hakkarainen, T., Oksanen, T., Mikkola, E., *Fire Behaviour of Facades in Multi-storey Wood-framed Houses*, VTT Research Notes 1823, Technical Research Centre of Finland, 1997.
14) Hedskog, B., Ryber, F., *The Classification Systems for Surface Lining Materials used in Buildings in Europe and Japan – A Summary and Comparison*, Report 5023, Department of Fire Safety Engineering, Lund University, Sweden, 1998.
15) Höglander, K., Sundström, B., *Design Fires for Pre-flashover Fires - Characteristic Heat release rates of Building Contents*, SP Swedish National Testing and Research Institute, SP Report 1997:36, Sweden, 1997.
16) International Organisation for Standardisation (ISO), *Fire Safety Engineering – Part 1: The Application of Fire Performance Concepts to Design Objectives*, Committee Draft, Report ISO/PDTR 13387-1, 1998.
17) Karlsson, B., *Modelling Fire Growth on combustible Wall Lining Materials in Enclosures*, Report TVBB-1009, Department of Fire Safety Engineering, Lund University, Sweden, 1992.
18) Karlsson, B., Quintiere, J.G., *Enclosure Fire Dynamics - A First Draft of a Student Textbook*, Department of Fire Safety Engineering, Lund University, Sweden, August

1998.
19) Kokkala, M., Göransson, U., Söderbom, J., *Five Large-scale Room Fire Experiments, Project 3 of the EUREFIC Fire Research Programme*, VTT Publication 104, Technical Research Centre of Finland, Espoo 1992.
20) Kokkala, M., Mikkola, E., Immonen, M., Juutilainen, H., Manner, P., Parker, W. J., *Large-scale Upward Flame Spread Tests on Wood Products*, VTT Research Notes 1834, Technical Research Centre of Finland, 1997.
21) Lie, T.T., Fire Temperature-Time Relations, *The SFPE Handbook of Fire Protection Engineering*, National Fire Protection Association, Quincy, Second Edition, Section 4, Chapter 8, 1995.
22) Lønvik, L.E., Opstad, K., *Software User's Guide for DCS - A Data Converting System, Version 1.20*, SINTEF - The Foundation for Scientific and Industrial Research at the Norwegian Institute of Technology, Report Number STF25 A90003, Norway, 1991.
23) Messerschmidt, B., Van Hees, P., Wickström, U., *Prediction of SBI (Single Burning Item) Test Results by Means of Cone Calorimeter Test Results*, Danish Institute of Fire Technology, Denmark and SP Swedish National Testing and Research Institute, Sweden, 1999.
24) Mitler, H.E., *User's Guide for the Harvard Computer Fire Code*, Harvard University, Division of Applied Sciences, 1979
25) Mitler, H.E, Rockett, J.A., *User's Guide to FIRST - A Comprehensive Single-Room Fire Model*, U.S. Dept of Commerce - National Bureau of Standards (NBS), 1987.
26) New Zealand Fire Service, *New Zealand Fire Service Database Statistics, 1986-1997*, National Headquarters, Wellington, New Zealand, 1998.
27) North, G., *An Analytical Model for Vertical Flame Spread on Solid Materials – An Initial Investigation*, Fire Engineering Research Report, School of Engineering, University of Canterbury, New Zealand, May 1999.
28) Palisade, *Guide to Using @RISK: Risk Analysis and Simulation Add-In for Microsoft Excel or Lotus 1-2-3*, Palisade Corporation, New York, September 1996.
29) Palisade, *PRECISION TREE User's Guide: Decision Analysis Add-In for Microsoft Excel*, Palisade Corporation, New York, July 1997.
30) Proposed European Standard, prEN SBI 1999, *Reaction to fire tests for building products - Building products excluding floorings exposed to the thermal attack by a single burning item ("SBI test")*, Technical Committee CEN/TC 127 "Fire Safety in Buildings", BSI, June 1999.
31) Quintiere, J.G., Surface Flame Spread, *The SFPE Handbook of Fire Protection Engineering*, National Fire Protection Association, Quincy, Second Edition, Section 2, Chapter 14, 1995.
32) Saito, K., Quintiere, J.G., Williams, F.A., *Upward Turbulent Flame Spread*, Proc. First International Symposium on Fire Safety Science, Hemisphere Publishing, New York, 1984.
33) Sundström, B., *A New Generation of Large Scale Fire Test Methods*, SP Swedish National Testing and Research Institute, SP Report 1990:12, Sweden, 1990.
34) Sundström, B., Van Hees, P., Thureson, P., *Results and Analysis from Fire Tests of Building Products in ISO 9705, the Room/Corner Test – The SBI Research*

*Programme*, SP Swedish National Testing and Research Institute, SP Report 1998:11, Sweden, 1998.
35) Thureson, P., *EUREFIC - Cone Calorimeter Test Results, Project 4 of the EUREFIC Fire Research Programme*, SP Swedish National Testing and Research Institute, SP Report 1991:24, Sweden, 1991.
36) Tsantaridis, L., *CEN Ignitability test results for wood building products*, Trätek Report L 9702010, TräteknikCentrum, Stockholm, Sweden, 1997.
37) Tsantaridis, L., Östman, B., *Smoke, Gas and Heat Release Data for building Products in the Cone Calorimeter*, Trätek Report I 8903013, TräteknikCentrum, Stockholm, Sweden, 1991.
38) Tsantaridis, L., Östman, B., *Cone Calorimeter Data and Comparisons for the SBI RR Products*, Trätek Report I 9806XXX, ISSN 1102-1071, TräteknikCentrum, Stockholm, Sweden, 1998.
39) Walton, W.D., Thomas, P.H., Estimating Temperatures in Compartment Fires, *The SFPE Handbook of Fire Protection Engineering*, National Fire Protection Association, Quincy, Second Edition, Section 3, Chapter 6, 1995.
40) Williams, F.A., *Mechanisms of Fire Spread*, 16th International Symposium on Combustion, pp. 1281-1294, 1976.
41) ASTM E-1321-90, *Standard Method for Determining Ignition and Flame Spread Properties*, American Society for Testing and Materials, Philadelphia, 1990

# 10. APPENDIX LIST

# APPENDIX A: PARAMETERS USED IN THE ANALYTICAL CALCULATION

## Input Values used in the Analytical Flame Spread Model

**Table A.1:** Swedish "S" series Input Values

| Material No. | Material Name | Wall Height (m) | Burner Output | Burner Width (m) |
|---|---|---|---|---|
| S1 | Insulating Fibre Board | 27 | 100 | 0.34 |
| S2 | Medium Density Fibre Board | 27 | 100 | 0.34 |
| S3 | Particle Board | 27 | 100 | 0.34 |
| S4 | Gypsum Plasterboard | 27 | 100 | 0.34 |
| S5 | PVC covering on S4 | 27 | 100 | 0.34 |
| S6 | Paper covering on S4 | 27 | 100 | 0.34 |
| S7 | Textile covering on S4 | 27 | 100 | 0.34 |
| S8 | Textile covering on Mineral Wool | 27 | 100 | 0.34 |
| S9 | Melamine-faced Particle Board | 27 | 100 | 0.34 |
| S10 | Expanded Polystyrene | 27 | 100 | 0.34 |
| S11 | Rigid Polyurethane Foam | 27 | 100 | 0.34 |
| S12 | Wood Panel (Spruce) | 27 | 100 | 0.34 |
| S13 | Paper covering on S3 | 27 | 100 | 0.34 |

**Table A.2:** Eurefic "E" series Input Values

| Material No. | Material Name | Wall Height (m) | Burner Output | Burner Width (m) |
|---|---|---|---|---|
| E1 | Painted Gypsum Paper Plaster Board | 27 | 100 | 0.34 |
| E2 | Ordinary Plywood | 27 | 100 | 0.34 |
| E3 | Textile Wall-covering on Gypsum Paper Plaster Board | 27 | 100 | 0.34 |
| E4 | Melamine Faced High Density Non-combustible Board | 27 | 100 | 0.34 |
| E5 | Plastic Faced Steel Sheet on Mineral Wool | 27 | 100 | 0.34 |
| E6 | FR Particle Board - type B1 | 27 | 100 | 0.34 |
| E7 | Faced Rockwool | 27 | 100 | 0.34 |
| E8 | FR Particle Board | 27 | 100 | 0.34 |
| E9 | Polyurethane Foam Covered with Steel Sheet | 27 | 100 | 0.34 |
| E10 | PVC-wall Carpet on Gypsum Paper Plaster Board | 27 | 100 | 0.34 |
| E11 | FR Polystyrene | 27 | 100 | 0.34 |

**Table A.3:** SBI "M" series Input Values

| Material No. | Material Name | Wall Height (m) | Burner Output | Burner Width (m) |
|---|---|---|---|---|
| M1 | Plasterboard | 1.5 | 30 | 0.5 |
| M2 | FR PVC | 1.5 | 30 | 0.5 |
| M3 | FR extruded Polystyrene board | 1.5 | 30 | 0.5 |
| M4 | PUR foam panel with Al. Foil faces | 1.5 | 30 | 0.5 |
| M5 | Varnished mass timber, Pine | 1.5 | 30 | 0.5 |
| M6 | FR Chipboard | 1.5 | 30 | 0.5 |
| M7 | FR Polycarbonate panel (3 layered) | 1.5 | 30 | 0.5 |
| M8 | Painted Plasterboard | 1.5 | 30 | 0.5 |
| M9 | Paper wall covering on Plasterboard | 1.5 | 30 | 0.5 |
| M10 | PVC wall carpet on Plasterboard | 1.5 | 30 | 0.5 |
| M11 | Plastic-faced Steel sheet on Mineral Wool | 1.5 | 30 | 0.5 |
| M12 | Unvarnished mass timber, Spruce | 1.5 | 30 | 0.5 |
| M13 | Plasterboard on Polystyrene | 1.5 | 30 | 0.5 |
| M14 | Phenolic foam | 1.5 | 30 | 0.5 |
| M15 | Intumescent coat on Particle board | 1.5 | 30 | 0.5 |
| M16 | Melamine faced MDF board | 1.5 | 30 | 0.5 |

| | | | | |
|---|---|---|---|---|
| M17 | PVC water pipes | 1.5 | 30 | 0.5 |
| M18 | PVC covered electric cables | 1.5 | 30 | 0.5 |
| M19 | Unfaced Rockwool | 1.5 | 30 | 0.5 |
| M20 | Melamine faced Particle board | 1.5 | 30 | 0.5 |
| M21 | Steel clad expanded Polystyrene sandwich panel | 1.5 | 30 | 0.5 |
| M22 | Ordinary Particle board | 1.5 | 30 | 0.5 |
| M23 | Ordinary Plywood, Birch | 1.5 | 30 | 0.5 |
| M24 | Paper wall covering on Particle board | 1.5 | 30 | 0.5 |
| M25 | Medium density fibre tiles | 1.5 | 30 | 0.5 |
| M26 | Low density fibre board | 1.5 | 30 | 0.5 |
| M27 | Plasterboard/FR PUR foam core | 1.5 | 30 | 0.5 |
| M28 | Acoustic mineral fibre tiles | 1.5 | 30 | 0.5 |
| M29 | Textile wall paper on Calcium silicate board | 1.5 | 30 | 0.5 |
| M30 | Paper-faced glass wool | 1.5 | 30 | 0.5 |

## Material Parameters used in the Analytical Flame Spread Model

**Table A.4:** Swedish "S" series Material Parameters

| Material No. | Material Name | Density, $\rho$ ($kgm^{-3}$) | $Q_{max}$ ($kWm^{-2}$) | $\lambda$ ($s^{-1}$) |
|---|---|---|---|---|
| S1 | Insulating Fibre Board | 250 | 184 | 0.0090 |
| S2 | Medium Density Fibre Board | 600 | 208 | 0.0027 |
| S3 | Particle Board | 750 | 204 | 0.0030 |
| S4 | Gypsum Plasterboard | 700 | 151 | 0.0390 |
| S5 | PVC covering on S4 | 682 | 210 | 0.0600 |
| S6 | Paper covering on S4 | 684 | 254 | 0.0600 |
| S7 | Textile covering on S4 | 691 | 408 | 0.0700 |
| S8 | Textile covering on Mineral Wool | 184 | 466 | 0.0800 |
| S9 | Melamine-faced Particle Board | 810 | 150 | 0.0016 |
| S10 | Expanded Polystyrene | 20 | 325 | 0.0120 |
| S11 | Rigid Polyurethane Foam | 30 | 247 | 0.0200 |
| S12 | Wood Panel (Spruce) | 527 | 168 | 0.0075 |
| S13 | Paper covering on S3 | 726 | 197 | 0.0041 |

**Table A.5:** Eurefic "E" series Material Parameters

| Material No. | Material Name | Density, $\rho$ ($kgm^{-3}$) | $Q_{max}$ ($kWm^{-2}$) | $\lambda$ ($s^{-1}$) |
|---|---|---|---|---|
| E1 | Painted Gypsum Paper Plaster Board | 681 | 213 | 0.0850 |
| E2 | Ordinary Plywood | 600 | 275 | 0.0060 |
| E3 | Textile Wall-covering on Gypsum Paper Plaster Board | 724 | 312 | 0.0400 |
| E4 | Melamine Faced High Density Non-combustible Board | 1055 | 106 | 0.0175 |
| E5 | Plastic Faced Steel Sheet on Mineral Wool | 640 | 71 | 0.2000 |
| E6 | FR Particle Board - type B1 | 630 | 152 | 0.0250 |
| E7 | Faced Rockwool | 87 | 126 | 0.0800 |
| E8 | FR Particle Board | 755 | 69 | 0.0175 |
| E9 | Polyurethane Foam Covered with Steel Sheet | 170 | 259 | 0.0125 |
| E10 | PVC-wall Carpet on Gypsum Paper Plaster Board | 750 | 137 | 0.0095 |
| E11 | FR Polystyrene | 37 | 667 | 0.0450 |

**Table A.6:** SBI "M" series Material Parameters

| Material Number | Material Name | Density [1] r ($kgm^{-3}$) | Cone A Data $Q_{max}$ ($kWm^{-2}$) | Cone A Data $\lambda$ ($s^{-1}$) | Cone B Data $Q_{max}$ ($kWm^{-2}$) | Cone B Data $\lambda$ ($s^{-1}$) |
|---|---|---|---|---|---|---|
| M1 | Plasterboard | 716 | 138.86 | 0.0800 | 103.93 | 0.1500 |
| M2 | FR PVC | 1453 | 280.80 | 0.0120 | 356.33 | 0.0400 |
| M3 | FR extruded Polystyrene board | 30 | 372.30 | 0.0100 | 545.68 | 0.0150 |
| M4 | PUR foam panel with Al. Foil faces | 57 | 124.73 | 0.0050 | 104.74 | 0.0055 |
| M5 | Varnished mass timber, Pine | 455 | 238.78 | 0.0200 | 227.90 | 0.0200 |

| | | | | | | |
|---|---|---|---|---|---|---|
| M6 | FR Chipboard | 789 | 101.39 | 0.0160 | 110.58 | 0.0120 |
| M7 | FR Polycarbonate panel (3 layered) | 174 | 628.89 | 0.0240 | 649.13 | 0.0400 |
| M8 | Painted Plasterboard | 731 | 168.69 | 0.1750 | 127.14 | 0.2500 |
| M9 | Paper wall covering on Plasterboard | 717 | 237.47 | 0.0700 | 173.52 | 0.0700 |
| M10 | PVC wall carpet on Plasterboard | 811 | 165.86 | 0.0150 | 159.78 | 0.0175 |
| M11 | Plastic-faced Steel sheet on Mineral Wool | 620 | 75.67 | 0.0650 | 114.44 | 0.0750 |
| M12 | Unvarnished mass timber, Spruce | 451 | 187.92 | 0.0125 | 213.81 | 0.0175 |
| M13 | Plasterboard on Polystyrene | 724 | 129.94 | 0.0500 | 126.15 | 0.0500 |
| M14 | Phenolic foam | 59 | 48.93 | 0.0035 | 43.32 | 0.0040 |
| M15 | Intumescent coat on Particle board | 350 | 25.89 | 0.1500 | 20.47 | 0.0700 |
| M16 | Melamine faced MDF board | 767 | 268.52 | 0.0150 | 267.48 | 0.0120 |
| M17 | PVC water pipes | (-) [2] | 0.00 | 0.0000 | 0.00 | 0.0000 |
| M18 | PVC covered electric cables | (-) [3] | 0.00 | 0.0000 | 0.00 | 0.0000 |
| M19 | Unfaced Rockwool | 151 | 11.60 | 0.0080 | 9.11 | 0.0070 |
| M20 | Melamine faced Particle board | 710 | 290.44 | 0.0120 | 232.50 | 0.0060 |
| M21 | Steel clad expanded Polystyrene sandwich panel | 107 | 34.46 | 0.0500 | 29.23 | 0.0450 |
| M22 | Ordinary Particle board | 705 | 235.83 | 0.0050 | 236.08 | 0.0050 |
| M23 | Ordinary Plywood, Birch | 718 | 187.16 | 0.0020 | 229.27 | 0.0020 |
| M24 | Paper wall covering on Particle board | 693 | 220.47 | 0.0060 | 238.32 | 0.0050 |
| M25 | Medium density fibre tiles | 848 | 255.57 | 0.0040 | 261.47 | 0.0040 |
| M26 | Low density fibre board | 296 | 164.45 | 0.0075 | 183.13 | 0.0080 |
| M27 | Plasterboard/FR PUR foam core | 846 | 122.22 | 0.0400 | 118.79 | 0.0550 |
| M28 | Acoustic mineral fibre tiles | 252 | 37.70 | 0.0500 | 70.67 | 0.2000 |
| M29 | Textile wall paper on Calcium silicate board | 945 | 273.88 | 0.1200 | 242.90 | 0.1300 |
| M30 | Paper-faced glass wool | 18 | 222.00 | 0.0850 | | |

[1] Value quoted is the “effective” density, ie. For a composite material, it’s the combined density value of each material

[2] Not quoted

[3] Not quoted

# APPENDIX B: @RISK SIMULATION OUTPUT DATA

**Table B.1:** @RISK Summary Output Data

| Name | Average $R^2$ Values | |
|---|---|---|
| **Description** | **Room/Corner Scenario** | **SBI Scenario** |
| **Minimum =** | 19646.54 | 20.67 |
| **Maximum =** | 40244.7 | 26.34 |
| **Mean =** | 24921.54 | 23.19 |
| **Std Deviation =** | 7661.24 | 1.14 |
| **Variance =** | 5.87E+07 | 1.29 |
| **Skewness =** | 1.115 | 0.25 |
| **Kurtosis =** | 2.293 | 2.48 |
| **Mode =** | 19749.87 | 22.11 |
| **5% Perc =** | 19725.42 | 21.44 |
| **10% Perc =** | 19773.83 | 21.75 |
| **15% Perc =** | 19822.47 | 21.95 |
| **20% Perc =** | 19879.74 | 22.13 |
| **25% Perc =** | 19951.33 | 22.32 |
| **30% Perc =** | 20045.42 | 22.49 |
| **35% Perc =** | 20174.14 | 22.64 |
| **40% Perc =** | 20331.43 | 22.81 |
| **45% Perc =** | 20432.49 | 22.98 |
| **50% Perc =** | 20564.38 | 23.15 |
| **55% Perc =** | 20764.86 | 23.30 |
| **60% Perc =** | 21071.24 | 23.47 |
| **65% Perc =** | 21526.81 | 23.65 |
| **70% Perc =** | 22066.65 | 23.82 |
| **75% Perc =** | 35713.38 | 24.00 |
| **80% Perc =** | 37897.75 | 24.18 |
| **85% Perc =** | 38060.68 | 24.38 |
| **90% Perc =** | 38385.63 | 24.72 |
| **95% Perc =** | 38511.87 | 25.26 |

# APPENDIX C: NUMERICAL MODEL DATA FILES

## C.1 Input Data File for the Flame Spread Algorithm

The first row, in this input data file example, contains a list of dummy variables. These should not be changed. The second, third and fourth rows consists of material properties and some constants that relate to the flame spread algorithm. Below this is the cone data presented in two columns, in the left column is the post-ignition time and in the right column is the heat flux per unit area.

**Table C.1:** Numerical Model Sample Input Data File

```
1       13       10
NDIM    NPROP    NPRINT

1  0  .2  .65E-5 37  0.  1.2  83.33E3 1  50.E3  20.0E6  41.7E6  0.65
n  x0  xp0     K    tig  t0  Wburner   Qb     α   qcone,0  ΔHc,wall  ΔHc,burner  χ

1.       0.  1200.
Δt     tmin  tmax

.2         2.4
y0          ymax

RHR-curve      [W/m2]:
0      50000
5      117000
10     137000
15     124000
20     115000
25     124000
30     114000
35     106000
40     102000
45     95000
50     90000
55     86000
60     82000
65     78000
70     75000
75     73000
80     71000
85     70000
90     68000
95     66000
100    66000
120    61000
140    69000
160    70000
180    83000
200    88000
```

```
220    137000
240    104000
250    112000
300    74000
350    80000
500          0
```

# C.2 Output Data File from the Zone Model

This Appendix shows a part of an output data file from the zone model, WPI/Fire Code, after 20 seconds simulation time. The output variables are coded by a special system. The specific data that is of most use for this research is TEOZZ as this data specifies the energy release rate for the burning object (e.g. the burning wall) [1].

**Table C.2:** Numerical Model Sample Output Data File

```
0-----------------------------------------------------------------------
 Time (sec) =     20.0            Total number of iterations =    2419

 ROOM= 1:    TELZR=-6.6618E+03   TELZD=-7.7904E+04   ZMLZZ= 6.5309E+00
             TMLZZ= 2.6433E-02   ZELZZ= 2.8251E+06   TELZZ= 2.7404E+04
             ZHLZZ= 8.9351E-01   ZKLZZ= 4.3085E+02   ZYLOZ= 2.2533E-01
             ZYLDZ= 4.1846E-03   ZYLMZ= 3.2600E-05   ZYLSZ= 9.0880E-04
             ZYLWZ= 1.7489E-03   ZPRZZ=-4.3374E-03   ZKDZZ= 3.0003E+02
             ZYCO = 2.3180E-01   ZYCD = 5.0078E-04   ZYCM = 6.9103E-09
             ZYCS = 1.9264E-07   ZYCW = 3.7071E-07   TMIXM= 1.0827E-03
   OBJ= 1:   FQLOR= 2.5843E+02   FQWOR= 1.7924E+02   FQPOR= 1.2681E+04
   (ID= 1)   ZKOZZ= 7.2700E+02   ZMOZZ= 6.8520E+00   TMOZZ=-2.6531E-03
             TEOZZ=-1.4897E+05
             ZHPZZ= 9.3489E-01   TMPZZ= 3.6900E-01   TEPZZ= 2.6015E+05
             TEPZR= 7.7214E+02
             ZRFZZ= 8.0000E-02
 VENT= 1:    TEUZZ= 3.1111E+04   TMUZZ= 7.1920E-02   TMDZZ= 0.0000E+00
 VENT= 2:    TEUZZ= 1.1660E+05   TMUZZ= 2.6956E-01   TMDZZ=-2.7384E-01
 WALL= 1,1:  FQLWR= 4.3495E+02   FQPWR= 6.6965E+00   FQLWD= 3.9057E+03
             ZKWZZ= 3.5274E+02
 WALL= 1,2:  FQLWR= 0.0000E+00   FQPWR= 0.0000E+00   FQLWD= 0.0000E+00
             ZKWZZ= 3.0000E+02
 WALL= 2,1:  FQLWR= 0.0000E+00   FQPWR= 0.0000E+00   FQLWD= 0.0000E+00
             ZKWZZ= 3.0000E+02
 WALL= 2,2:  FQLWR= 0.0000E+00   FQPWR= 0.0000E+00   FQLWD= 0.0000E+00
             ZKWZZ= 3.0000E+02
 -----------------------------------------------------------------------
```

# APPENDIX D: ROOM/CORNER SCENARIO - SWEDISH MATERIALS

| Global Variable Constants | | |
|---|---|---|
| f | 0.18 | (-) |
| $q''_{fs}$ | 30 | ($kWm^{-2}$) |
| $q''_{start}$ | 50 | ($kWm^{-2}$) |
| K | 0.018 | ($m^2kW^{-1}$) |

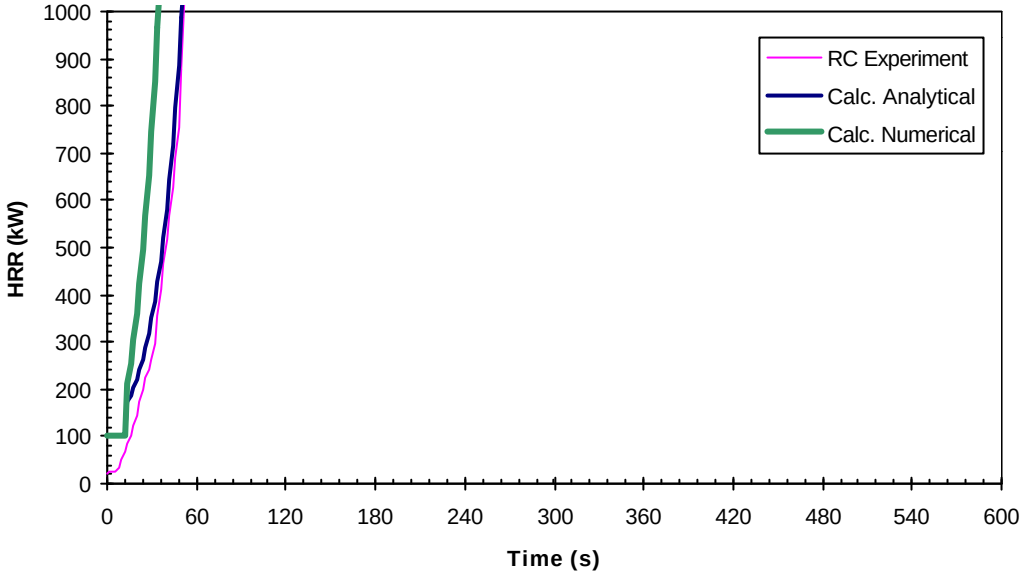


**Figure D.1:** Material S1 (insulating Fibre board) HRR Comparison – RC Test Scenario

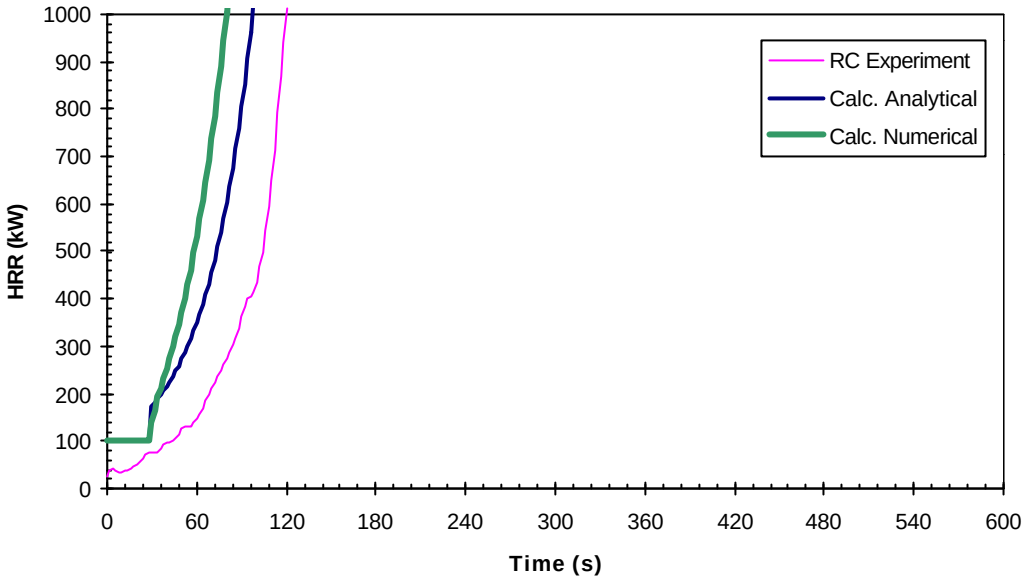


**Figure D.2:** Material S2 (Medium Density Fibre board) HRR Comparison – RC Test Scenario

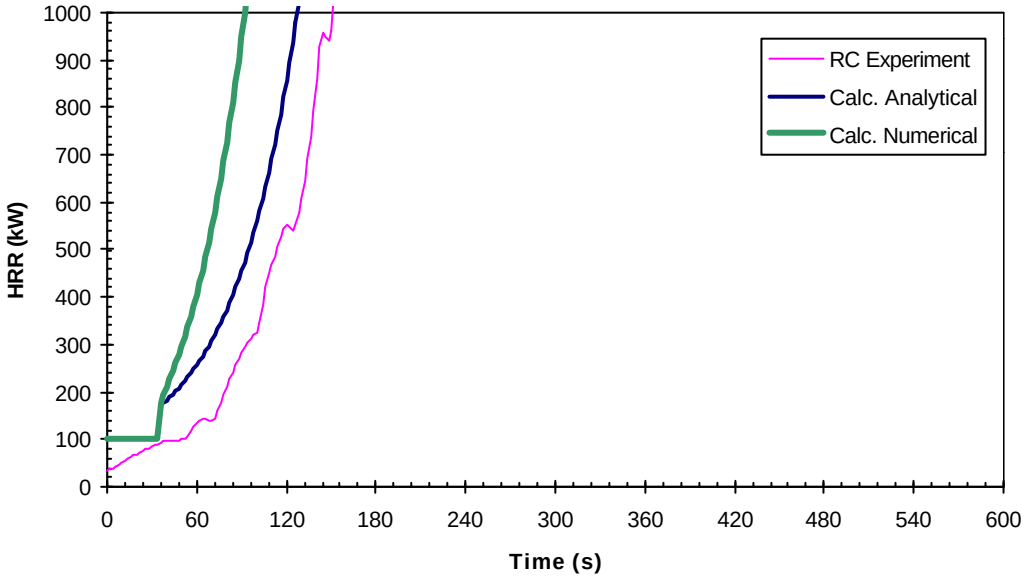


**Figure D.3:** Material S3 (Particle board) HRR Comparison – RC Test Scenario

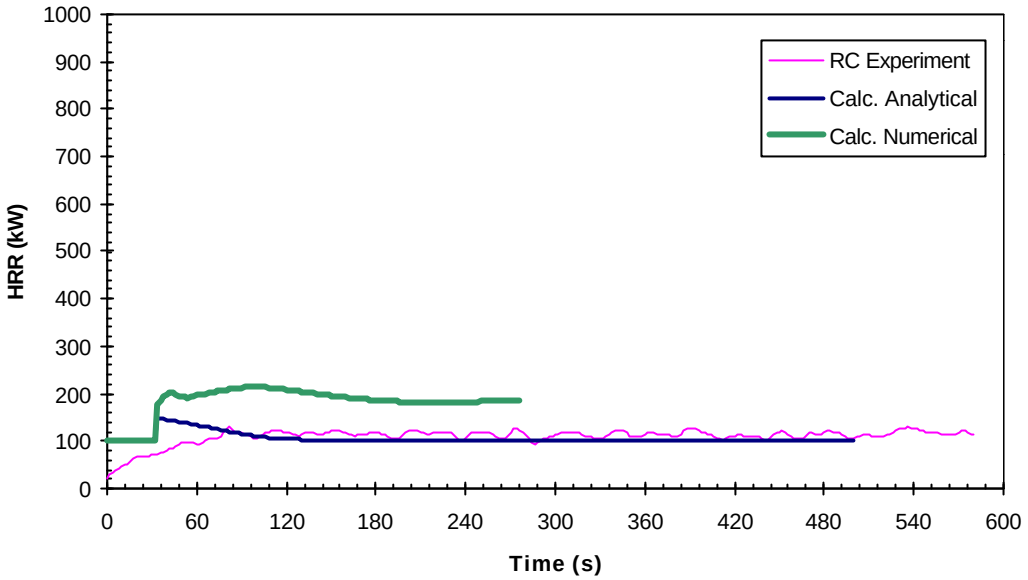


**Figure D.4:** Material S4 (Gypsum Plasterboard) HRR Comparison – RC Test Scenario

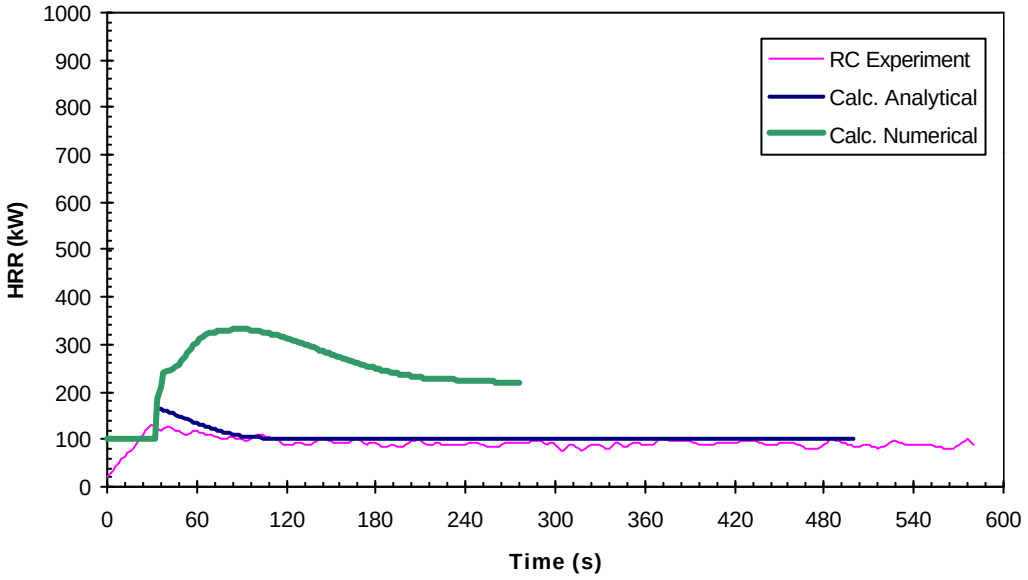


**Figure D.5:** Material S5 (PVC covering on S4) HRR Comparison – RC Test Scenario

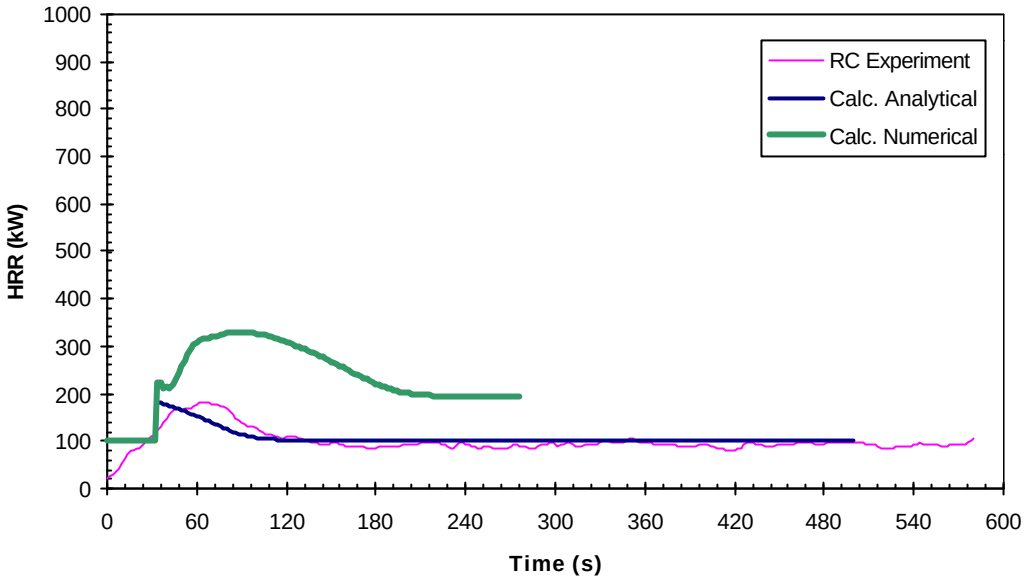


**Figure D.6:** Material S6 (Paper covering on S4) HRR Comparison – RC Test Scenario

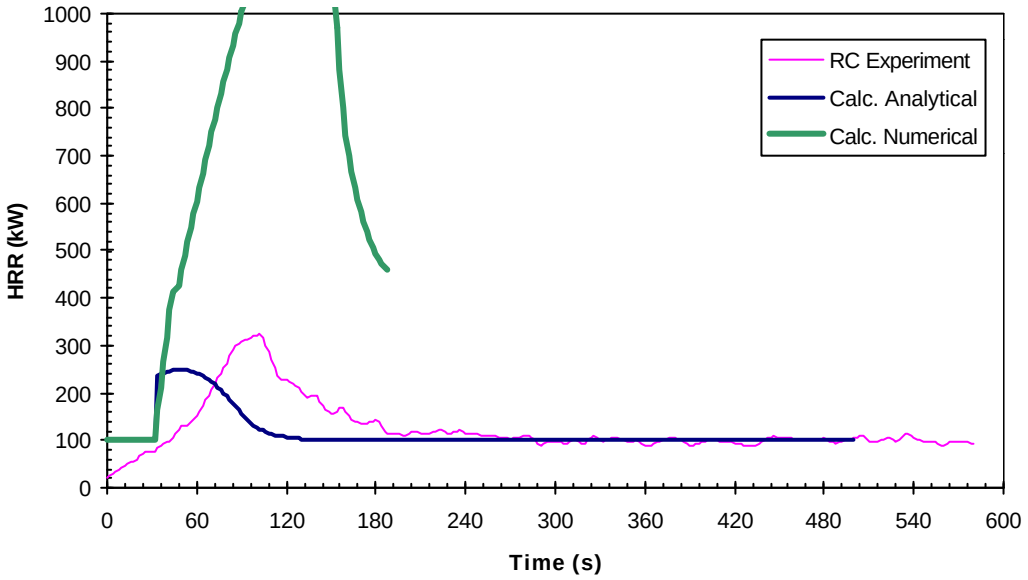


**Figure D.7:** Material S7 (Textile covering on S4) HRR Comparison – RC Test Scenario

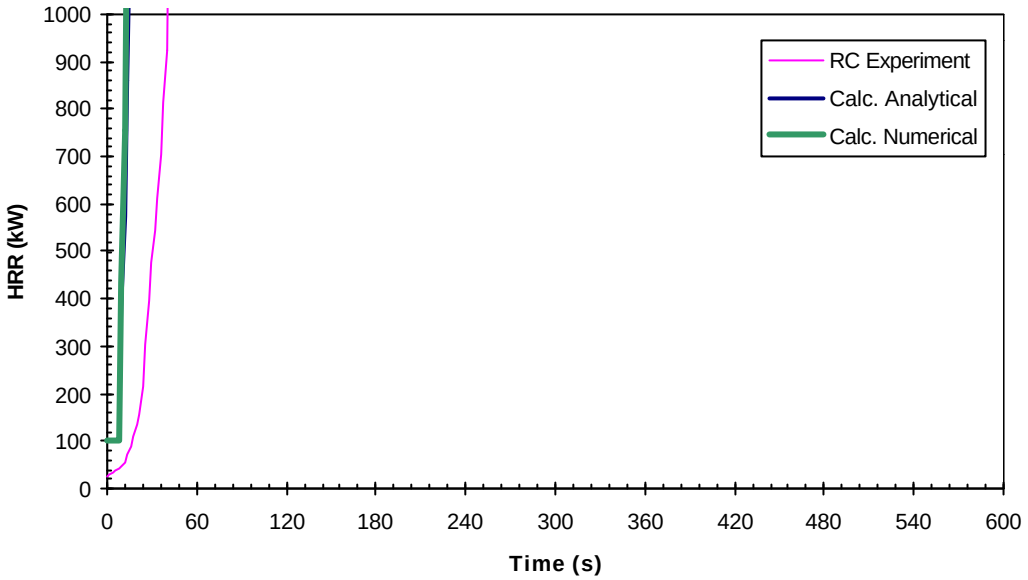


**Figure D.8:** Material S8 (Textile covering on Mineral Wool) HRR Comparison – RC Test Scenario

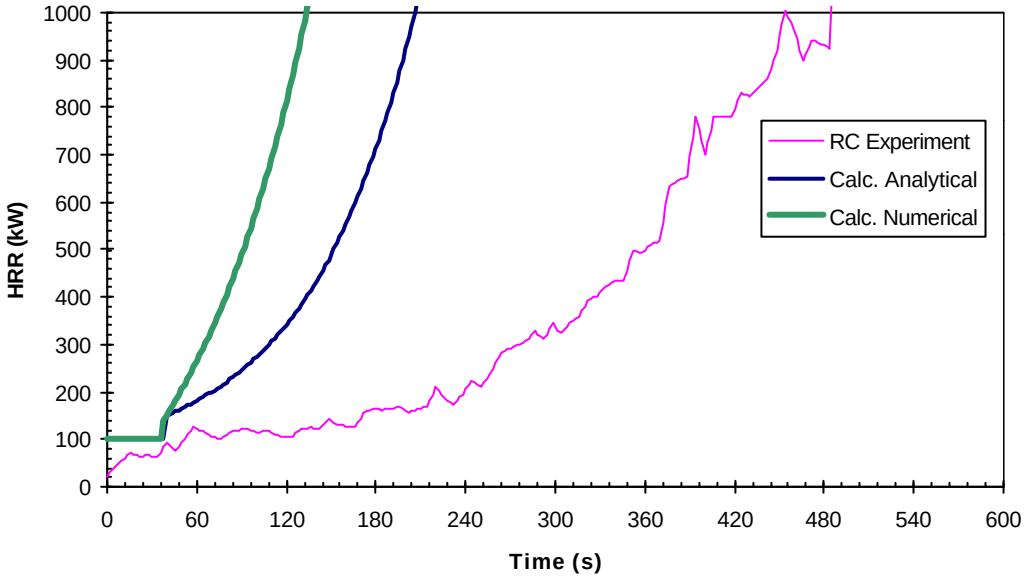


**Figure D.9:** Material S9 (Melamine-faced Particle board) HRR Comparison – RC Test Scenario

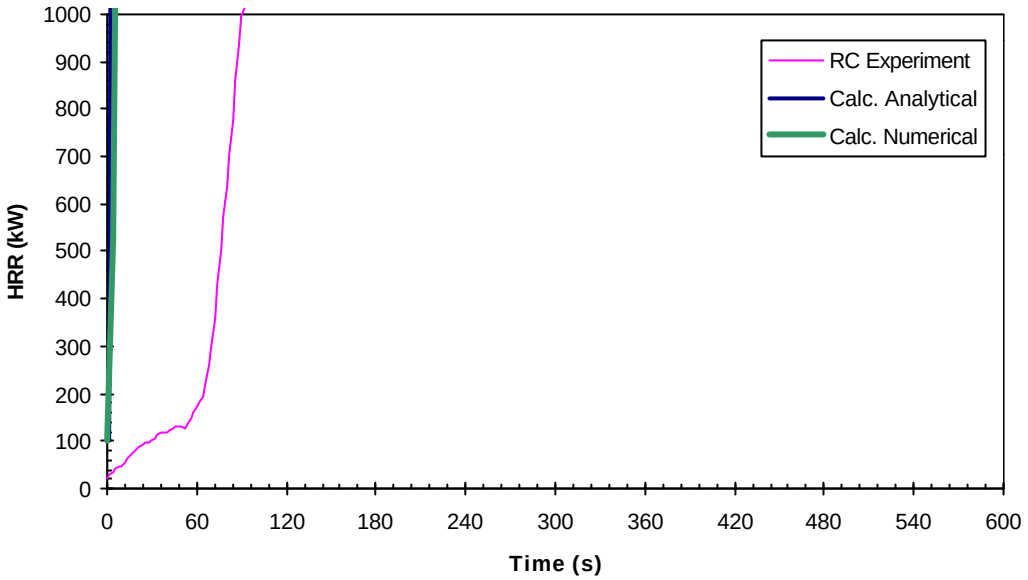


**Figure D.10:** Material S10 (expanded Polystyrene) HRR Comparison – RC Test Scenario

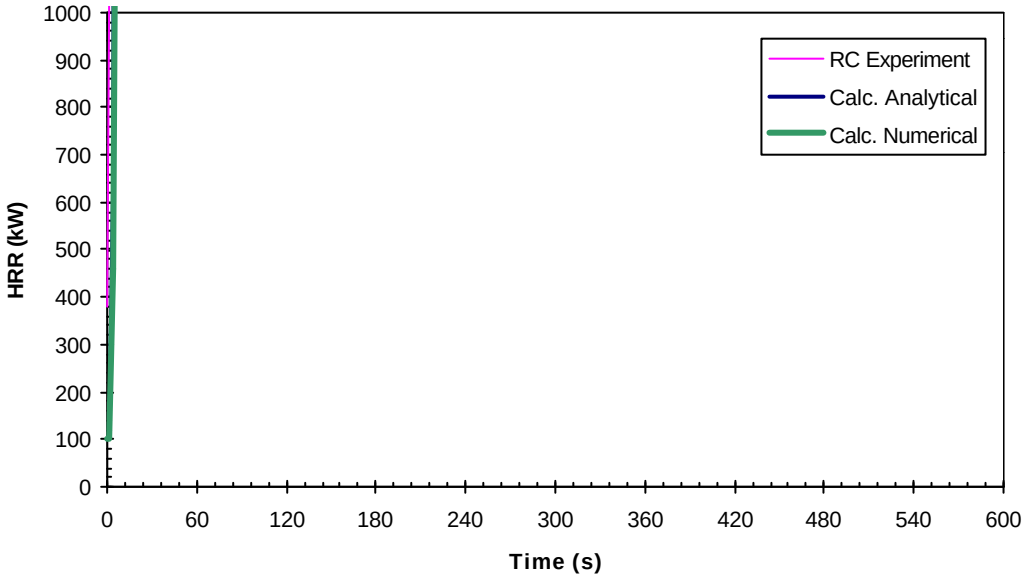


**Figure D.11:** Material S11 (rigid Polyurethane foam) HRR Comparison – RC Test Scenario

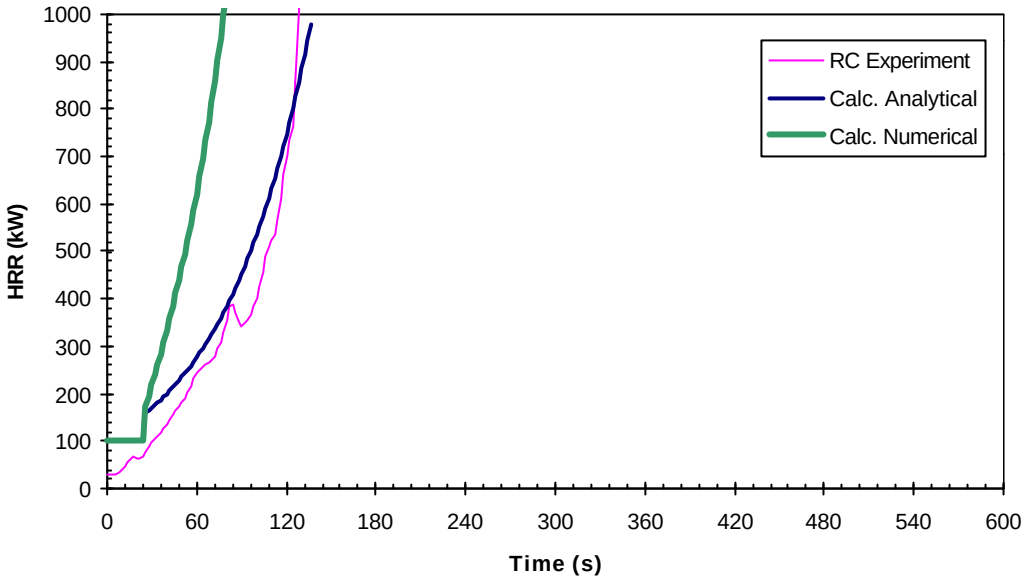


**Figure D.12:** Material S12 (Wood panel (Spruce)) HRR Comparison – RC Test Scenario

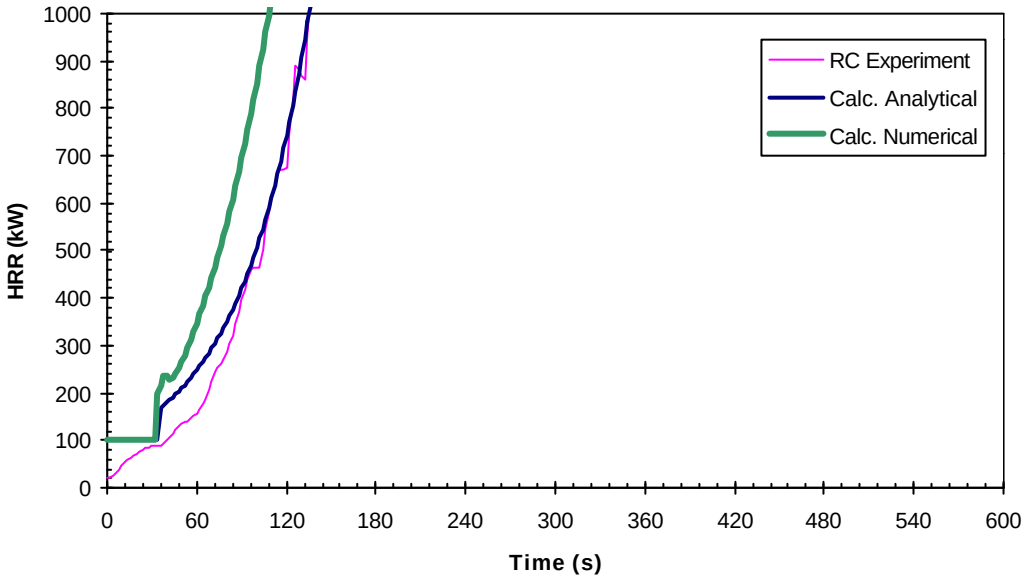


**Figure D.13:** Material S13 (Paper covering on S3) HRR Comparison – RC Test Scenario

# APPENDIX E: ROOM/CORNER SCENARIO – EUREFIC MATERIALS

| Global Variable Constants | | |
|---|---|---|
| f | 0.18 | (-) |
| $q''_{fs}$ | 30 | ($kWm^{-2}$) |
| $q''_{start}$ | 50 | ($kWm^{-2}$) |
| K | 0.018 | ($m^2kW^{-1}$) |

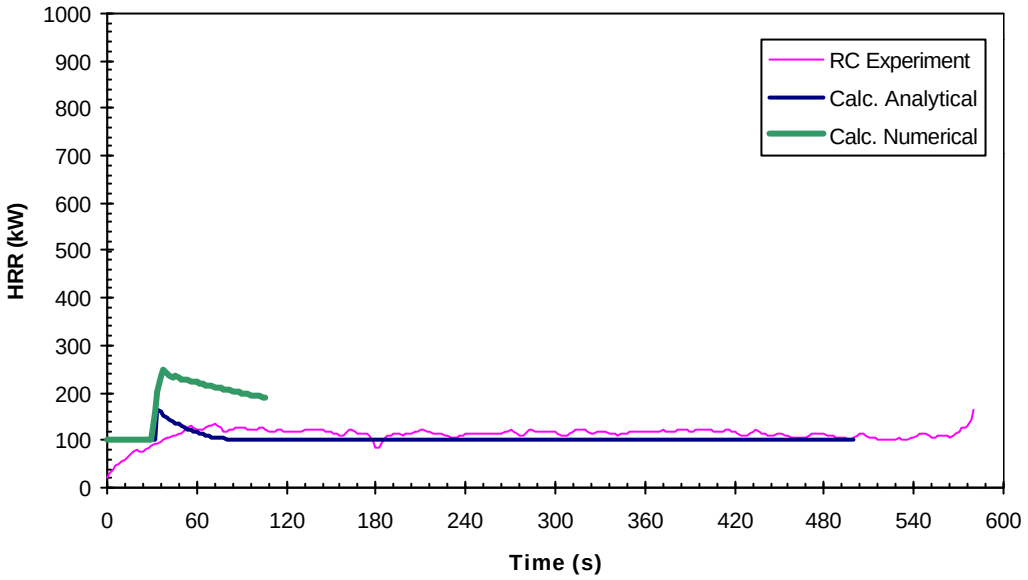


**Figure E.1** Material E1 (painted Gypsum Paper Plaster board) HRR Comparison – RC Test Scenario

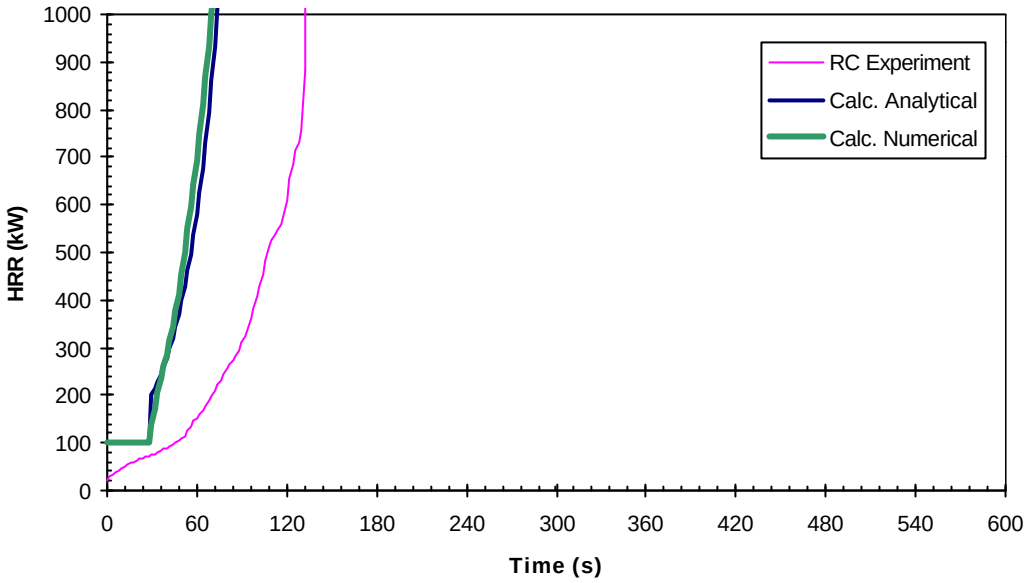


**Figure E.2:** Material E2 (ordinary Plywood) HRR Comparison – RC Test Scenario

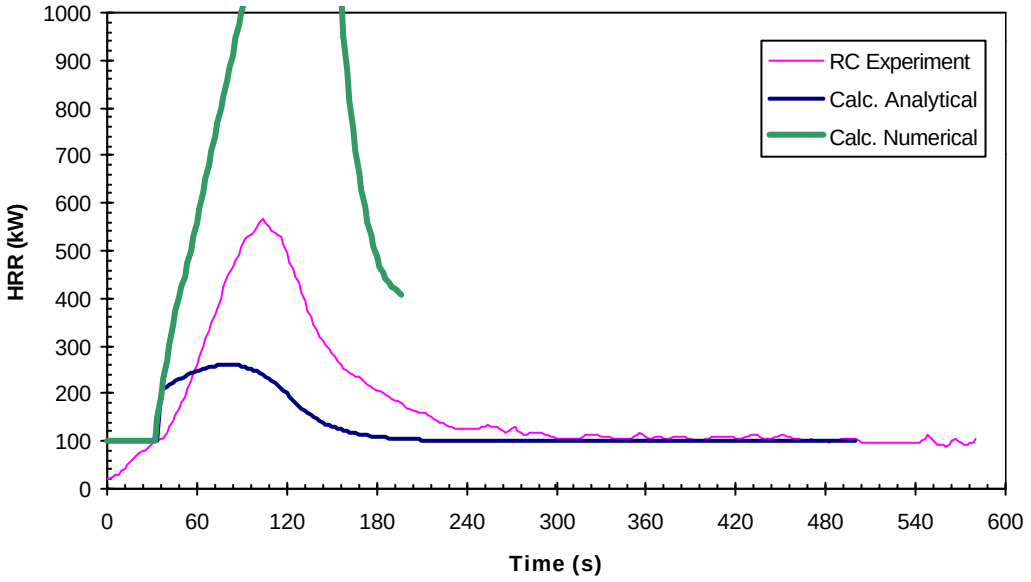


**Figure E.3:** Material E3 (Textile Wall-covering on Gypsum Paper Plaster board) HRR Comparison – RC Test Scenario

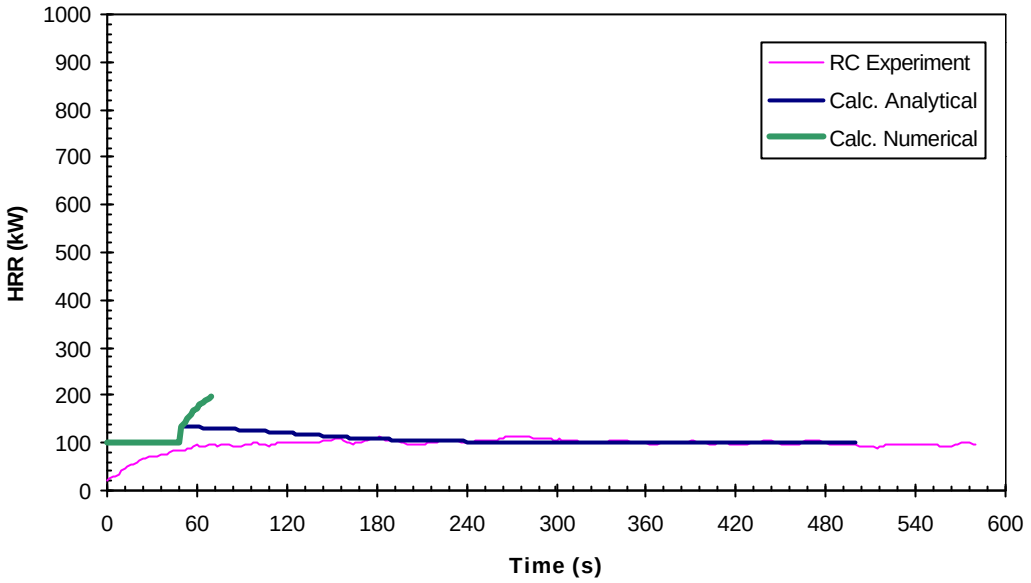


**Figure E.4:** Material E4 (Melamine faced High Density Non-combustible board) HRR Comparison – RC Test Scenario

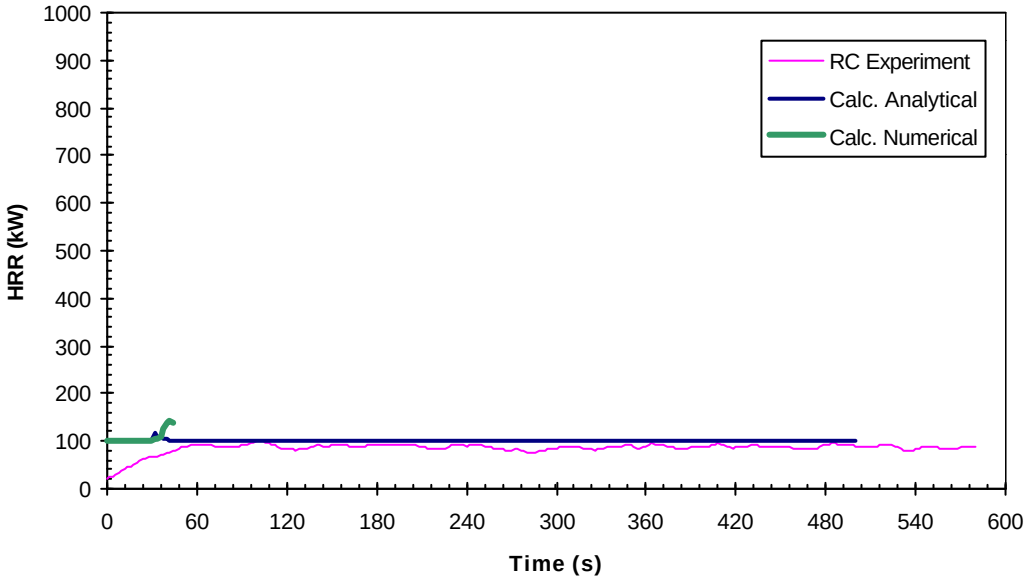


**Figure E.5:** Material E5 (Plastic faced Steel sheet on Mineral Wool) HRR Comparison – RC Test Scenario

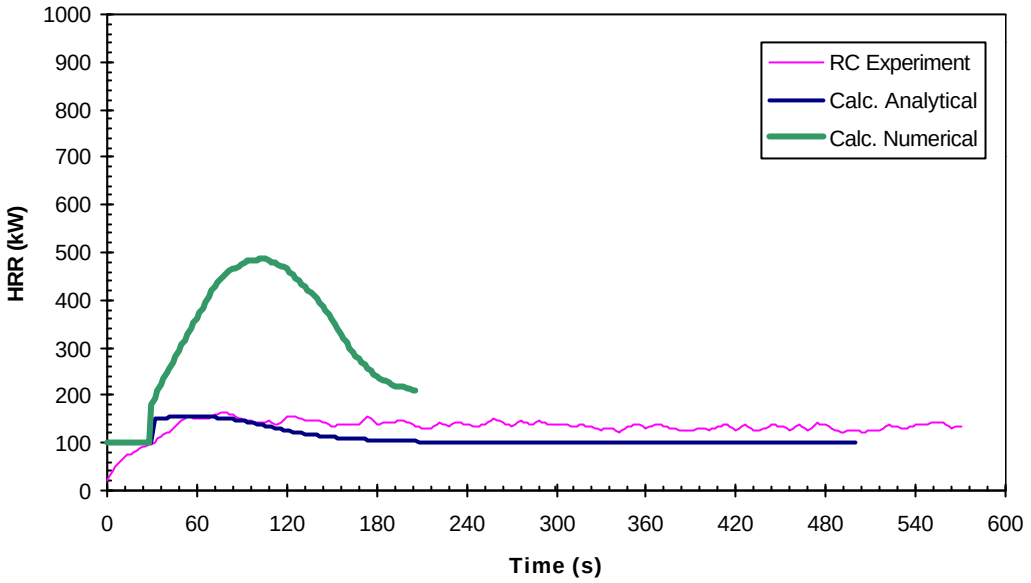


**Figure E.6:** Material E6 (FR Particle board - type B1) HRR Comparison – RC Test Scenario

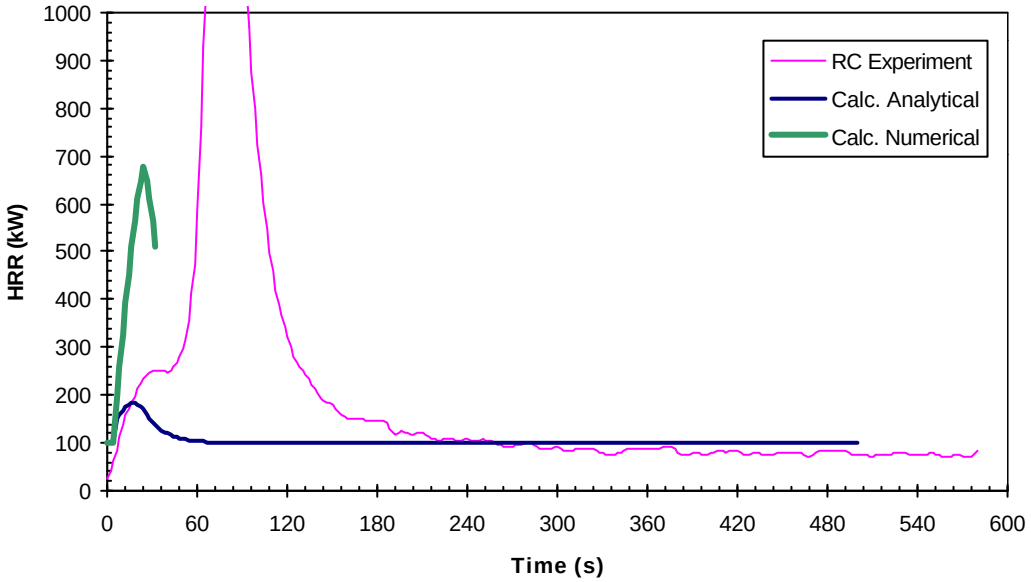


**Figure E.7:** Material E7 (faced Rockwool) HRR Comparison – RC Test Scenario

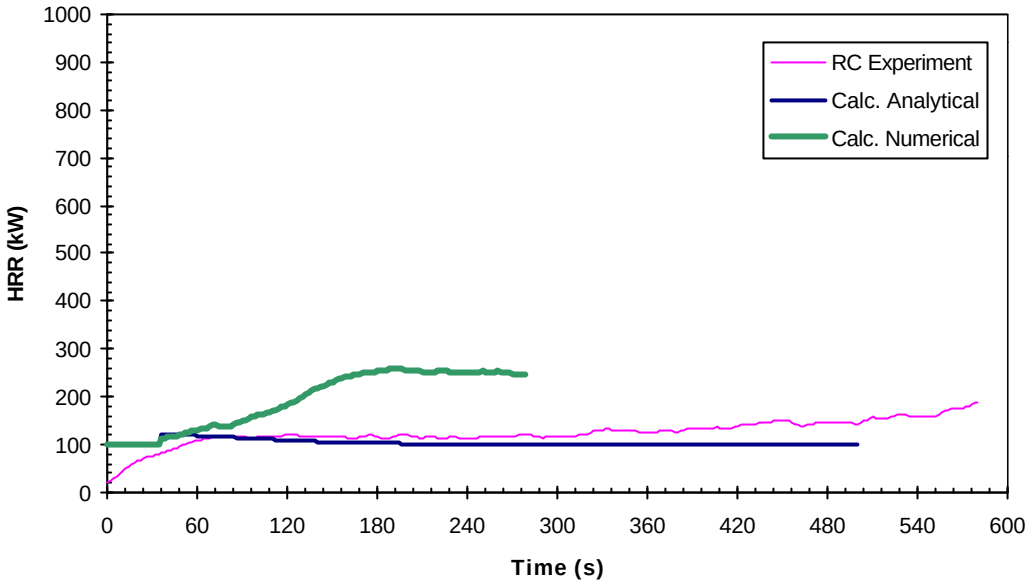


**Figure E.8:** Material E8 (FR Particle board) HRR Comparison – RC Test Scenario

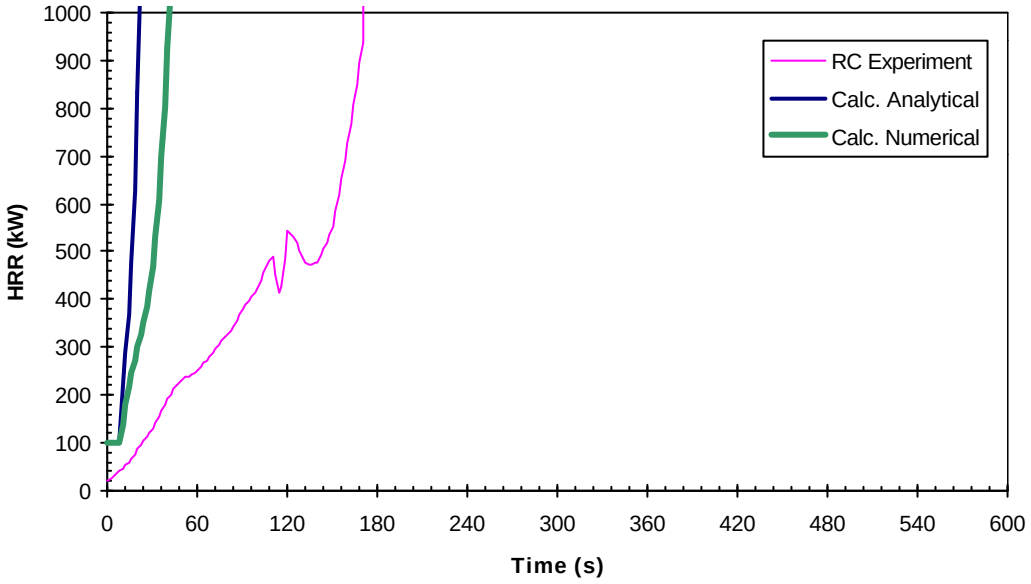


**Figure E.9:** Material E9 (Polyurethane foam covered with Steel sheet) HRR Comparison – RC Test Scenario

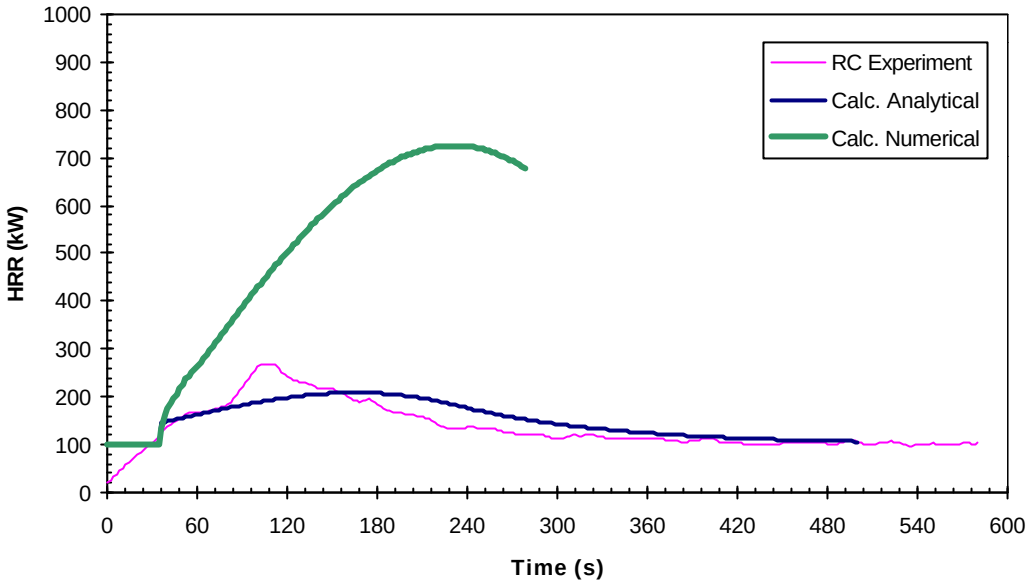


**Figure E.10:** Material E10 (PVC wall Carpet on Gypsum Paper Plaster board) HRR Comparison – RC Test Scenario

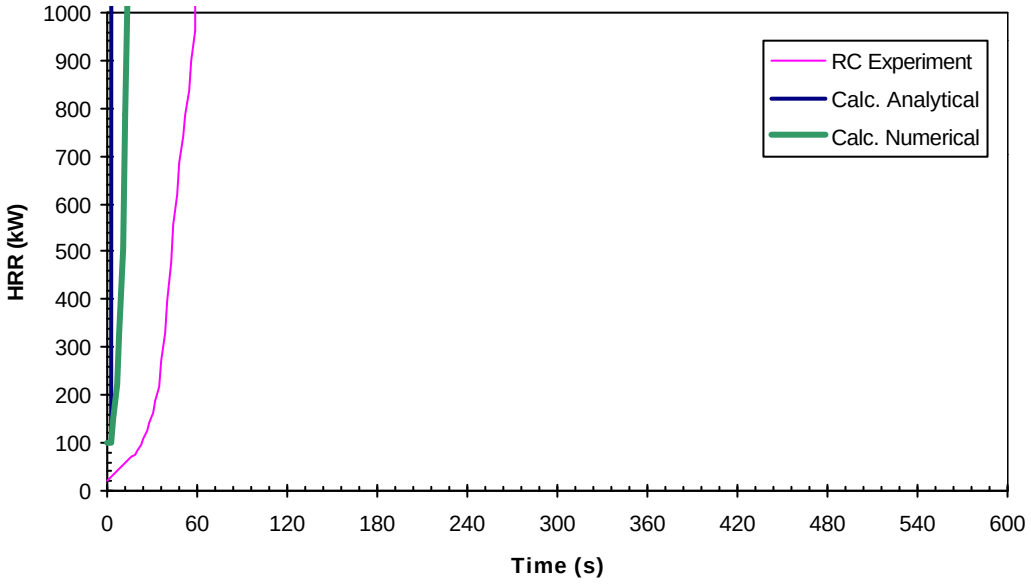


**Figure E.11:** Material E11 (FR Polystyrene) HRR Comparison – RC Test Scenario

# APPENDIX F: ROOM/CORNER SCENARIO – "M SERIES" MATERIALS

| Global Variable Constants | | |
|---|---|---|
| f | 0.18 | (-) |
| $q''_{fs}$ | 30 | ($kWm^{-2}$) |
| $q''_{start}$ | 50 | ($kWm^{-2}$) |
| K | 0.018 | ($m^2kW^{-1}$) |

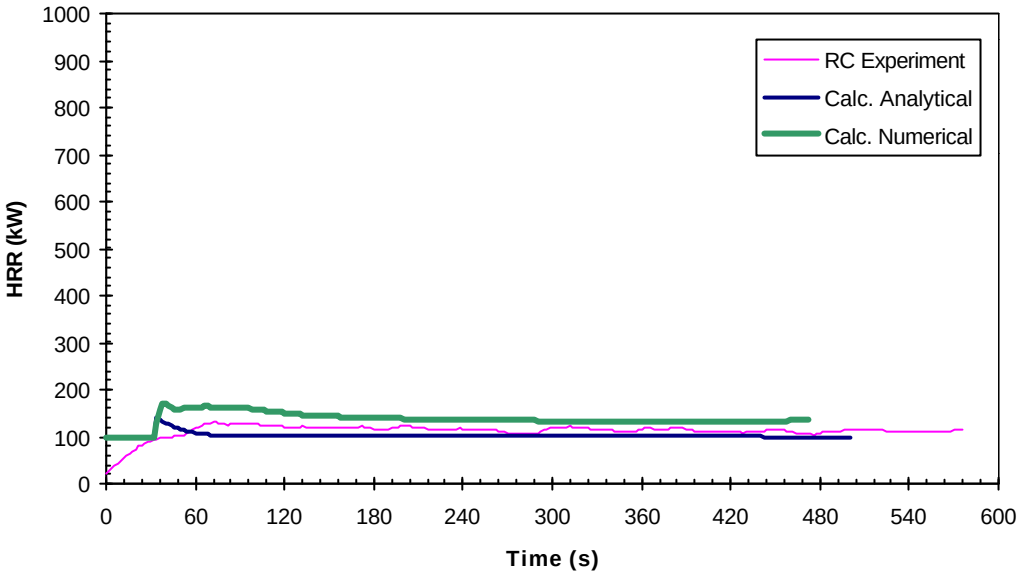


**Figure F.1:** Material M1 (Plasterboard) HRR Comparison – RC Test Scenario

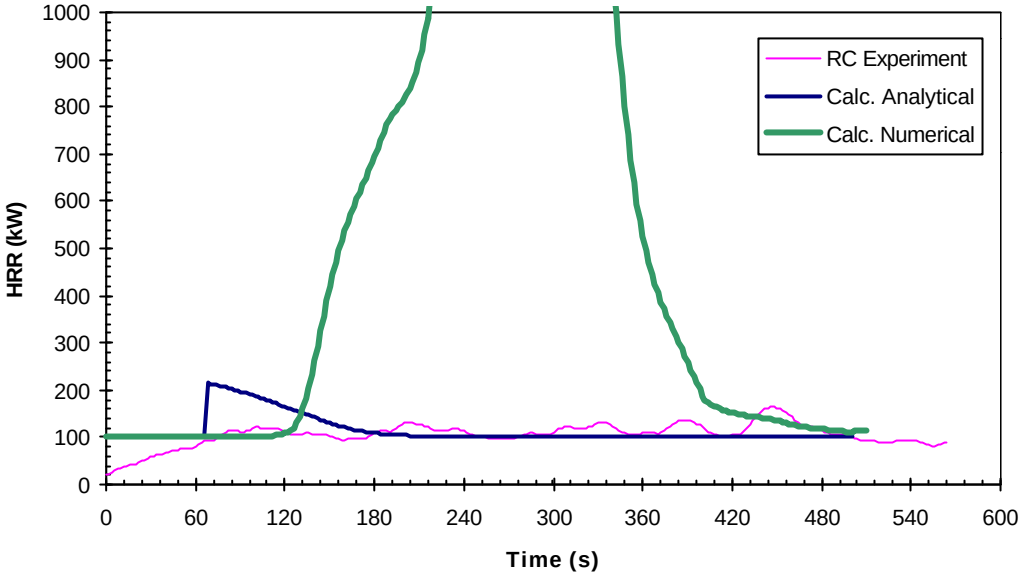


**Figure F.2:** Material M2 (FR PVC) HRR Comparison – RC Test Scenario

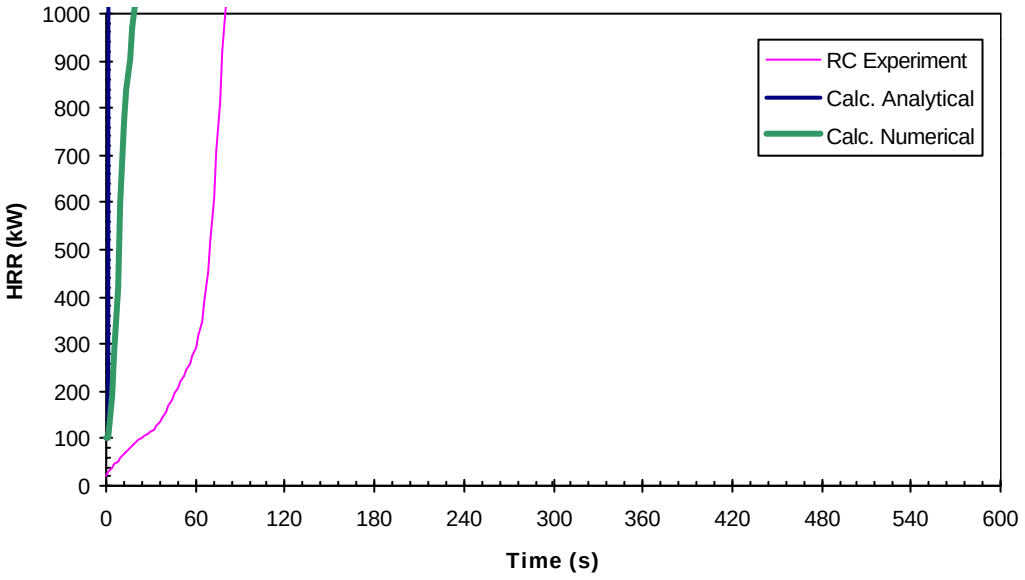


**Figure F.3:** Material M3 (FR extruded Polystyrene board) HRR Comparison – RC Test Scenario

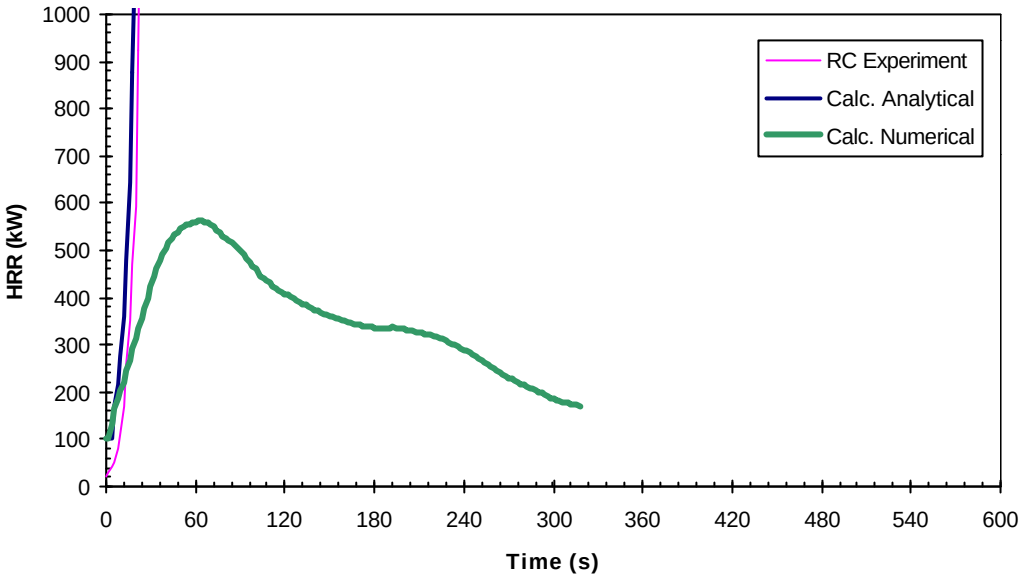


**Figure F.4:** Material M4 (PUR foam panel with Aluminium foil faces) HRR Comparison – RC Test Scenario

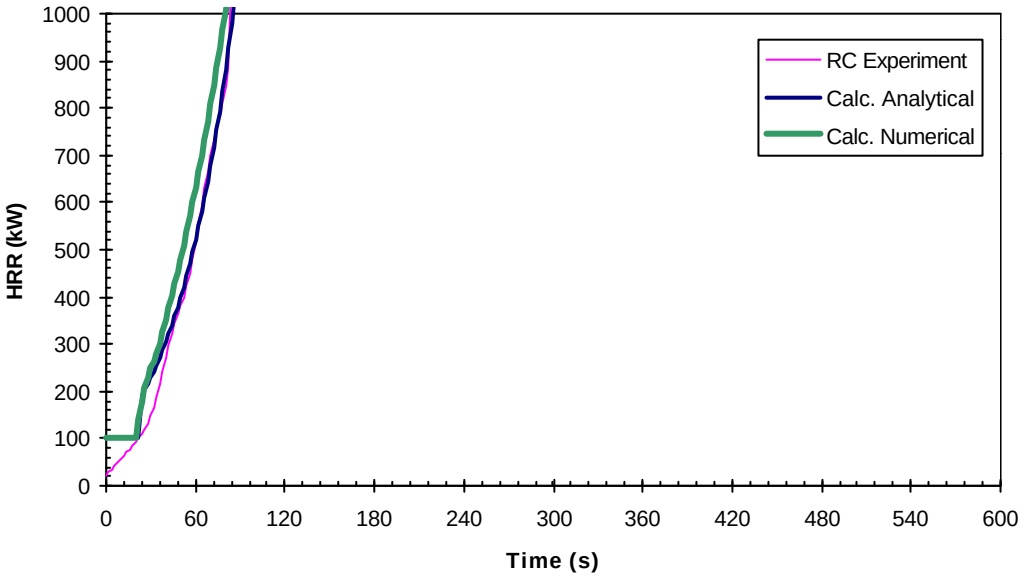


**Figure F.5:** Material M5 (varnished mass Timber, Pine) HRR Comparison – RC Test Scenario

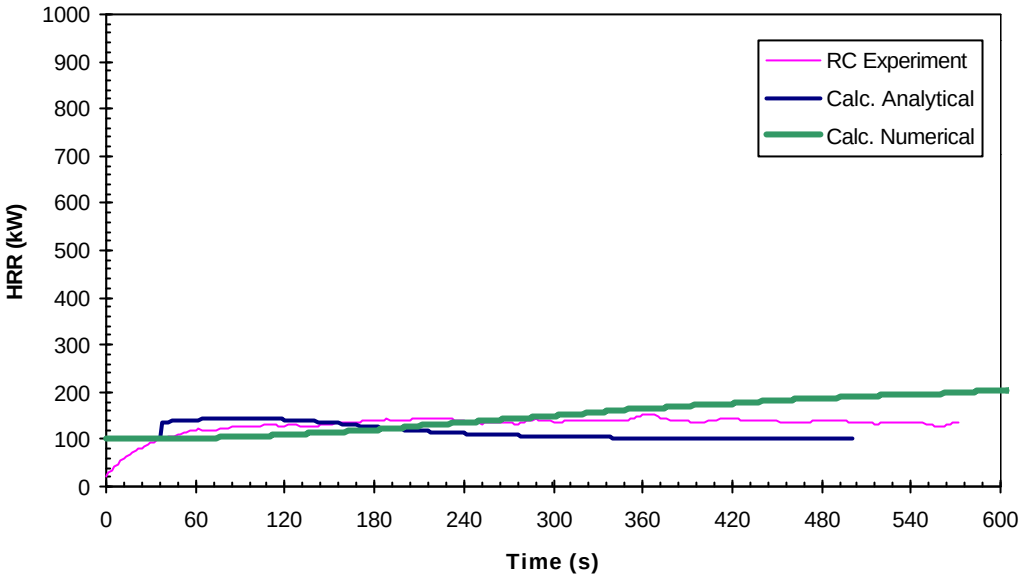


**Figure F.6:** Material M6 (FR Chipboard) HRR Comparison – RC Test Scenario

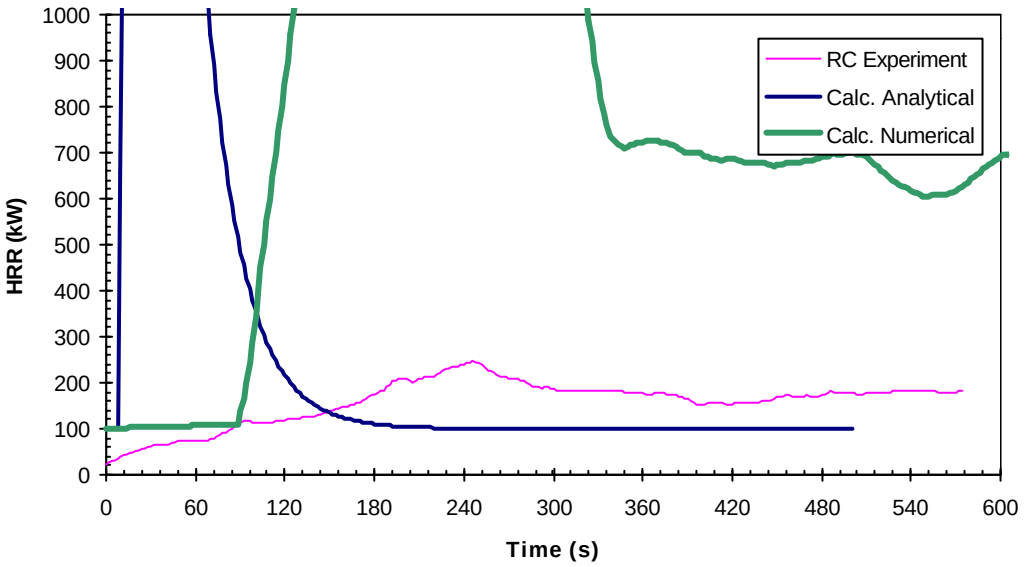


**Figure F.7:** Material M7 (FR Polycarbonate panel (3 layered)) HRR Comparison – RC Test Scenario

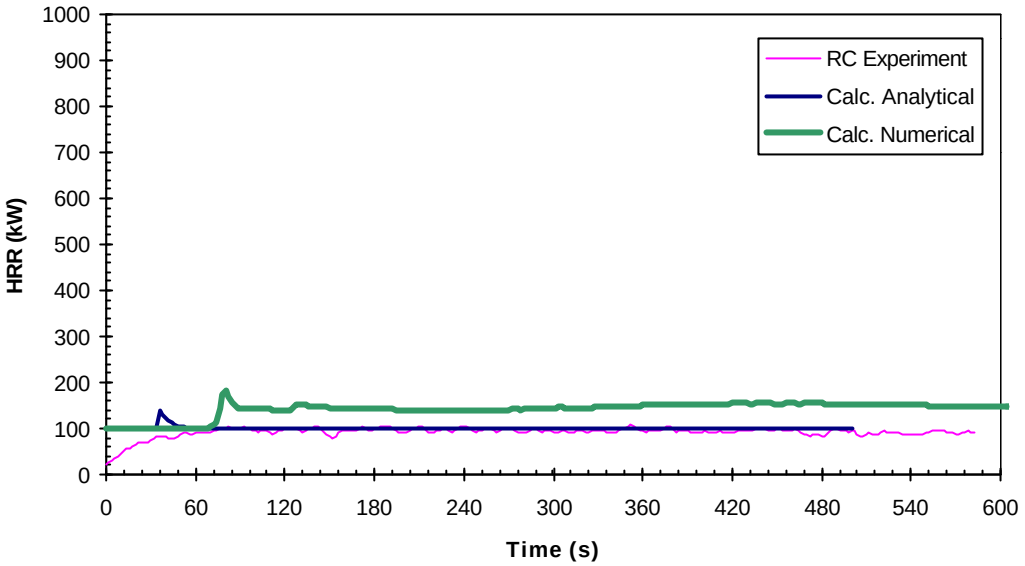


**Figure F.8:** Material M8 (painted Plasterboard) HRR Comparison – RC Test Scenario

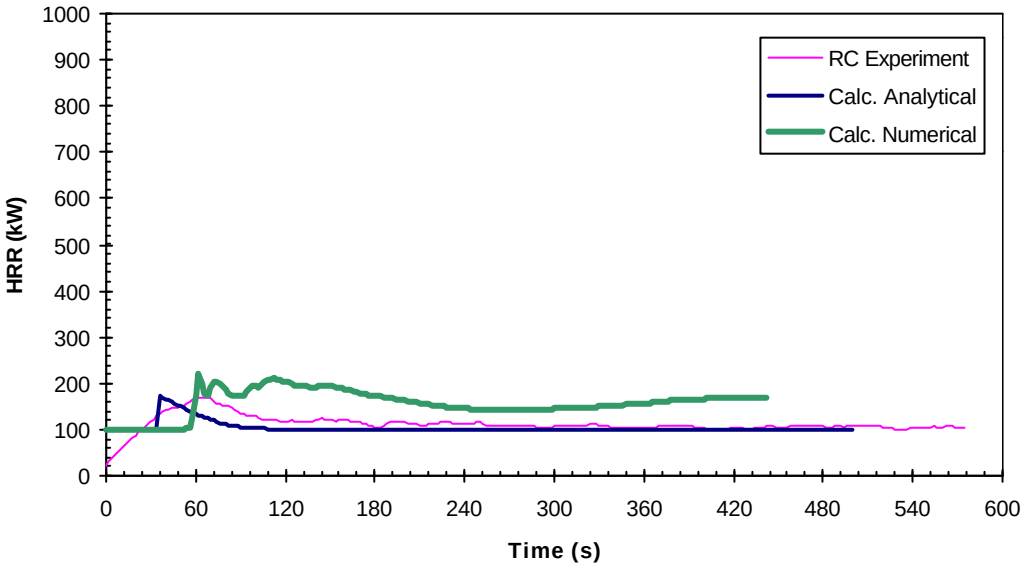


**Figure F.9:** Material M9 (Paper wall covering on Plasterboard) HRR Comparison – RC Test Scenario

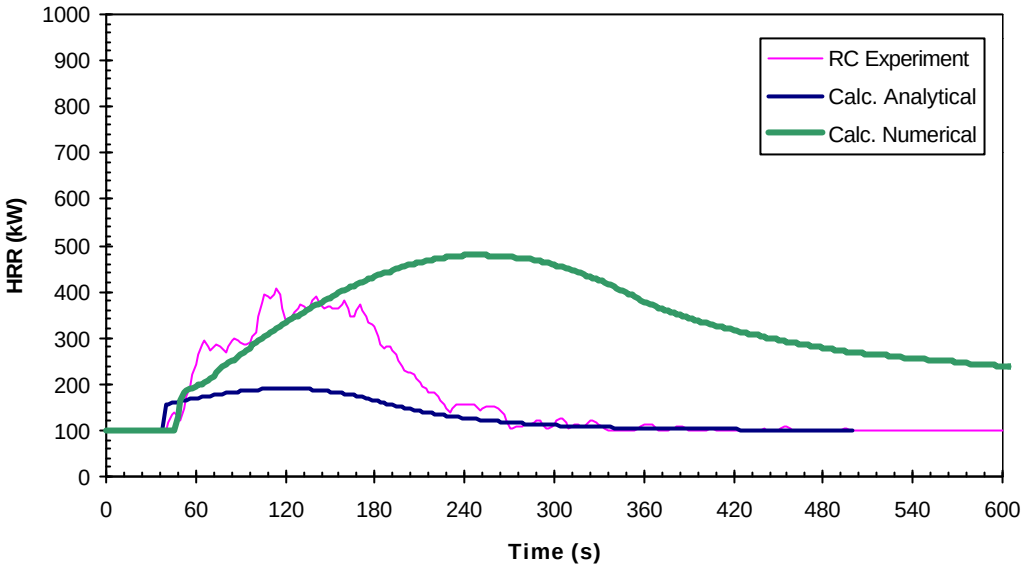


**Figure F.10:** Material M10 (PVC wall carpet on Plasterboard) HRR Comparison – RC Test Scenario

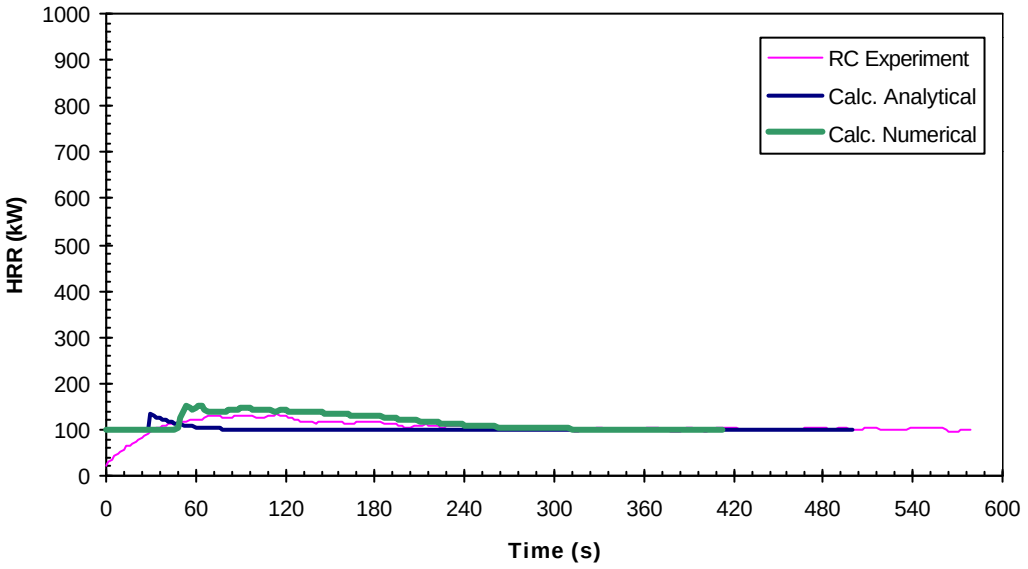


**Figure F.11:** Material M11 (Plastic-faced Steel sheet on Mineral Wool) HRR Comparison – RC Test Scenario

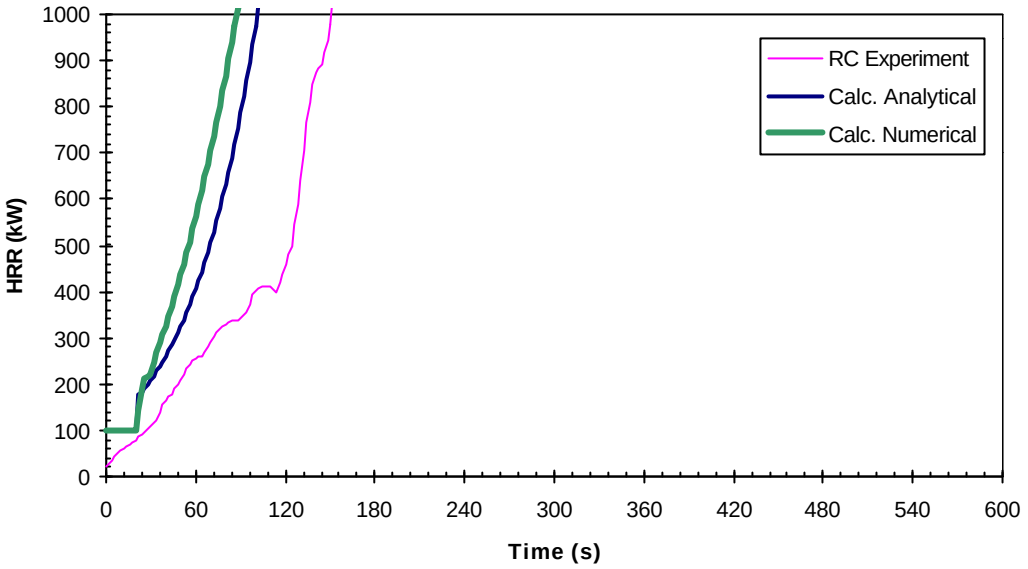


**Figure F.12:** Material M12 (unvarnished mass Timber, Spruce) HRR Comparison – RC Test Scenario

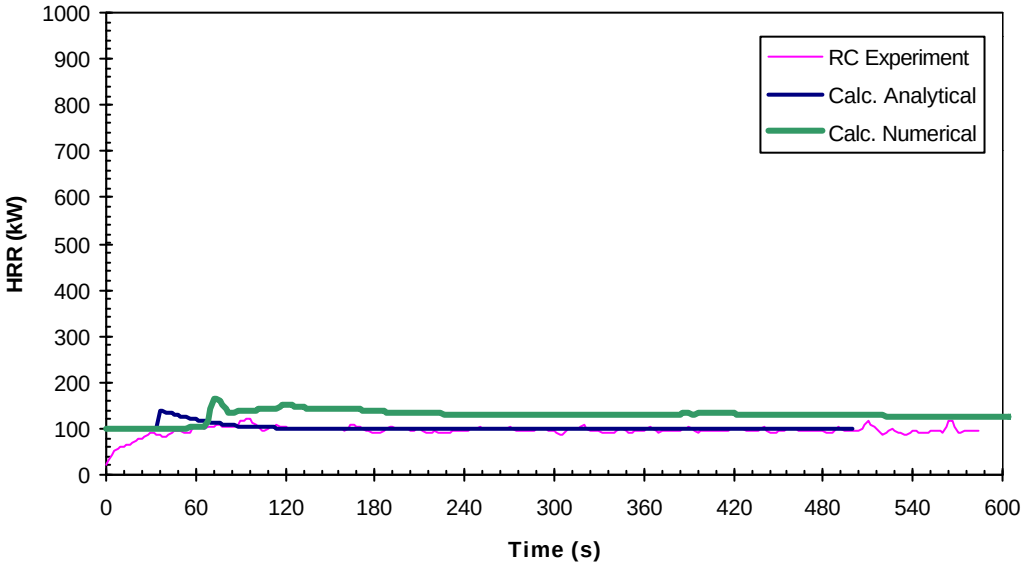


**Figure F.13:** Material M13 (Plasterboard on Polystyrene) HRR Comparison – RC Test Scenario

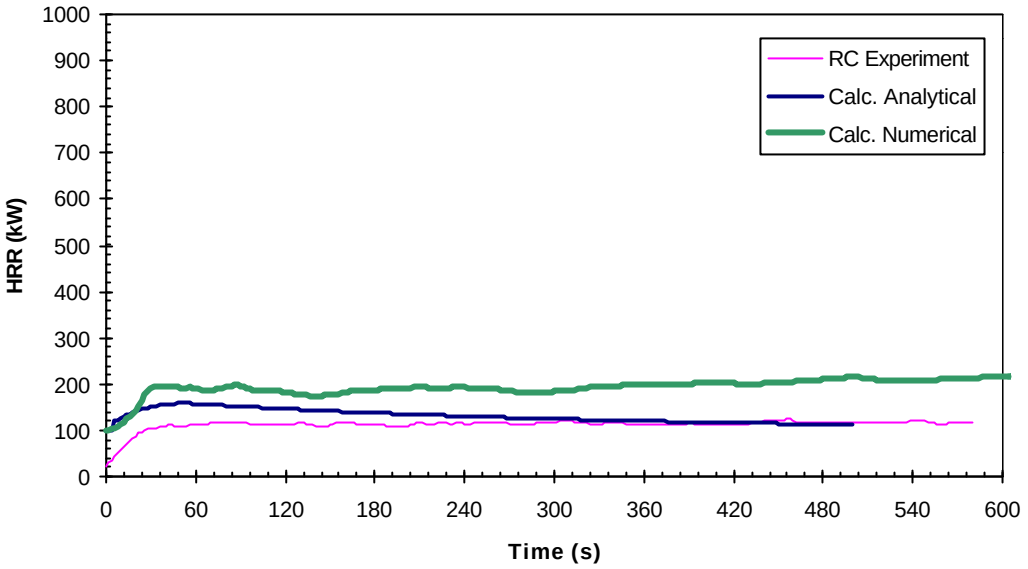


**Figure F.14:** Material M14 (Phenolic foam) HRR Comparison – RC Test Scenario

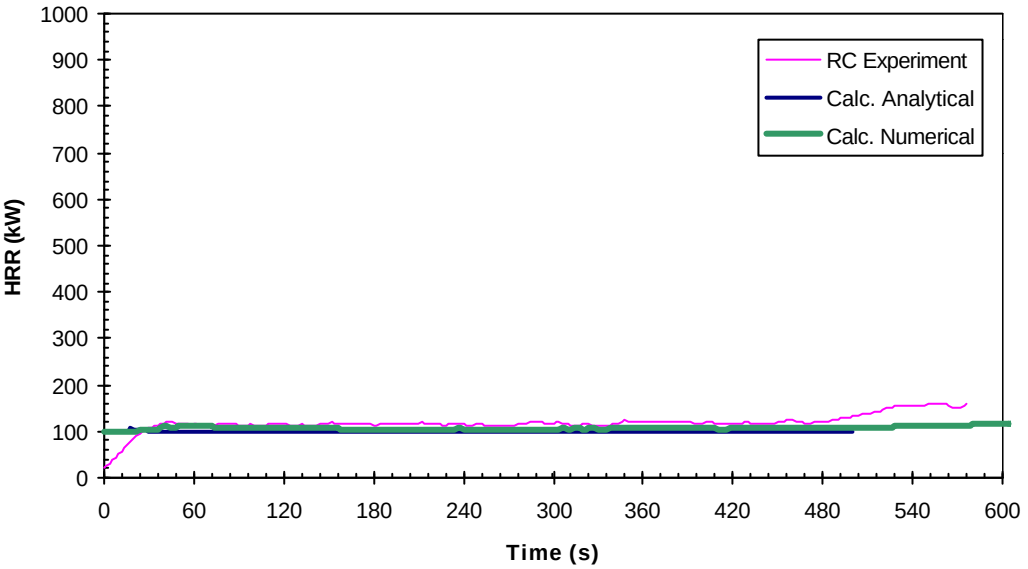


**Figure F.15:** Material M15 (Intumescent coat on Particle board) HRR Comparison – RC Test Scenario

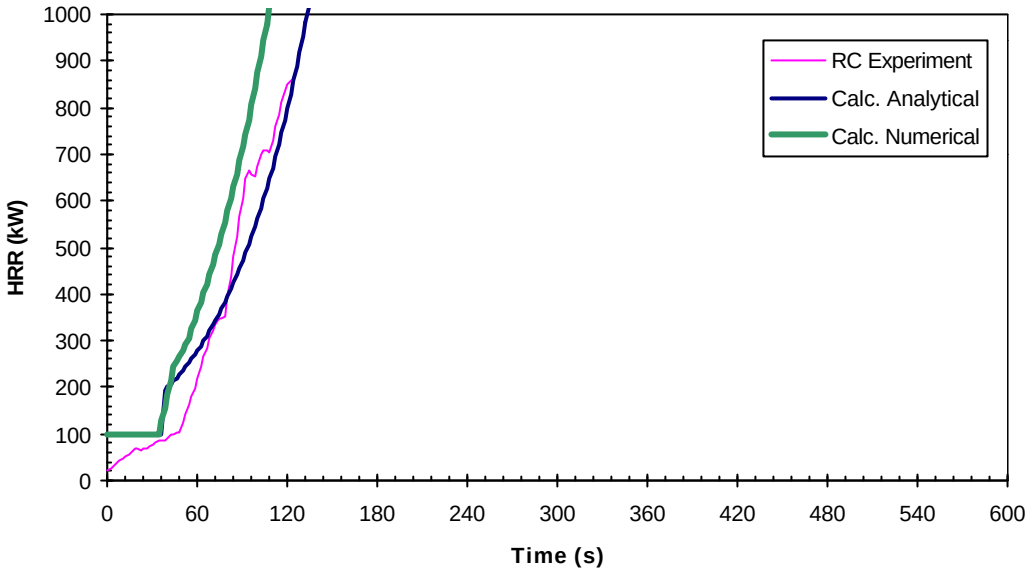


**Figure F.16:** Material M16 (Melamine faced MDF board) HRR Comparison – RC Test Scenario

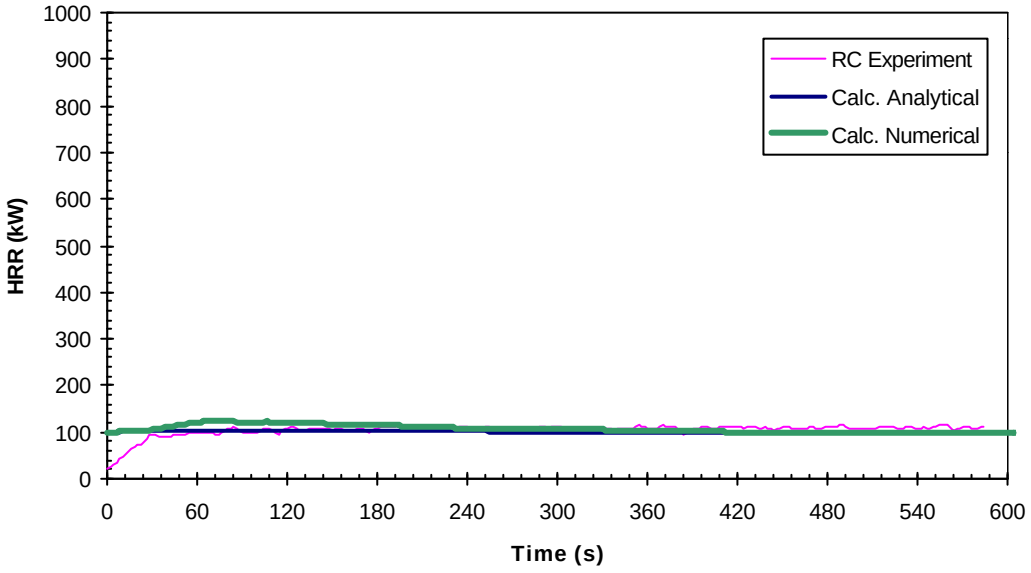


**Figure F.17:** Material M19 (unfaced Rockwool) HRR Comparison – RC Test Scenario

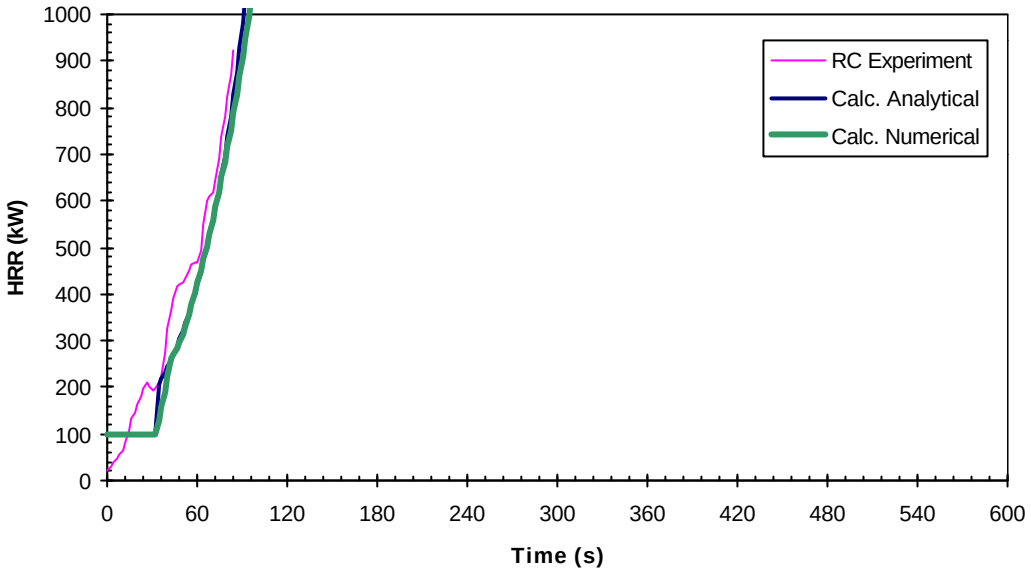


**Figure F.18:** Material M20 (Melamine faced Particle board) HRR Comparison – RC Test Scenario

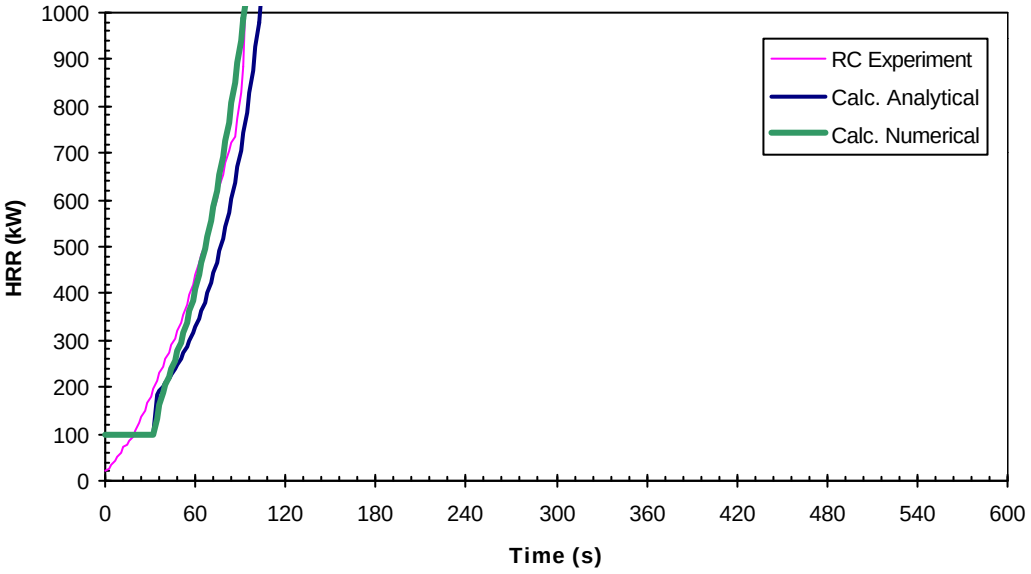


**Figure F.19:** Material M22 (ordinary Particle board) HRR Comparison – RC Test Scenario

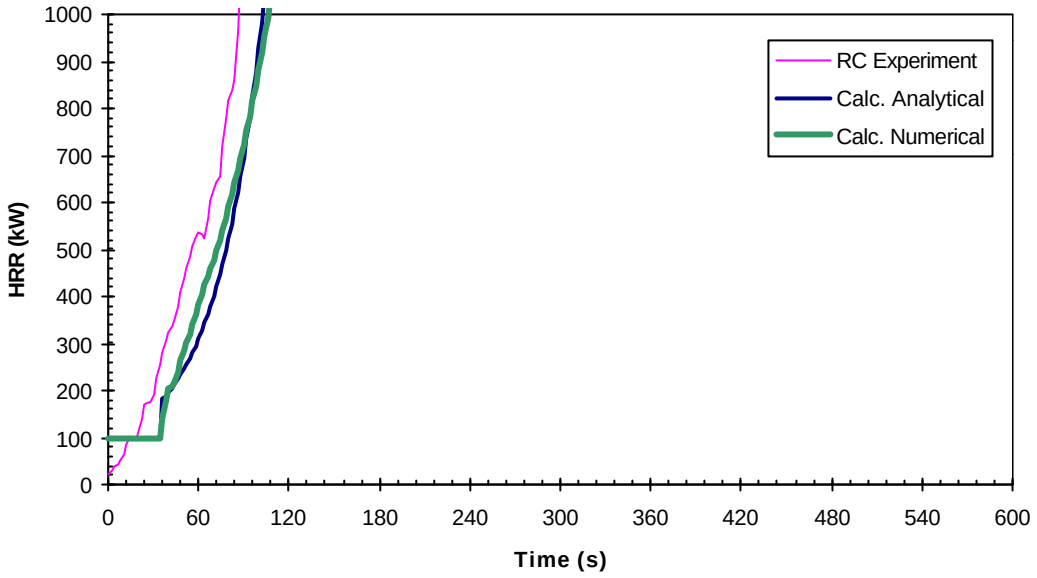


**Figure F.20:** Material M23 (ordinary Plywood, Birch) HRR Comparison – RC Test Scenario

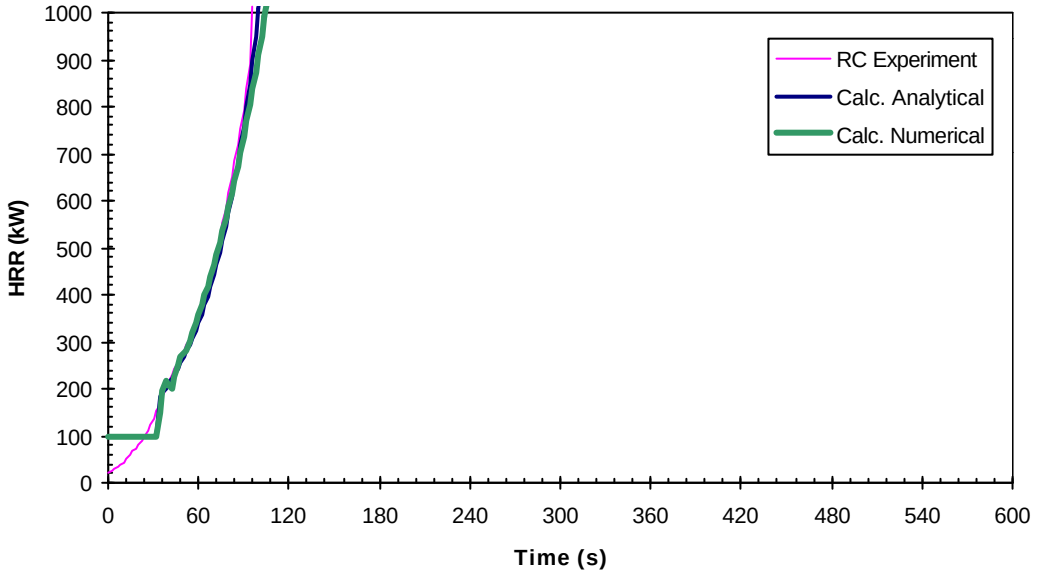


**Figure F.21:** Material M24 (Paper wall covering on Particle board) HRR Comparison – RC Test Scenario

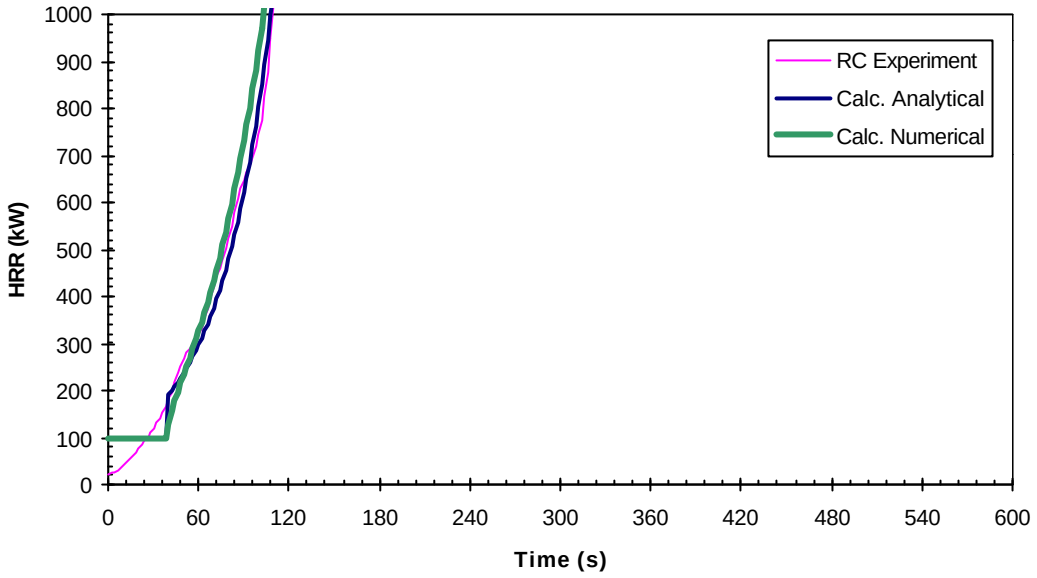


**Figure F.22:** Material M25 (Medium Density Fibre tiles) HRR Comparison – RC Test Scenario

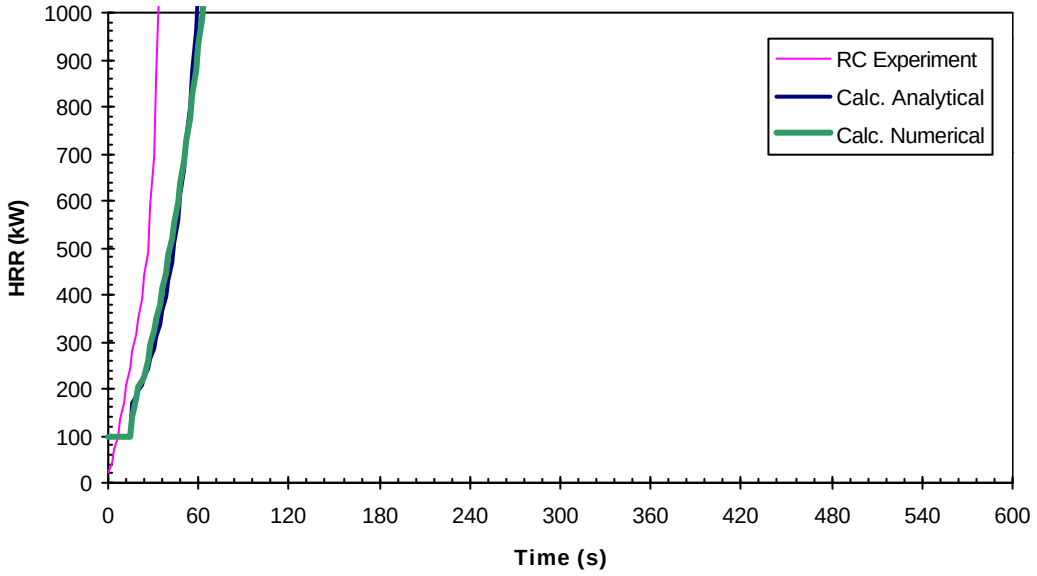


**Figure F.23:** Material M26 (Low Density Fibre board) HRR Comparison – RC Test Scenario

# APPENDIX G: SBI SCENARIO – "M SERIES" MATERIALS

| Global Variable Constants | | |
|---|---|---|
| f | 0.55 | (-) |
| $q''_{fs}$ | 10 | ($kWm^{-2}$) |
| $q''_{start}$ | 30 | ($kWm^{-2}$) |
| K | 0.020 | ($m^2kW^{-1}$) |

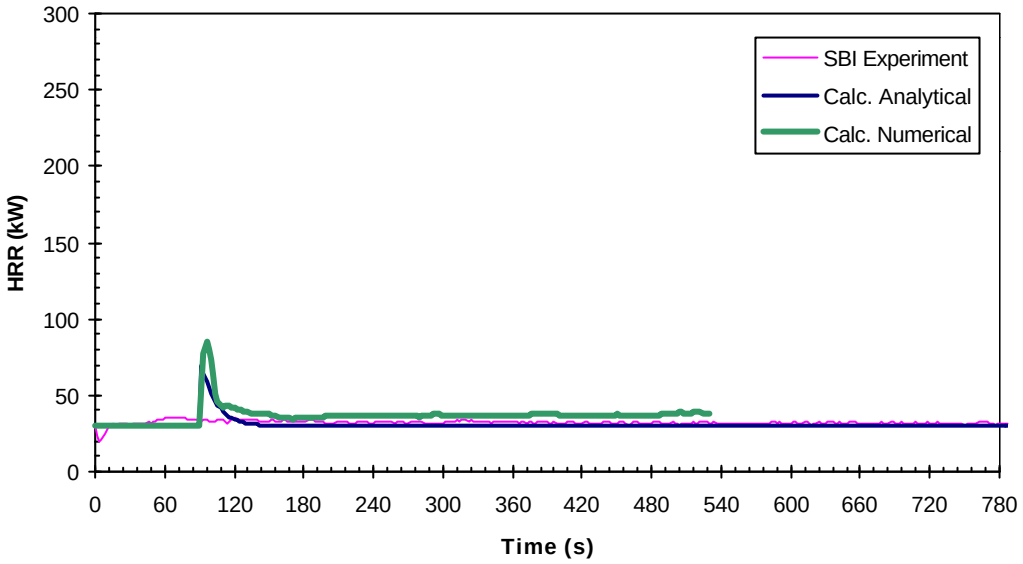


**Figure G.1:** Material M1 (Plasterboard) HRR Comparison – SBI Test Scenario

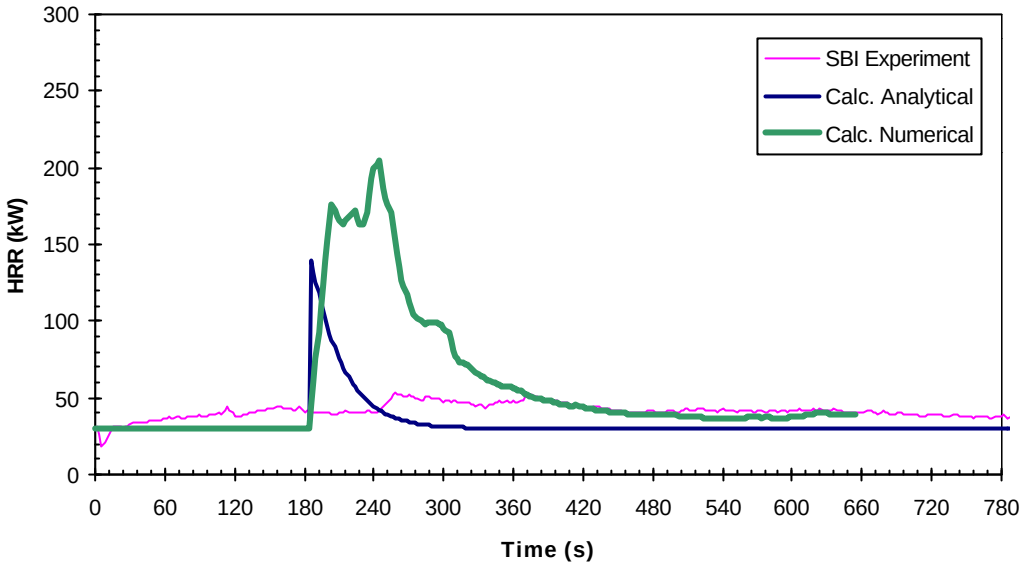


**Figure G.2:** Material M2 (FR PVC) HRR Comparison – SBI Test Scenario

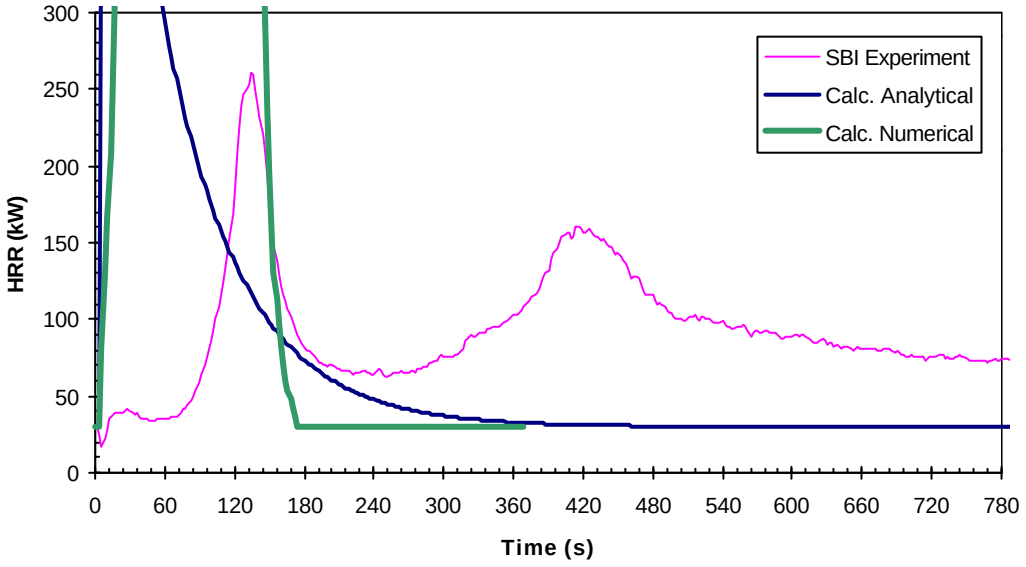


**Figure G.3:** Material M3 (FR extruded Polystyrene board) HRR Comparison – SBI Test Scenario

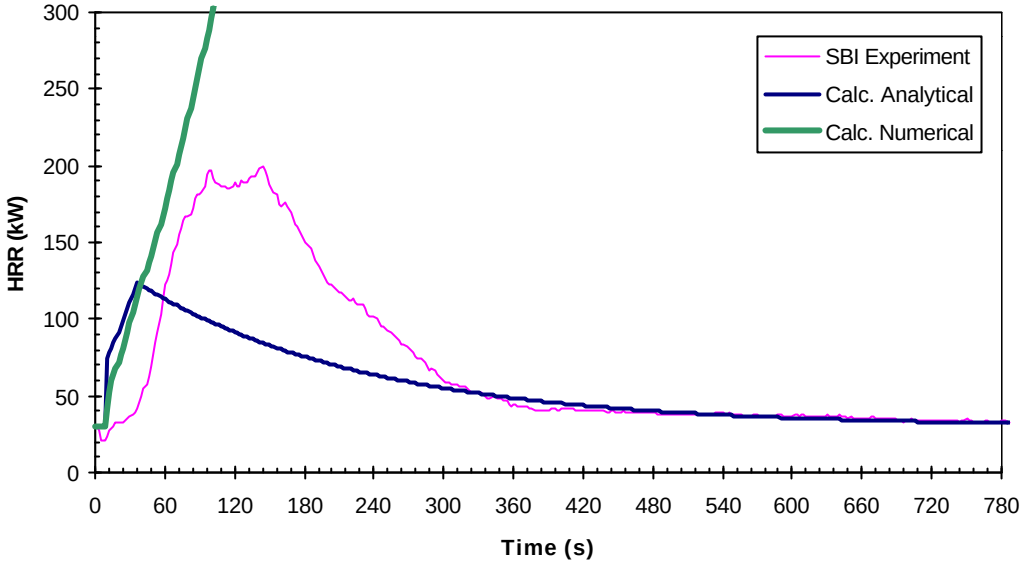


**Figure G.4:** Material M4 (PUR foam panel with Aluminium foil faces) HRR Comparison – SBI Test Scenario

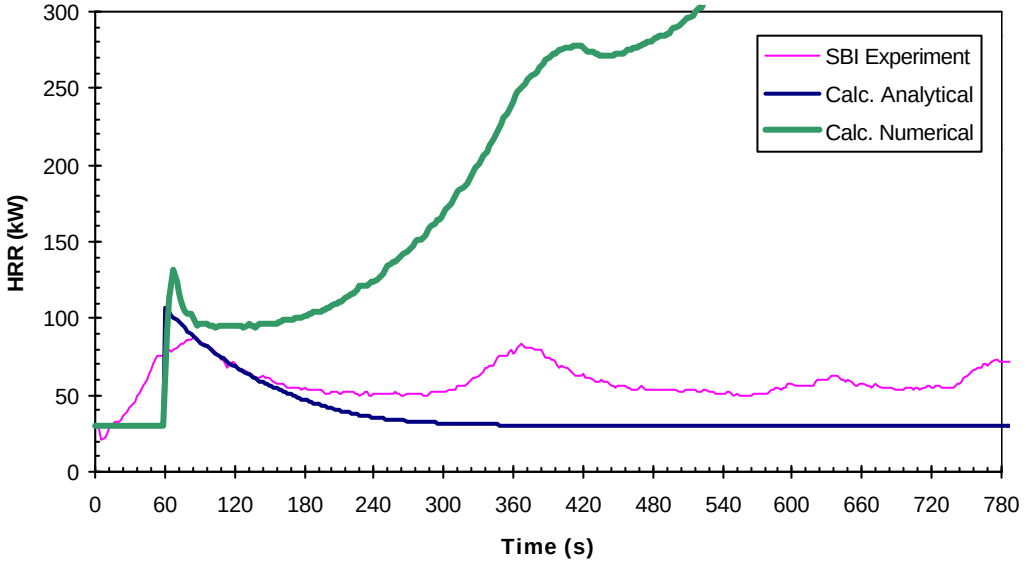


**Figure G.5:** Material M5 (varnished mass Timber, Pine) HRR Comparison – SBI Test Scenario

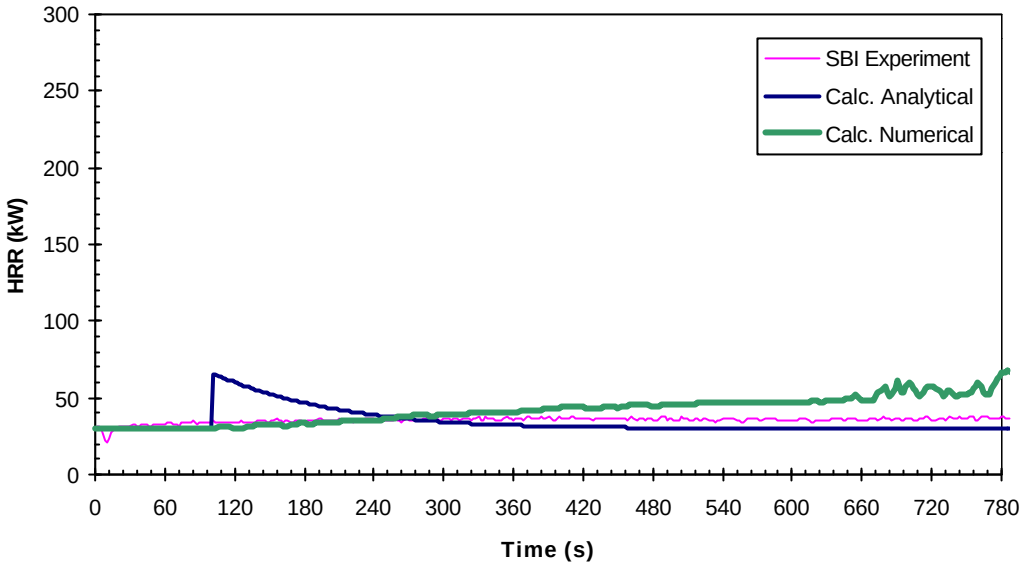


**Figure G.6:** Material M6 (FR Chipboard) HRR Comparison – SBI Test Scenario

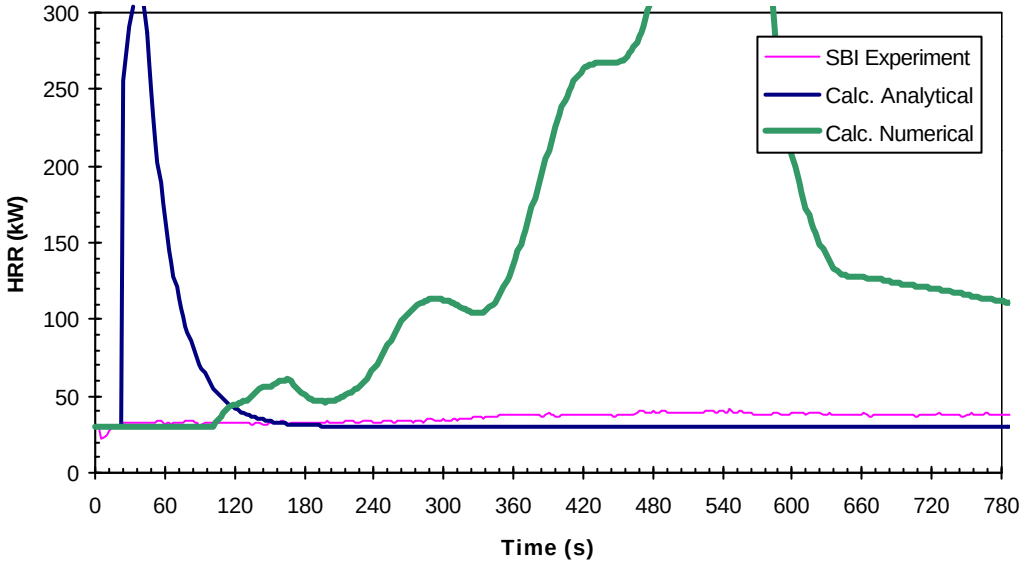


**Figure G.7:** Material M7 (FR Polycarbonate panel (3 layered)) HRR Comparison – SBI Test Scenario

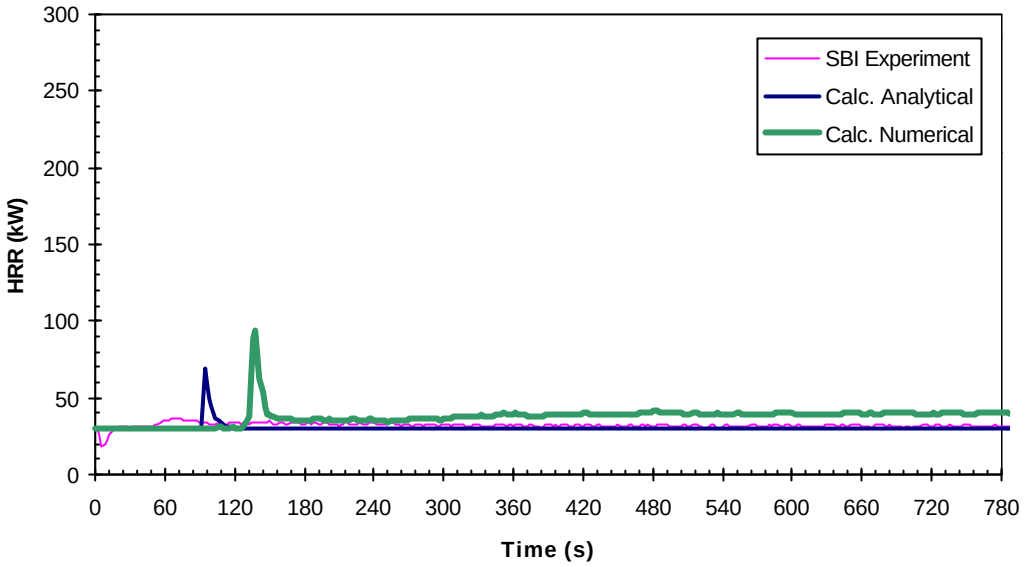


**Figure G.8:** Material M8 (painted Plasterboard) HRR Comparison – SBI Test Scenario

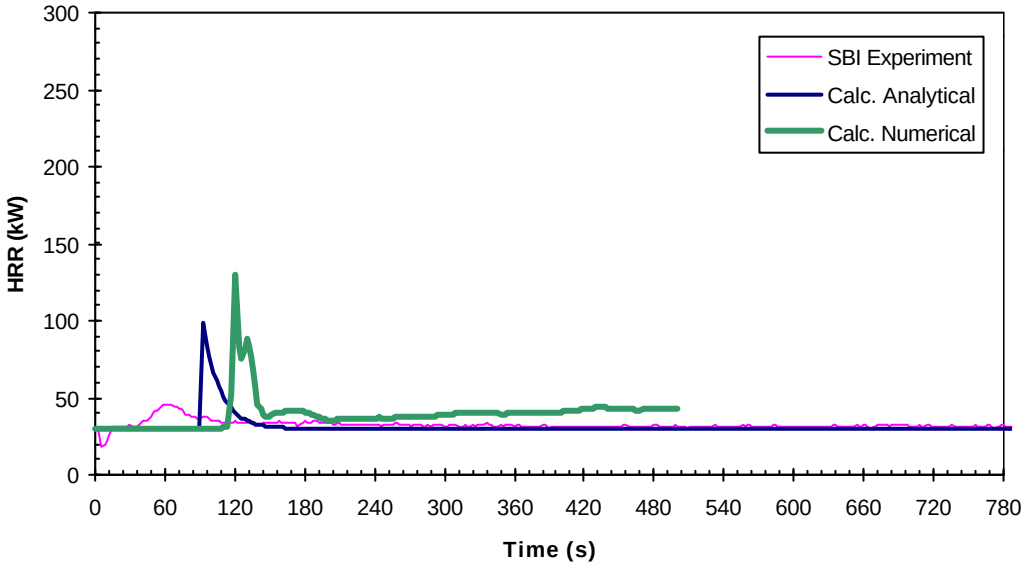


**Figure G.9:** Material M9 (Paper wall covering on Plasterboard) HRR Comparison – SBI Test Scenario

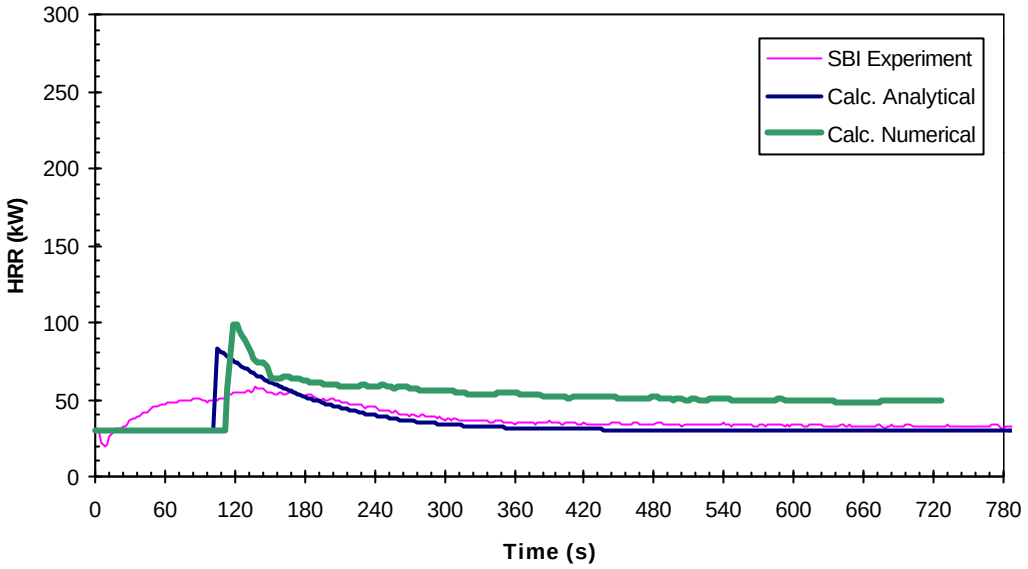


**Figure G.10:** Material M10 (PVC wall carpet on Plasterboard) HRR Comparison – SBI Test Scenario

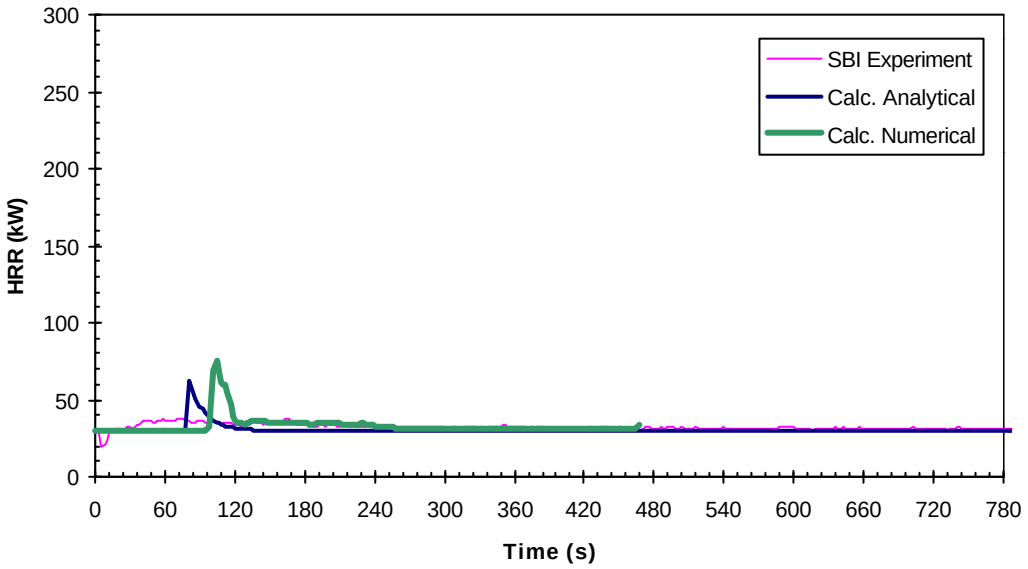


**Figure G.11:** Material M11 (Plastic-faced Steel sheet on Mineral Wool) HRR Comparison – SBI Test Scenario

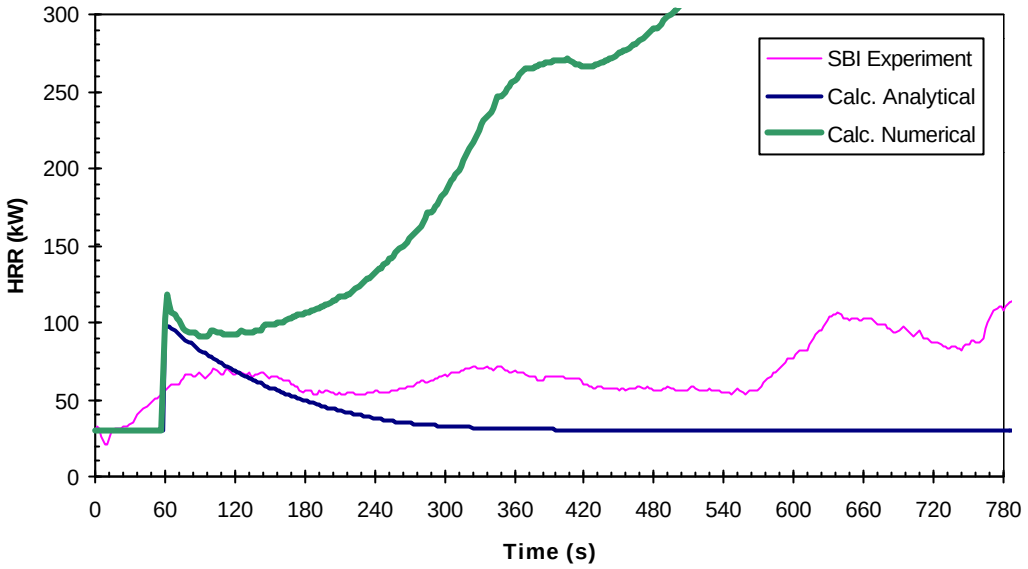


**Figure G.12:** Material M12 (unvarnished mass Timber, Spruce) HRR Comparison – SBI Test Scenario

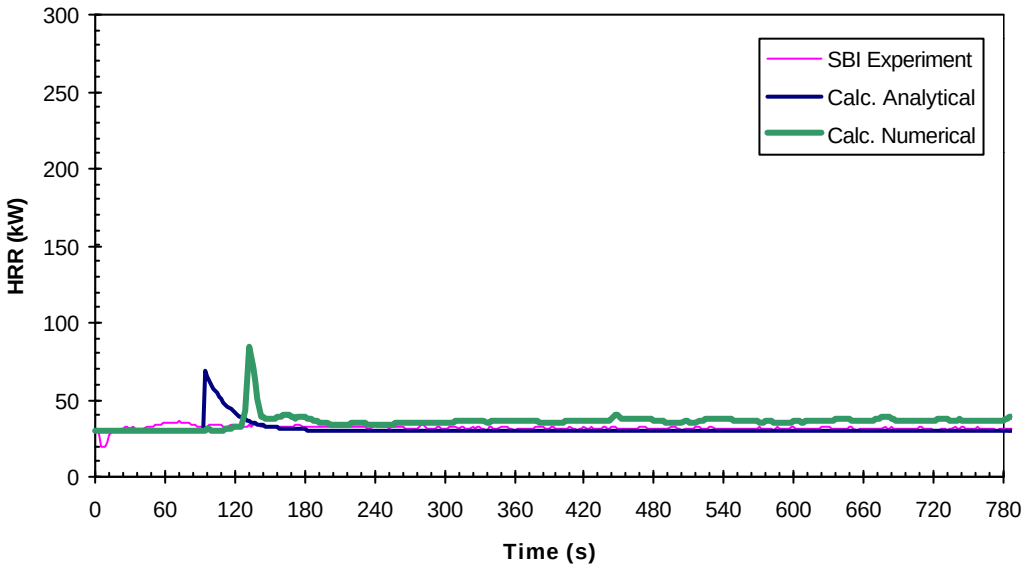


**Figure G.13:** Material M13 (Plasterboard on Polystyrene) HRR Comparison – SBI Test Scenario

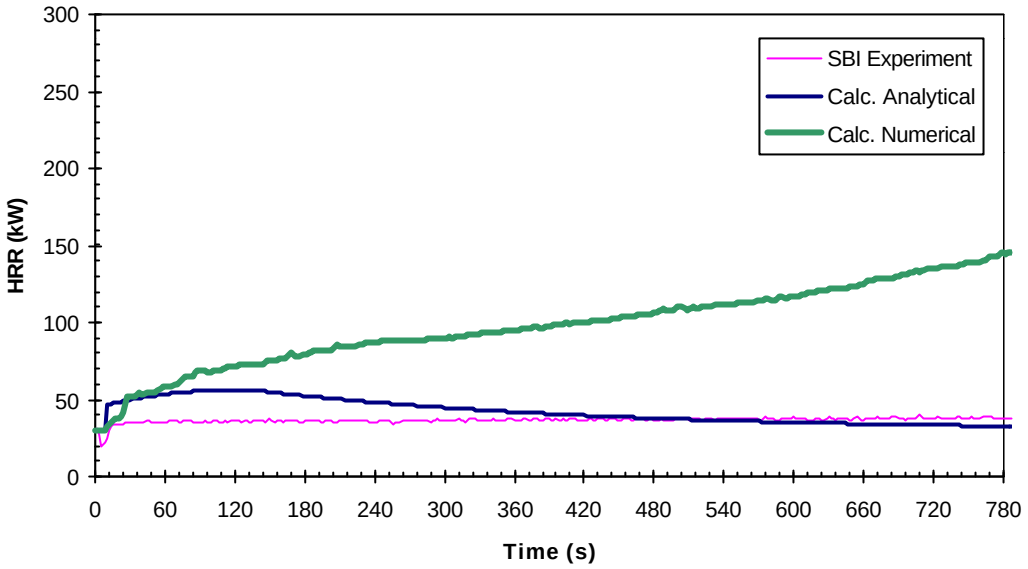


**Figure G.14:** Material M14 (Phenolic foam) HRR Comparison – SBI Test Scenario

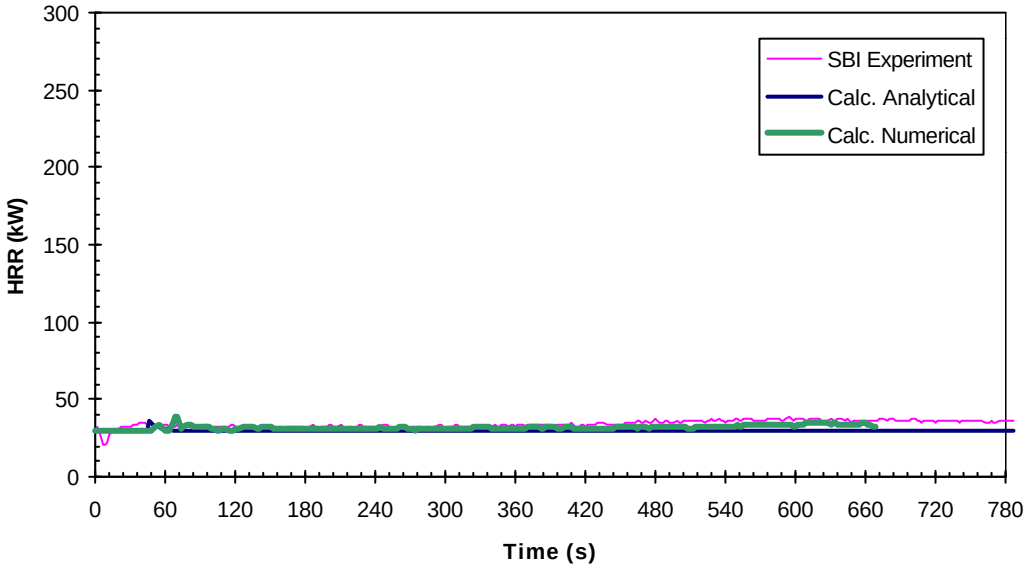


**Figure G.15:** Material M15 (Intumescent coat on Particle board) HRR Comparison – SBI Test Scenario

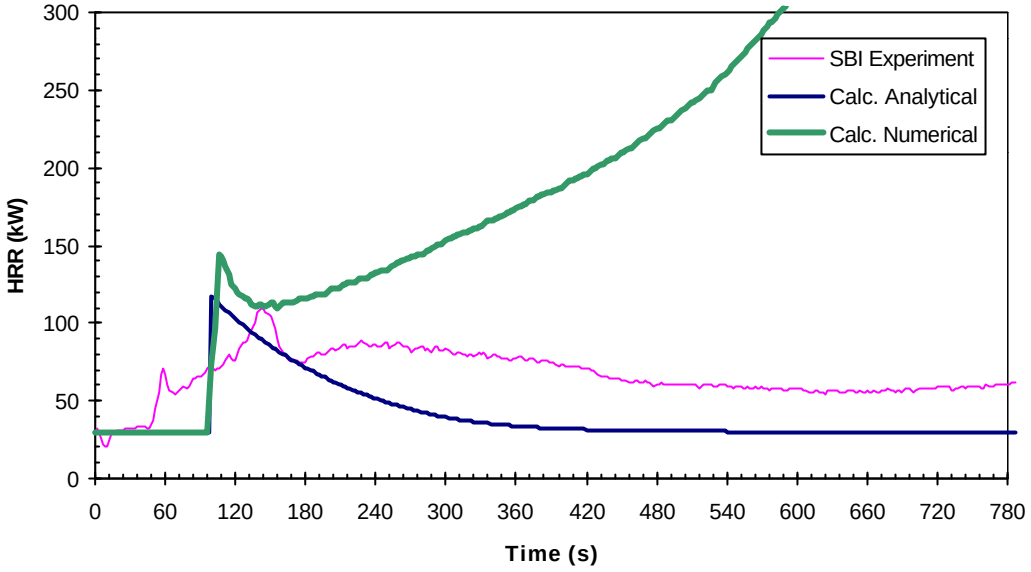


**Figure G.16:** Material M16 (Melamine faced MDF board) HRR Comparison – SBI Test Scenario

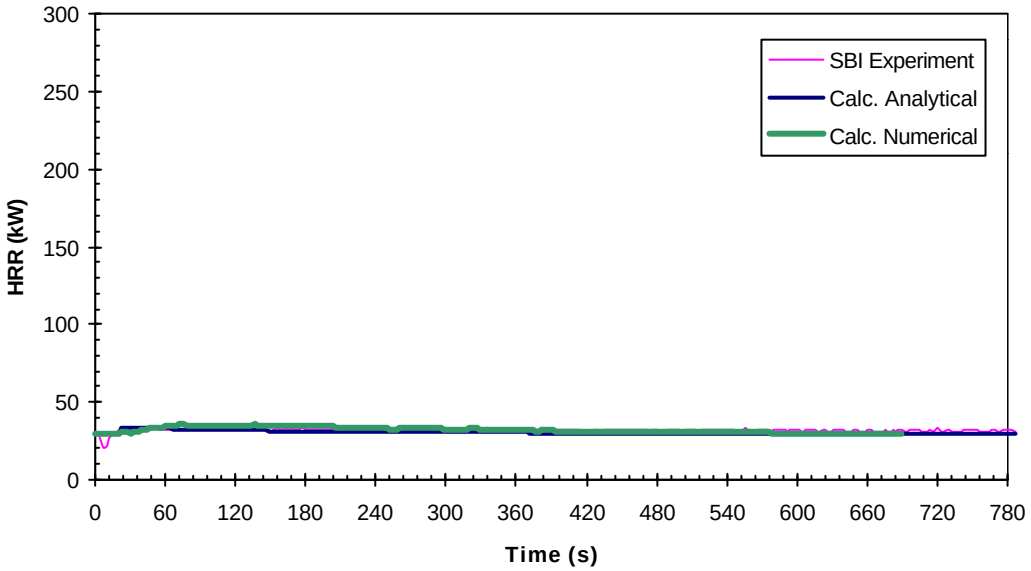


**Figure G.17:** Material M19 (unfaced Rockwool) HRR Comparison – SBI Test Scenario

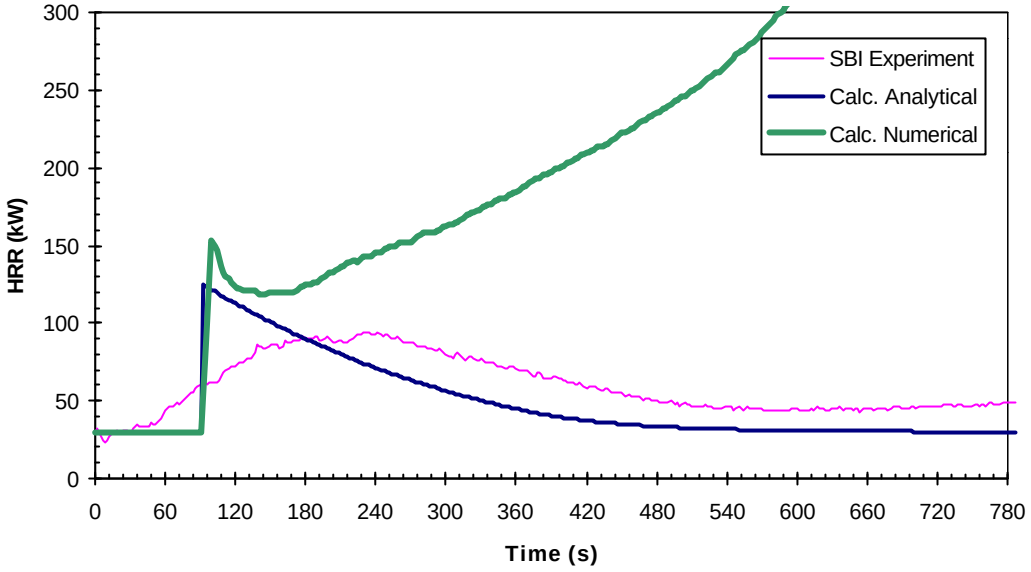


**Figure G.18:** Material M20 (Melamine faced Particle board) HRR Comparison – SBI Test Scenario

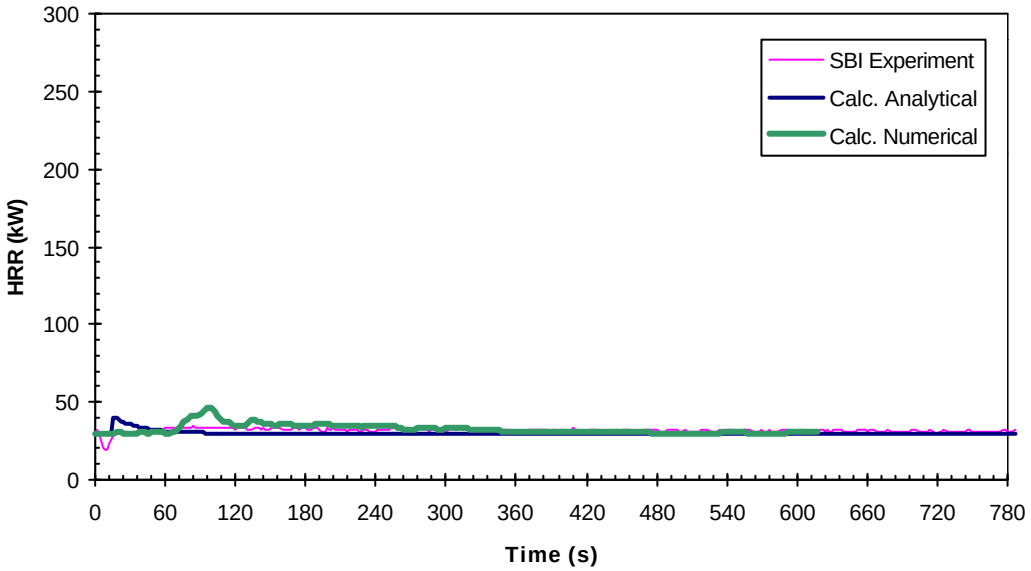


**Figure G.19:** Material M21 (Steel clad expanded Polystyrene sandwich panel) HRR Comparison – SBI Test Scenario

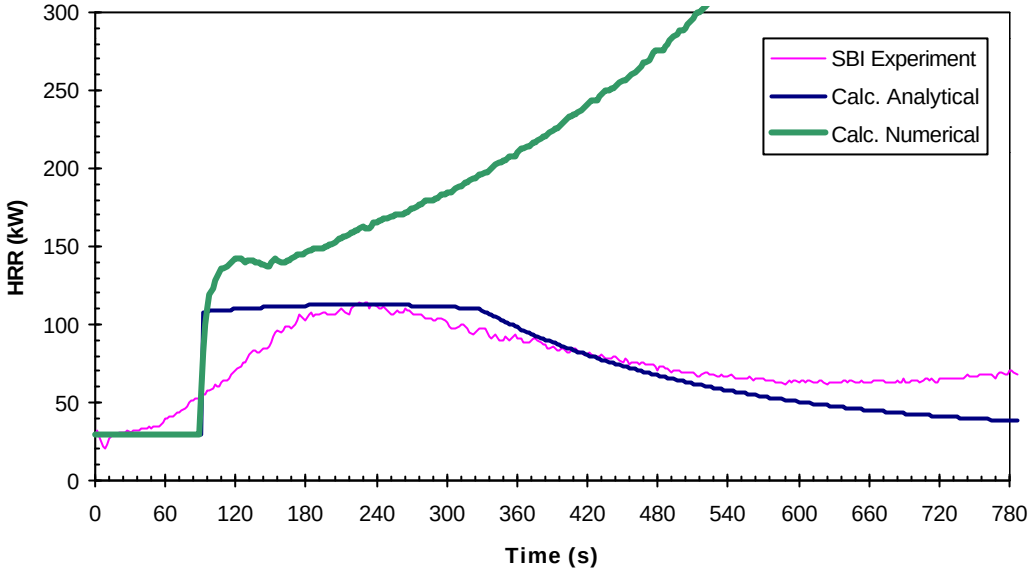


**Figure G.20:** Material M22 (ordinary Particle board) HRR Comparison – SBI Test Scenario

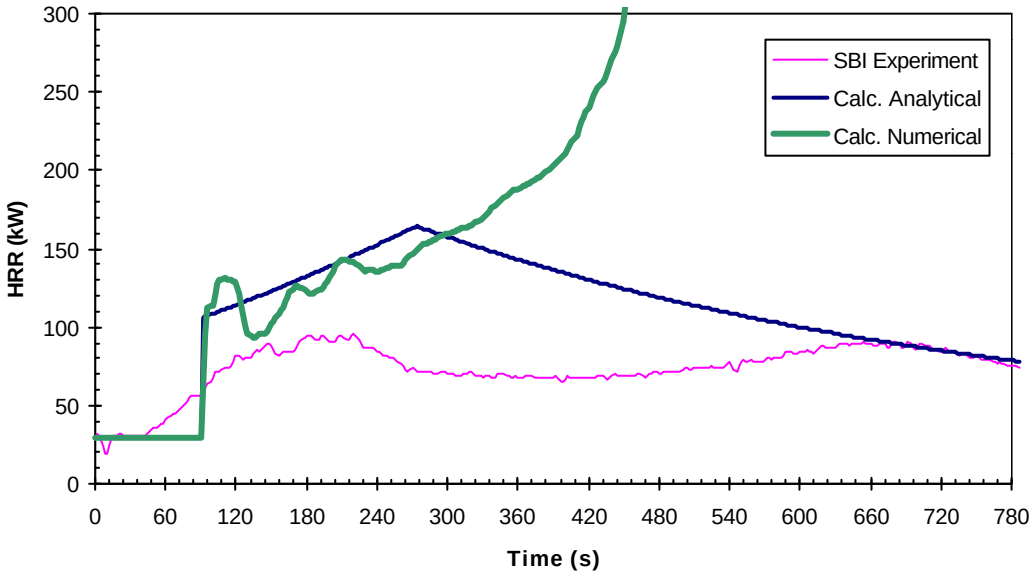


**Figure G.21:** Material M23 (ordinary Plywood, Birch) HRR Comparison – SBI Test Scenario

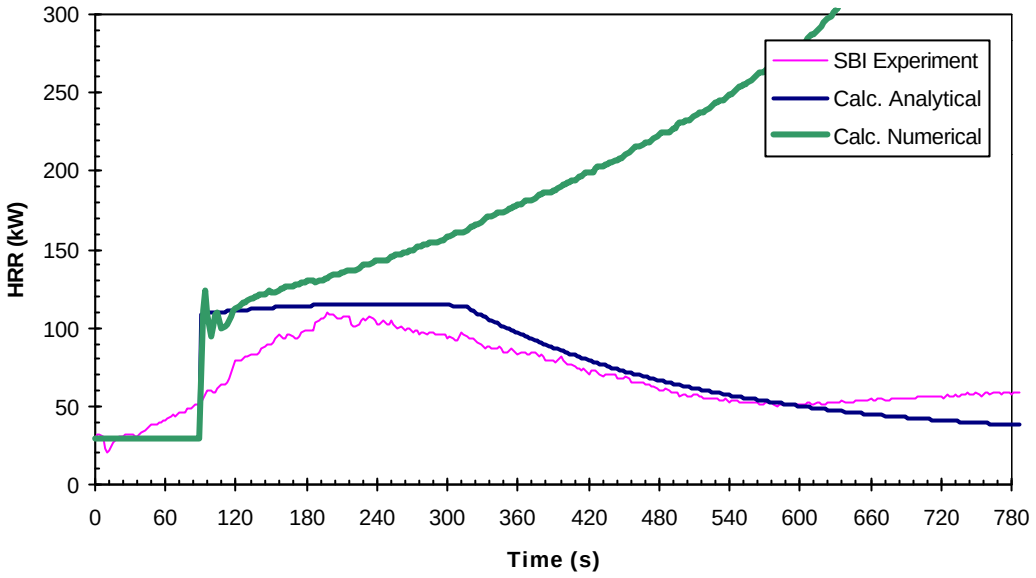


**Figure G.22:** Material M24 (Paper wall covering on Particle board) HRR Comparison – SBI Test Scenario

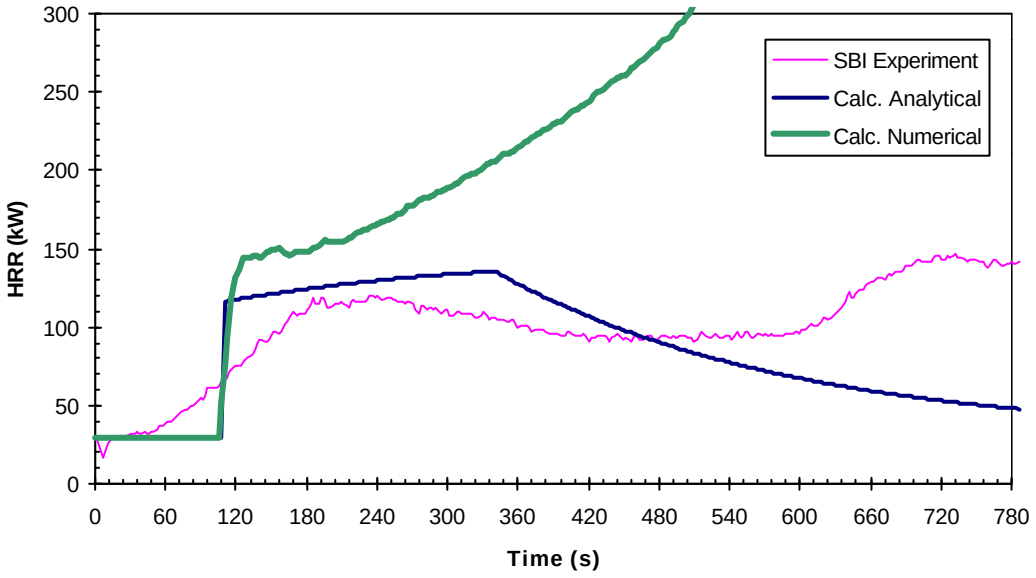


**Figure G.23:** Material M25 (Medium Density Fibre tiles) HRR Comparison – SBI Test Scenario

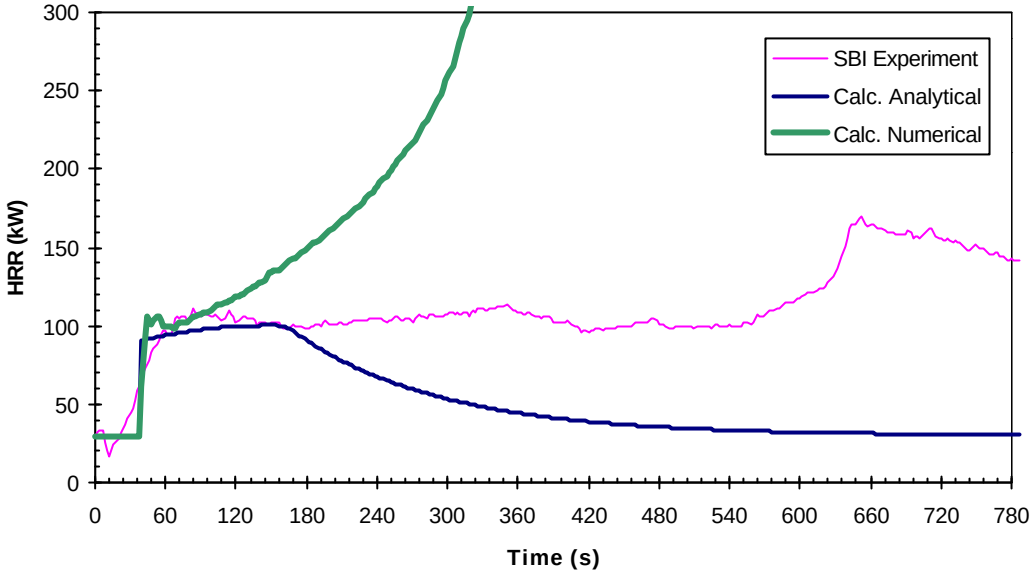


**Figure G.24:** Material M26 (Low Density Fibre board) HRR Comparison – SBI Test Scenario

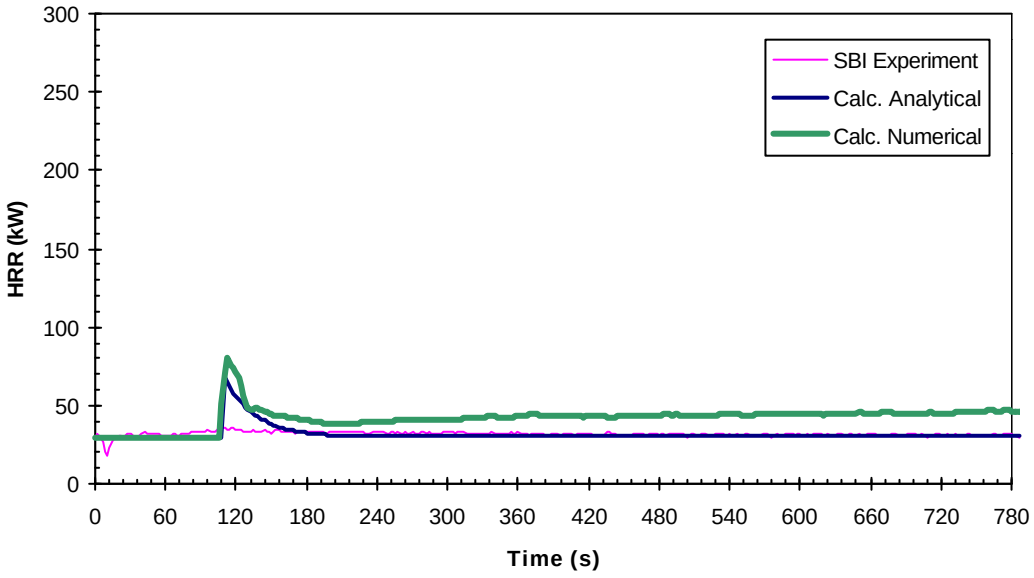


**Figure G.25:** Material M27 (Plasterboard/FR PUR foam core) HRR Comparison – SBI Test Scenario

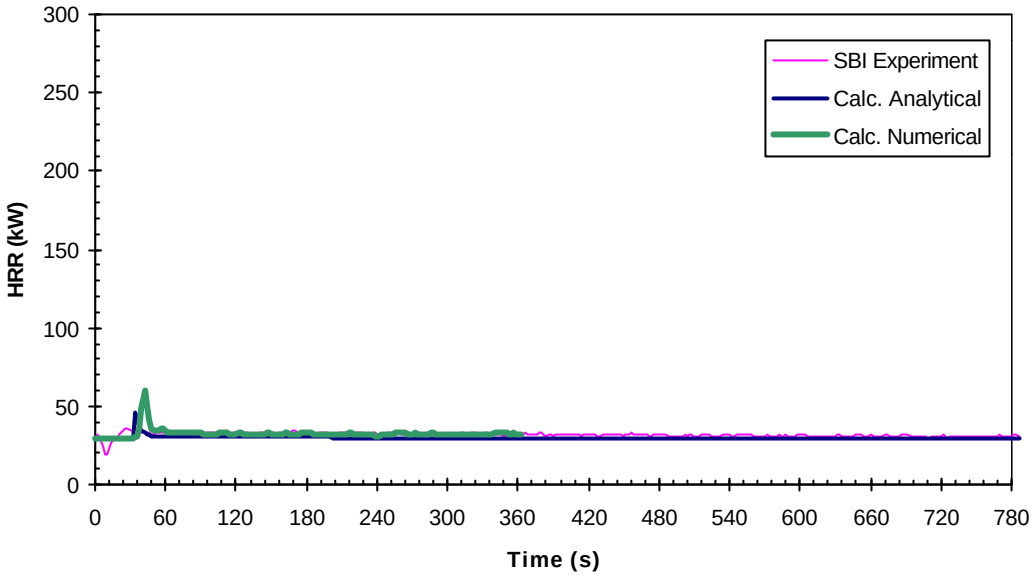


**Figure G.26:** Material M28 (Acoustic Mineral Fibre tiles) HRR Comparison – SBI Test Scenario

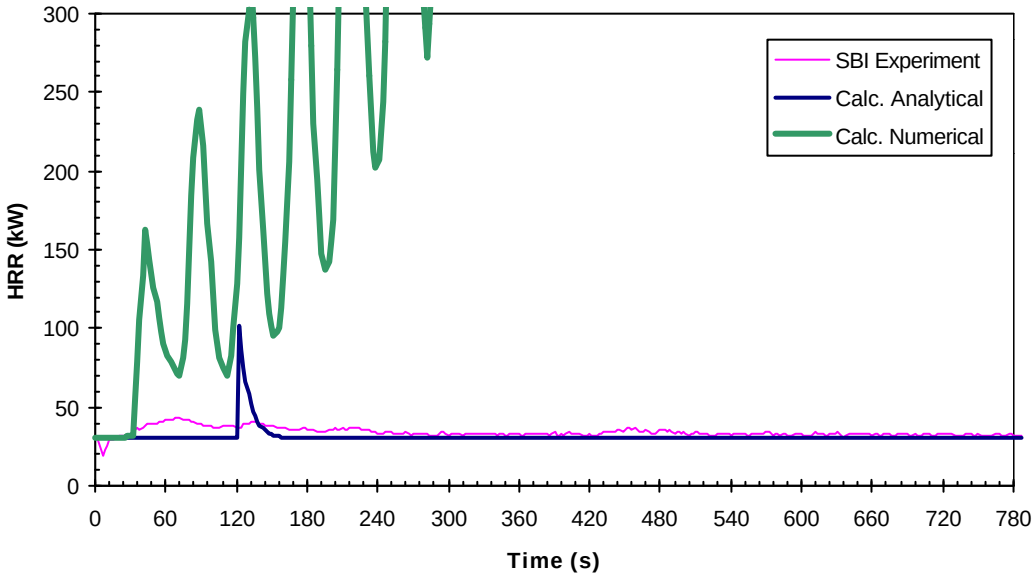


**Figure G.27:** Material M29 (Textile wall paper on Calcium Silicate board) HRR Comparison – SBI Test Scenario

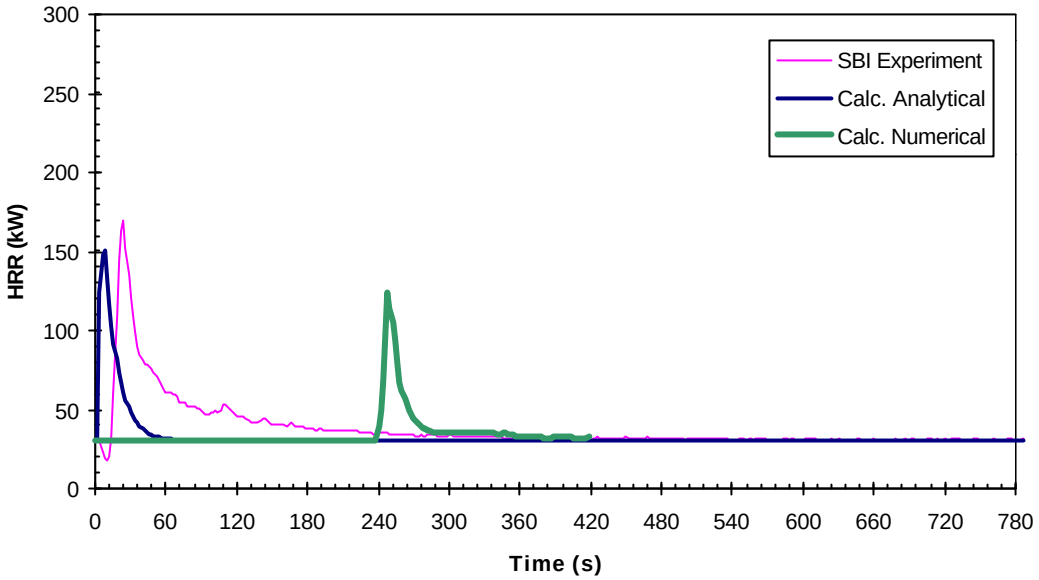


**Figure G.28:** Material M30 (Paper-faced Glass wool) HRR Comparison – SBI Test Scenario